

National Chiao Tung University PhD Thesis

國立交通大學博士學位論文

**Characterization of PslB and PA3346, Two Bifunctional Enzymes in
Pseudomonas aeruginosa PAO1, and Analysis of the Galactose Stress on Gene
Expression of a *Klebsiella pneumoniae* CG43S3 $\Delta galU$ Mutant**

綠膿桿菌 PAO1 中兩個雙功能酵素 PslB 和 PA3346 功能特性之
研究與克雷白氏肺炎桿菌 CG43 *galU* 突變株在半乳糖壓力下其轉錄體之分析



研究生：李蕙如

Student：Hui-Ju Lee

指導教授：張晃猷 博士

彭慧玲 博士

Advisor：Hwan-You Chang, Ph.D

Hwei-Ling Peng, Ph.D

中華民國一零三年一月

January, 2014

綠膿桿菌 PAO1 中兩個雙功能酵素 PslB 和 PA3346 功能特性之研究
與克雷白氏肺炎桿菌 CG43 *galU* 突變株在半乳糖壓力下其轉錄體之分析
Characterization of PslB and PA3346, Two Bifunctional Enzymes in
Pseudomonas aeruginosa PAO1, and Analysis of the Galactose Stress on
Gene Expression of a *Klebsiella pneumoniae* CG43S3 $\Delta galU$ Mutant

研究生：李蕙如

Student：Hui-Ju Lee

指導教授：張晃猷

Advisor：Hwan-You Chang

彭慧玲

Hwei-Ling Peng



National Chiao Tung University
Department of Biological Science and Technology
PhD Thesis

中華民國一零三年一月

January 2014

中文摘要

本論文共分為三個章節，第一章和第二章主要是探討綠膿桿菌 PAO1 中兩個雙功能酵素 PslB 與 PA3346 之酵素特性，第三章則是分析克雷白氏肺炎桿菌 CG43 尿嘧啶雙磷酸葡萄糖焦磷酸化酶(GalU)突變株在半乳糖存在下其基因轉錄之變化。

綠膿桿菌中 PslB 是具有磷酸甘露糖異構酶(PMI)與鳥苷雙磷酸甘露糖焦磷酸化酶(GDP-man PPase)的雙功能酵素，分別參與鳥苷雙磷酸甘露糖(GDP-man)合成的第一步和第三步催化反應。而目前為止，PslB 的酵素活性及參與催化反應的重要胺基酸位置尚未被報導。在第一章的研究裡，我們證實了 PslB 的確具有 PMI 與 GDP-man PPase 的酵素功能。GDP-man PPase 酵素反應需要正二價鎂離子的幫助；PMI 酵素反應則是需要正二價鈷離子，而且其活性會被 GDP-man 所抑制。另外，2,3-丁二酮(2,3-butanedione)能將 PslB 的 PMI 活性去活化，顯示 PslB 上某個位置的精胺酸(Arg)可能在催化過程中扮演重要的角色。我們進一步利用點突變的實驗技術，發現將 PslB 第 408 號位置的精胺酸更改為賴胺酸(Lys)或者丙胺酸(Ala)後，其 PMI 的活性則是完全消失。經由圓二色光譜的分析，野生株及定點突變株的 PslB 在蛋白質二級結構上未有改變。此結果證實 PslB Arg408 的確是參與催化反應的重要胺基酸，亦可做為未來了解 PMI 催化機制的初步依據。

第二章主要研究綠膿桿菌另一雙功能酵素 PA3346。先前的研究發現，HptB 訊息傳

遞路徑在綠膿桿菌 PAO1 細菌群體移動與生物膜形成中扮演重要的調控角色。當細菌接受到環境的刺激，感應激酶蛋白(PA1611, PA1976, PA2824)會自我磷酸化，其磷酸根再經由 HptB 傳遞給下游的反應調控子 PA3346。PA3346 N 端磷酸化後，使得其絲胺酸蛋白磷酸酶活性增加，並將 anti-sigma factor 拮抗子 PA3347 Ser56 上之磷酸根去除。然而，能將 PA3347 Ser56 位置磷酸化的絲胺酸蛋白激酶仍然未知。經由蛋白質結構域分析，我們發現 PA3346 C 端 (PA3346^{L408-A571}) 的結構域與枯草桿菌的 SpoIIAB (絲胺酸蛋白激酶/anti-sigma factor) 極為相似，因此推測 PA3346^{L408-A571} 具有絲胺酸蛋白激酶的活性；而且，PA3346-PA3347 可能與枯草桿菌 SpoIIE-SpoIIAB-SpoIIAA 的調控系統類似，形成所謂的 partner-switching 調控模組。本論文建構 PA3346^{L408-A571} 與 PA3347 重組蛋白質，以進行試管內磷酸化反應。結果證實 PA3346^{L408-A571} 能將 PA3347 Ser56 位置磷酸化，其絲胺酸蛋白激酶的活性需要 Mg²⁺, Ca²⁺ 與 Mn²⁺ 等正二價金屬離子的幫助。在進行 GST pull-down assay 與 GFP assembly assay 後，我們發現 PA3346^{L408-A571} 與 PA3347 蛋白質不管是在試管內或是在細菌體內，都能夠互相結合。這些結果證實了 PA3346^{L408-A571} 的確具有絲胺酸蛋白激酶/anti-sigma factor 的功能。為了尋找參與 partner-switching 調控系統的 sigma factor，我們亦進行了雙分子螢光互補實驗，而詳細的分子調控機制需要進一步的探討研究。

本論文的第三章，主要對克雷白氏肺炎桿菌 *galU* 突變株進行研究。當使用 *galU* 突變株進行半乳糖紙錠擴散實驗時，紙錠周圍會出現清晰的抑菌圈；將細菌培養在以 2%

甘油為主要碳源的 M9 培養液時，加入半乳糖會使得細菌生長緩慢並且有死亡的現象。

半乳糖對克雷白氏肺炎桿菌 *galU* 突變株的毒性，主要是因為尿嘧啶雙磷酸葡萄糖焦磷酸化酶(UDP-glc PPase)缺損，導致了有毒的半乳糖代謝產物累積。然而，這些代謝產物如何影響細菌基因表現及造成細菌死亡的原因仍然未知。因此，我們利用 RNA-seq 技術研究在半乳糖存在的狀況下，克雷白氏肺炎桿菌 *galU* 突變株的基因表現變化。我們發現在半乳糖的存在下，*galETKM*、*galP*、*lacYZ* 以及胺基酸合成相關的基因表現有上升的趨勢；而甘油代謝(*pduCDE*)、鐵離子攝取系統(*sitABCD*、*feoABC*)與 12 個調控因子(*hns*、*csrA* 與 10 個轉錄調控子)的基因表現則被抑制。廣泛型調控因子 H-NS 與 CsrA 控制許多細菌的重要生理作用，如碳源代謝、毒性、移動與應激反應系統。我們推測本研究使用的培養條件使得有毒的半乳糖代謝產物累積，並間接地抑制 H-NS、CsrA 與其它轉錄調控子的基因表現，影響細菌的轉譯與轉錄作用，最後因為生理系統紊亂導致死亡。

Abstract

This thesis consists of three chapters. Chapter 1 and chapter 2 describe the functional studies of two bifunctional enzymes, PslB and PA3346, in *Pseudomonas aeruginosa* PAO1. Chapter 3 describes the results of transcriptome analysis of *Klebsiella pneumoniae* CG43S3 $\Delta galU$ mutant under galactose stress.

Pseudomonas aeruginosa pslB gene encodes a bifunctional enzyme phosphomannose isomerase/GDP-D-mannose pyrophosphorylase (PMI-GDP-man PPase). The enzyme catalyzes the first and third steps in the GDP-D-mannose biosynthetic pathway, an important precursor of many polysaccharides. So far, very little is known about PslB. In Chapter 1, we demonstrate that *Pseudomonas aeruginosa pslB* encodes a protein with GDP-man PPase/PMI dual activities. The GDP-man PPase activity is Mg^{2+} -dependent, whereas the PMI activity is Co^{2+} -dependent and could be inhibited by GDP-mannose in a competitive manner. Furthermore, the PMI activity could be inactivated by 2, 3-butanedione suggesting the presence of a catalytic Arg residue. Site-specific mutations at R373, R472, R479, E410, H411, N433 and E458 increase the K_M approximately 8- to 20-fold. The PMI activity of PslB was completely diminished with a R408K or R408A, reflecting the importance of this residue in catalysis. The CD spectra of R408A, R408K and wild type PslB are nearly identical,

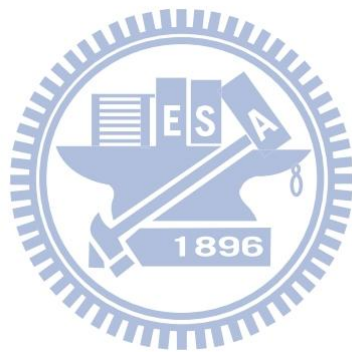
indicating that there is nearly no alterations of their secondary structures. Overall, these results provide a basis for understanding the catalytic mechanism of PMI.

In chapter 2, we focus on the other bifunctional enzyme PA3346. We have previously observed that the HptB-mediated phosphorelay pathway plays an important role in swarming phenotype and biofilm formation in *P. aeruginosa* PAO1. Upon activation by an environmental stress, sensor kinase (PA1611, PA1976 and PA2824) autophosphorylates itself and then transfers a phosphoryl group to HptB, which then relays the signal to response regulator PA3346. The phosphorylation on PA3346 N-terminal receiver domain results in an increase in its Ser protein phosphatase activity leading to dephosphorylation of the putative anti-sigma factor antagonist PA3347. While the target phosphorylation site on PA3347 has been shown to be located at Ser-56, the corresponding serine protein kinase and anti-sigma factor remain elusive. Protein domain analysis revealed that the C-terminal region of PA3346 (PA3346^{L408-A571}) contains conserved domains similar to the Ser protein kinase/anti-sigma factor SpoIIAB in *Bacillus subtilis*. Thus, we proposed that PA3346-PA3347 forms a partner-switching regulatory module as observed for SpoIIE-SpoIIAB-SpoIIAA in *B. subtilis*. This thesis has cloned and purified PA3346^{L408-A571} and PA3347-GST for *in vitro* phosphorylation and GST pull-down assays. The results clearly demonstrate that PA3346^{L408-A571} possesses a kinase activity toward PA3347 and the activity is divalent cation,

especially Mg^{2+} , Ca^{2+} and Mn^{2+} dependent. The PA3347-S56A mutant protein could not serve as a substrate for the kinase. In the GST pull-down assay, PA3346^{L408-A571} could be co-eluted with PA3347-GST in the presence of ADP. As for the GFP fragment reassembly assay, the bacterial cells harboring the plasmids of PA3346^{L408-A571}-CGFP and PA3347-NGFP display the green fluorescence signals. These data indicate that PA3346^{L408-A571} is a serine protein kinase/anti-sigma factor playing a key role in the partner-switching regulatory module. In order to identify the specific sigma factor participated in this partner-switching system, *in vivo* bimolecular fluorescence complementation assay are performed and the detailed molecular regulation mechanism is under investigation.

Chapter 3 focuses on the response of *K. pneumoniae* CG43 $\Delta galU$ mutant to the galactose stress. *K. pneumoniae* $\Delta galU$ mutant, which is defective in UDP-Glc PPase, exhibited a growth-inhibition zone in the galactose disk diffusion assay. Galactose can increase the mortality when the $\Delta galU$ mutant was cultivated in M9 minimal medium with 2% glycerol as the sole carbon source. The toxic galactose metabolite affecting the gene expression and causing the cell death remains unclear. Therefore, we investigate the gene expression profiles of the *K. pneumoniae* $\Delta galU$ mutant under the galactose stress by RNA-seq. The results indicate that *galETKM*, *galP*, *lacYZ* and genes responsible for biosynthesis of certain amino acids are upregulated in the presence of galactose. The gene

expressions of glycerol metabolism (*pduCDE*), iron-acquisition systems (*sitABCD* and *feoABC*) and 12 regulatory factors (*hns*, *csrA* and 10 transcriptional regulators) are repressed. Notably, H-NS and CsrA are global regulatory proteins controlling a variety of physiological processes. Besides, *E. coli* *csrA* gene was shown to be essential for bacterial growth in both LB and minimal medium. The toxic galactose metabolites might indirectly repress the gene transcription of H-NS, CsrA and several other transcriptional regulators and lead to the bacterial growth arrest and death.



Acknowledgement

博士班期間，受到了許多師長、同儕與朋友們的幫忙，才得以完成博士學業，要感謝的人真的非常多。首先，最感謝的是我的指導教授張晃猷老師與彭慧玲老師。謝謝清大分醫所張晃猷老師這幾年來的指導，讓我有機會跟不同領域的人合作，並參與許多研究計畫。也謝謝張老師在百忙之中，抽空修改我的論文，使我的論文得以完善。謝謝彭慧玲老師，在我最無助的時候，對我伸出援手，收我當研究生。老師總是設身處地為我著想，替我做最好的安排，對於彭老師的感謝，真的不是言語能夠完全表達的。

謝謝楊昀良老師、梁美智老師與中國醫藥學大學林靖婷老師撥冗擔任我的博士班畢業口試委員，老師們親切的提問，讓我回答問題時不那麼緊張，在口試時給了我許多建議，而且非常仔細地看我的論文，幫我挑出很多小錯誤。謝謝林志生老師與中興大學鄧文玲老師，在兩次的博士班資格考中擔任我的口試委員時，給我很多實驗設計與規劃的建議，提醒我要加強報告與回答問題的技巧。最後，要感謝我的大學專題與碩士班指導教授邱顯泰老師，在邱老師的實驗室裡，學到許多分生、生化實驗技術與實驗設計邏輯，奠定了我做生物實驗的良好基礎。

感謝實驗室所有的成員們，尤其是同組的敏潔學姐，很懷念以前和學姐一起討論實驗，一起出去吃飯，還有參加清大校園健走活動的日子；謝謝靜柔學姐，我們一起當了微生物實驗課助教，而且，在兩次博士班資格考時，學姊幾乎一手包辦了大小瑣事，讓

我能夠專心準備資格考資料，真的非常謝謝學姊這些年來的幫忙與照顧；謝謝健誠學長與小新學長，雖然與學長們相處的時間不多，但每次不管是聊實驗相關或是生活上的事情，總是非常開心；要感謝的還有清大實驗室的貞儀學姊、韻如學姊、莉芳學姊、Poki學長、錢小豬、婉禎、方瑜、宗葆、芊瑜、芝瑄、明融、幸珊、艾婷、吉姆、克萊兒、柏融、Hubert、哈哈、小辣椒、Cain、楊不理、小蛙、毛毛、翼軒、小杜、慈芳、Maybe、鄒宇、瑟玉、Maysam、Minh、Daniel Liu 與 Manish，大家在實驗室生活上的幫助、關心與包容，讓我在清大的這幾年過得不孤單☺。

謝謝我的朋友們，偶爾與妳們聚餐聊天，是我攻讀博士班期間，最棒的生活點綴；感謝我親愛的家人們，你們不求回報的付出與無條件的支持，對我而言，就是最大的鼓勵，讓我能夠毫無後顧之憂的完成博士學業，我內心由衷的感謝，願將我所有的喜悅與我親愛的家人們分享。



Abbreviations

AHL	N-acylhomoserine lactones
ADP	adenosine diphosphate
ATP	adenosine triphosphate
ADP-Glc	ADP-glucose
Ap	ampicillin
C ₄ -HSL	N-butyryl-L-Homoserine lactone
CAS	chrome azurol S
CD	circular dichroism
DTT	dithiothreitol
EDTA	ethylenediaminetetraacetic acid
Fru-6-p	fructose-6-phosphate
Gal	galactose
Gal-1-p	galactose-1-phosphate
GDP-Man	GDP-mannose
GDP-Man PPase	GDP-mannose pyrophosphorylase
Glc	glucose
Glc-6-p	glucose-6-phosphate
GFP	green fluorescent protein
GST	glutathione S-transferase
GTP	guanosine triphosphate
HDTMA	hexadecyltrimethylammonium bromide
HRP	horseradish peroxidase
IPTG	isopropyl thio- β -D-galactopyranoside
K _m	kanamycin
LB	Luria-Bertani
Man-1-p	mannose-1-phosphate
Man-6-p	mannose-6-phosphate
NADH	nicotinamide adenine dinucleotide
β -NADP	nicotinamide adenine dinucleotide phosphate
NB	nutrient broth
PBS	phosphate buffered saline
PIPES	piperazine-N,N'-bis(2-ethanesulfonic acid)
PMI	phosphomannose isomerase

PVDF	polyvinylidene fluoride
SDS	sodium dodecyl sulfate
Sm	streptomycin
TDP-glc	TDP-glucose
2CS	two-component system
UDP-Gal	UDP-galactose
UDP-Glc	UDP-glucose
UDP-GlcN	UDP-glucosamine
UDP-Glc PPase	UDP-glucose pyrophosphorylase



Table of Contents

中文摘要.....	I
ABSTRACT	IV
ACKNOWLEDGEMENT	VIII
ABBREVIATIONS.....	X
TABLE OF CONTENTS.....	XII
LIST OF TABLES	XV
LIST OF FIGURES.....	XVI
CHAPTER 1.....	1
1.1 ABSTRACT	2
1.2 INTRODUCTION	2
1.3 MATERIALS AND METHODS	4
1.3.1 Bacterial strains and growth conditions	4
1.3.2 Expression and purification of PslB	4
1.3.3 Determination of the enzyme activity	5
1.3.4 Inactivation of PslB by 2, 3-Butanedione	6
1.3.5 Amino acid sequence alignment and site-directed mutagenesis.....	6
1.3.6 Circular dichroism spectrum analysis	6
1.3.7 <i>In vivo</i> protein-protein interaction assay by GFP fragment reassembly.....	7
1.4 RESULT AND DISCUSSION	7
1.4.1 PslB possesses PMI and GDP-Man PPase activity	7
1.4.2 Divalent cation requirement for PslB	8
1.4.3 The PMI activity of PslB is inhibited by GDP-Man	9
1.4.4 An Arg residue participates in the <i>P. aeruginosa</i> PMI activity.....	10
1.4.5 Arg408 substitutions abolished the PMI activity of PslB.....	11
1.4.6 The R408 mutations did not affect GDP-Man PPase activity of PslB	12
1.4.7 The GMP domain and the PMI domain influence the activities of each other.....	12
1.4.8 PslB cannot form protein complex with AlgC	14
1.5 TABLES.....	16
1.6 FIGURES.....	23
CHAPTER2.....	32

2.1 ABSTRACT	33
2.2 INTRODUCTION	34
2.3 MATERIALS AND METHODS.....	36
2.3.1 Bacterial strains and growth conditions	36
2.3.2 Amino acid sequence alignments	36
2.3.3 Cloning, expression and purification of His-tag and GST-tag fusion protein	37
2.3.4 <i>In vitro</i> phosphorylation assay	38
2.3.5 Protein pull-down assays.....	38
2.3.6 Western blotting analysis.....	39
2.3.7 <i>In vivo</i> protein-protein interaction assay by GFP fragment reassembly	39
2.3.8 Chrome azurol S (CAS) plate assay	40
2.3.9 N-Acyl homoserine lactones (AHL) reporter plate bioassays	40
2.3.10 Congo red plate assay.....	41
2.4 RESULT AND DISCUSSION.....	41
2.4.1 PA3346 ^{L408-A571} contains the conserved N, G1 and G2 boxes	41
2.4.2 PA3346 ^{L408-A571} possesses a Ser protein kinase activity toward PA3347	42
2.4.3 PA2797 is not the substrate of PA3346 ^{L408-A571}	42
2.4.4 PA3346 ^{L408-A571} interacts with PA3347 in the presence of ADP <i>in vitro</i>	43
2.4.5 PA3346 ^{L408-A571} interacts with PA3347 <i>in vivo</i>	44
2.4.6 PA3346 ^{L408-A571} cannot interact with RpoN in the presence of ATP <i>in vitro</i>	45
2.4.7 $\Delta hptB$ mutant strain displays a higher production level of exopolysaccharides.....	46
2.4.8 No significant phenotype differences are found in CAS plate assay and AHL reporter assay	46
2.4.9 Is PA3346 ^{L408-A571} an anti-sigma factor?	47
2.5 TABLES	51
2.6 FIGURES.....	59
CHAPTER 3.....	74
3.1 ABSTRACT	75
3.2 INTRODUCTION	75
3.3 MATERIALS AND METHODS	77
3.3.1 Bacteria strains and growth medium	77
3.3.2 Bacterial growth curve	77
3.3.3 Disk diffusion assay	78
3.3.4 LIVE/DEAD [®] BacLight [™] Bacterial Viability assay	78
3.3.5 RNA purification.....	78
3.3.6 RNA sequencing	80
3.4 RESULT AND DISCUSSION.....	80

3.4.1 A growth-inhibition zone is observed in <i>K. pneumoniae</i> $\Delta galU$ mutant strain in galactose disk diffusion assay.....	80
3.4.2 Galactose inhibits growth of <i>K. pneumoniae</i> $\Delta galU$ mutant	81
3.4.3 Galactose induces death of <i>K. pneumoniae</i> $\Delta galU$ mutant.....	82
3.4.4 Transcriptome analysis of <i>K. pneumoniae</i> $\Delta galU$ gene expression profiles under galactose stress ...	82
3.5 TABLES	88
3.6 FIGURES.....	96
REFERENCES	99
APPENDIX I.....	112
APPENDIX II	120
CURRICULUM VITAE.....	122



List of Tables

Table 1.5.1 Bacterial strains and plasmids used in this study	16
Table 1.5.2 Primers used in this study	18
Table 1.5.3 Divalent cation effects on PslB	20
Table 1.5.4 Effects of potential inhibitors on the PMI activity	21
Table 1.5.5 PMI kinetic parameters of the wild type or mutated PslB	22
Table 2.5.1 Bacterial strains and plasmids used in this study	51
Table 2.5.2 Primers used in this study	54
Table 2.5.3 Genes used in the GFP assembly assay	58
Table 3.5.1 Upregulated genes in CG43S3 $\Delta galU$ (+Gal) comparing with CG43S3 $\Delta galU$	88
Table 3.5.2 Downregulated genes in CG43S3 $\Delta galU$ (+Gal) comparing with CG43S3 $\Delta galU$	90
Table 3.5.3 Predicted CRP binding site in the upstream region of galactose regulated genes	93
Table 3.5.4 Predicted H-NS binding site in the upstream region of the galactose regulated genes	94
Table 3.5.5 Predicted Fur binding site in the upstream region of the galactose regulated genes	95

List of Figures

Fig. 1.6.1 Protein purity of wild type and mutant PslB	23
Fig. 1.6.2 Effects of various concentrations of cobalt ion on the PMI activity	24
Fig. 1.6.3 Effects of Mg ²⁺ on the PMI activity of PslB.....	25
Fig. 1.6.4 Double reciprocal plot at various GDP-Man concentrations	26
Fig. 1.6.5 Inactivation of PslB by 2, 3-butanedione	27
Fig. 1.6.6 Amino acid sequence alignment of GDP-Man PPase /PMIs	28
Fig. 1.6.7 Circular dichroism spectra of wild type and mutant PslB	29
Fig. 1.6.8 Time dependent profiles of the GDP-man PPase activity assay	30
Fig. 1.6.9 Time dependent profile of PMI activity assay	31
Fig. 2.6.1 Multiple sequence alignment of PA3346 ^{L408-A571} with other Ser protein kinases.....	59
Fig. 2.6.2 Time course analysis of PA3347 <i>in vitro</i> phosphorylation.	60
Fig. 2.6.3 <i>In vitro</i> phosphorylation assay of purified PA3347 and PA3347S56A mutant protein	61
Fig. 2.6.4 Divalent cation dependence on phosphorylation reaction.	62
Fig. 2.6.5 Phosphorylation level of PA3347 analysis by Pro-Q Diamond staining	63
Fig. 2.6.6 Multiple sequence alignment of PA2797 with other anti-sigma factor antagonist.	64
Fig. 2.6.7 <i>In vitro</i> phosphorylation of purified GST, GST-PA2797 and GST-PA3347 proteins.....	65
Fig. 2.6.8 Analysis of PA3346 ^{L408A-A571} and PA3347 protein-protein interaction by using GST pull down assay.66	66
Fig. 2.6.9 Protein interaction of PA3347 and PA3346 ^{L408-A571} examined using the GFP fragment reassembly assay	67
Fig. 2.6.10 Analysis of PA3346 and RpoN protein-protein interaction using GST pull down assay.	68
Fig. 2.6.11 Colony morphology of <i>P. aeruginosa</i> PAO1 and mutants on Congo red plate.....	69
Fig. 2.6.12 The CAS plate assay.....	70
Fig. 2.6.13 The N-Acyl homoserine lactones (AHL) reporter plate bioassays	71
Fig. 2.6.14 A hypothetical model of the combination of the HptB-mediated phosphorelay and partner switching regulatory system.....	72

Fig. 3.6.1 Effects of glucose or galactose on *K. pneumoniae* CG43 S3 and $\Delta galU$ mutant using the disk diffusion assay 96

Fig. 3.6.2 Growth curve of *K. pneumoniae* CG43 S3 and the $\Delta galU$ mutant 97

Fig. 3.6.3 The growth curve and Live/Dead cell staining of the *K. pneumoniae* CG43 $\Delta galU$ mutant 98



Chapter 1

**Identification of amino acid residues important for the
phosphomannose isomerase activity of PslB in *Pseudomonas***



1.1 Abstract

Phosphomannose isomerase (PMI) plays a pivotal role in biosynthesis of GDP-mannose, an important precursor of many polysaccharides. We demonstrate in this study that *Pseudomonas aeruginosa* *pslB* encodes a protein with GDP-mannose pyrophosphorylase/PMI dual activities. The GDP-man PPase activity is Mg^{2+} -dependent, whereas the PMI activity is Co^{2+} -dependent and could be inhibited by GDP-mannose in a competitive manner. Furthermore, the PMI activity could be inactivated by 2, 3-butanedione suggesting the presence of a catalytic Arg residue. Site-specific mutations at R373, R472, R479, E410, H411, N433 and E458 increase the K_M approximately 8- to 20-fold. The PMI activity of PslB was completely diminished with a R408K or R408A, reflecting the importance of this residue in catalysis. The CD spectra of R408A, R408K and wild type PslB are nearly identical, indicating that there is nearly no alterations of their secondary structures. Overall, these results provide a basis for understanding the catalytic mechanism of PMI.

1.2 Introduction

Phosphomannose isomerase (PMI) catalyzes the reversible interconversion of fructose-6-phosphate (Fru-6-p) and mannose-6-phosphate (Man-6-p) (1). This reaction links Man-6-p into the mannose metabolism pathway resulting in the generation of GDP-mannose (GDP-Man), an important precursor of many nucleotide sugars such as GDP-rhamnose and

GDP-fucose, and for mannosylation of various bacterial structural components such as lipopolysaccharides and glycoproteins (2,3). PMI also plays an essential role in yeasts and therefore can be regarded as an appropriate target to combat both bacterial and mycotic infections (4).

PMI can be classified into three major types based on sequence similarity and domain organization (5,6). Type I PMIs are found in all eukaryotes including yeast *Candida albicans*, and certain bacteria including *Escherichia coli*. Type II PMIs are bifunctional enzymes possessing GDP-mannose pyrophosphorylase (GDP-Man PPase)/PMI dual activities and are primarily found in bacteria. Type III PMIs, first identified in *Rhizobium meliloti*, are evolutionally more distinct from the other two PMI types. The structural basis on how these seemingly unrelated proteins can catalyze an identical reaction is not clear.

Pseudomonas aeruginosa PAO1 contains three genes encoding a product homologous with the Type II PMI. These genes, designated *algA*, *wbpW* and *pslB*, are located individually within three distinct polysaccharide biosynthesis gene clusters (3). AlgA and WbpW have been shown to participate in the production of alginate and A-band lipopolysaccharide, respectively (3,7). The gene *pslB* is located in a 15-gene *psl* operon required for exopolysaccharide synthesis and biofilm formation (8,9). Whether PslB is indeed a bifunctional GDP-Man PPase/PMI has not been verified.

The major aim of this study is to address the structural-functional relationship of type II PMIs that is been largely unexplored. We have cloned, overexpressed, and characterized the PMI activity of PslB. This was followed by site-directed mutagenesis of conserved amino acid to identify important residues participating in the PMI activity.

1.3 Materials and Methods

1.3.1 Bacterial strains and growth conditions

E. coli XL-1 Blue was used for plasmid preparation and recombinant DNA manipulation. *E. coli* Nova Blue was used for protein expression. All bacteria used in this study were grown in Luria-Bertain medium containing ampicillin (100 µg/ml) or kanamycin (50 µg/ml), with 150 rpm shaking at 37°C. Bacteria strains and plasmids used in this study were listed in Table 1.5.1.

1.3.2 Expression and purification of PslB

E. coli Nova Blue harboring the *pslB* overexpression plasmid was grown in 200 ml Luria-Bertani broth supplemented with 50 µg/ml kanamycin and 100 µM isopropyl thio-β-D-galactopyranoside (IPTG) at 30°C with vigorous shaking. After 10 h, cells were collected by centrifugation at 3100 rpm for 15 min and washed with 20 mM Tris-HCl buffer pH 7.5. The pellets were resuspended in 20 mM Tris-HCl buffer and the bacteria were disrupted by sonication. Soluble proteins were separated from non-soluble proteins by

centrifugation at 14000 *g* for 20 min at 4°C. PslB was purified by nickel-charged affinity chromatography following the standard purification protocol (Novagen). The eluted protein was dialyzed against 20 mM Tris-HCl buffer (pH 7.5) to remove imidazole and the protein concentration was determined by the Bradford method with bovine serum albumin as a standard.

1.3.3 Determination of the enzyme activity

The PMI activity was determined in a 1-ml reaction mixture containing 50 mM Tris-HCl pH 7.0, 2 mM CoCl₂, 1 mM Man-6-p, 1 mM β-NADP, 5 U phosphoglucose isomerase and 5 U Glc-6-p dehydrogenase. The reduction of β-NADP was measured at 340 nm at 25°C using a spectrophotometer. The GDP-Man PPase activity was assayed in a reaction mixture containing GDP-Man, 5 mM sodium pyrophosphate, 2 mM MgCl₂, 2 mM 3-phosphoglycerate, 20 U glyceraldehyde-3-phosphate dehydrogenase and 10 U phosphoglycerate kinase. The decrease in NADH absorption at 340 nm was monitored by a spectrophotometer (10). Where indicated, 0.5 mM of Man-1-p, GDP-Man, GTP, UDP-Glc, UDP-Gal, ADP-Glc, TDP-Glc, UDP-GlcN, or sodium pyrophosphate was included in the PMI reaction to determine the inhibition activity of these compounds. For determination of the effects of divalent cation, PslB was dialyzed extensively in 20 mM Tris HCl pH 7.5, 140 mM NaCl and 1 mM EDTA. The enzyme activities were determined in the presence of 2 mM

chloride form divalent cation including CaCl₂, MnCl₂, MgCl₂, CoCl₂, NiCl₂ and ZnCl₂ (2,11).

1.3.4 Inactivation of PslB by 2, 3-Butanedione

PslB (3.2 mg/ml) was incubated with different concentrations of 2, 3-butanedione (150 mM borate buffer, pH 9.0) at 22°C in the dark for 0 to 60 min (12,13), then the excess 2,3-butanedione was removed by passing the reaction mixture through a Sephadex G-25 column (GE healthcare). The PMI activity was measured as described above.

1.3.5 Amino acid sequence alignment and site-directed mutagenesis

The multiple sequences alignment of several type II PMIs, including *Xanthomonas campestris* XanB (14), *Helicobacter pylori* HP0043 (2), *Gluconacetobacter xylinus* AceF (15), and *Vibrio vulnificus* YJ016 VV0352, were conducted by using the Vector NTI (Invitrogen) and the result is shown in Fig. 1.6.6. Site-specific mutations were performed using the QuikChange site-directed mutagenesis kit purchased from Stratagene. Oligonucleotide primer sequences are provided in Table 1.5.2.

1.3.6 Circular dichroism spectrum analysis

The CD spectra of wild type and mutant PslB were recorded by using a CD spectrophotometer (AVIV 62A PS) with 1-mm path length cell, 0.5 nm wavelength step, and an averaging time of 3×10^{-1} s. The protein samples were adjusted to 5 μM before

measurement. The CD spectra signals were collected from 190 nm to 260 nm in 20 mM Tris-HCl buffer at 25°C and averaged over three scans (16).

1.3.7 *In vivo* protein-protein interaction assay by GFP fragment reassembly

The vectors used in this study were provided by Dr. Lynne Regan of Yale University as a gift (17). Gene *algC* was cloned into pMRBAD-link-CGPF. Three GMP-PMIs (*algA*, *pslB* and *wbpW*) were cloned into pET11a-link-NGFP. The two plasmids were co-transformed into *E. coli* BL21 (DE3) and cultured in LB medium containing 100 µM ampicillin and 35 µM kanamycin at 37°C for 12 to 16 h. To perform the GFP reassembly, ten microliters of the overnight cultures were applied to the LB agar plates containing the same antibiotics, 100 µM IPTG and 0.05% arabinose. Then, the plates were statically incubated at 20°C for 2 to 3 days. The bacteria cells grown on the plates were re-suspended with PBS buffer and examined by fluorescence microscope. All images were captured with an upright microscope (BX-51; Olympus) connected with a CCD camera. The data were analyzed by using the SPOT Advanced Plus Imaging software (Sterling Heights, MI).

1.4 Result and Discussion

1.4.1 PslB possesses PMI and GDP-Man PPase activity

Based on the domain analysis result of InterProScan, the N-terminal domain of AlgA, PslB and WbpW is GMP domain and the C-terminal domain of those enzymes is the PMI

domain. Among the three PMI-GMPs in *P. aeruginosa* PAO1, the GDP-Man PPase/PMI activities of AlgA have been proved (7), whereas that of PslB has not been reported before. Therefore, we first examined whether PslB is indeed a GDP-Man PPase/PMI bifunctional enzyme. Recombinant PslB was purified from *E. coli* by nickel affinity chromatography and its purity was confirmed on a SDS-polyacrylamide gel (Fig. 1.6.1). Under the standard assay conditions, both GDP-Man PPase and PMI activities could clearly be detected for PslB. The K_M value of Man-6-p for the PMI activity was 1.18 mM, and the K_M of GDP-Man for GDP-Man PPase was 0.11 mM, both values are in good agreement with that reported for AlgA in *P. aeruginosa* 8822 (7). Bacteria with a large genome commonly harbor duplicated genes encoding functionally identical enzymes. For example, there are at least two UDP-Glc dehydrogenases in *P. aeruginosa* PAO1. The enzyme kinetic parameters and expression profiles are somewhat different for these UDP-Glc dehydrogenases that ensure the bacterium can adapt to broader environments (18). A similar mode of regulation may also occur for PMI. It has been demonstrated previously that a *P. aeruginosa* strain deficient in WbpW could not produce normal amounts of A-band lipopolysaccharide despite the presence of functional *algA* and *pslB* (3), suggesting that WbpW has distinct expression profiles or kinetic parameters from PslB and AlgA.

1.4.2 Divalent cation requirement for PslB

We measured the PMI and GDP-Man PPase activities of PslB at a fixed concentration (2 mM) of different divalent ions to evaluate cation dependence of the protein. The GDP-Man PPase of PslB could utilize different divalent metal ion with the highest activity in the presence of Mg^{2+} , followed by Co^{2+} , then Mn^{2+} (Table 1.5.3). The PMI activity of PslB showed high specificity to Co^{2+} , yielding about 3-fold higher activity than that observed with Mn^{2+} (Table 1.5.3). Other divalent cations, including Mg^{2+} , Zn^{2+} , Ca^{2+} , and Ni^{2+} , could not serve effectively as a cofactor for the PMI activity of PslB, consistent with several previous reports (2,7,19). The optimal Co^{2+} concentration for the PMI was 0.2 mM, which yielded an activity approximately 1.5 fold higher than that of 2.0 mM (Fig. 1.6.2). Mg^{2+} at 2.0 mM showed little interference on the PMI activity in the presence of either 0.2 mM or 2.0 mM Co^{2+} (Fig. 1.6.3), indicating that Co^{2+} is capable of functioning as a cofactor for the PMI in bacterial cells which commonly contain millimolar Mg^{2+} (20). Interestingly, both PMI and GDP-Man PPase activities in PslB could not be activated in $ZnCl_2$ despite the fact that the protein contains a zinc-binding sequence $Q^{403}XH^{405}$ (X represents any amino acid), a feature that is also present in type I PMIs (6).

1.4.3 The PMI activity of PslB is inhibited by GDP-Man

Several molecules participating in GDP-Man biosynthesis and six nucleotide sugars commonly found in bacteria were tested for their effects on the PMI activity of PslB. At 0.5

mM, only GDP-Man significantly inhibited the PMI activity, which decreased to approximately 47% than that observed for the control (Table 1.5.4). Further investigation on the GDP-Man inhibition type demonstrated a competitive inhibition (Fig. 1.6.4) indicating that the GDP-Man biosynthesis pathway is well controlled by the end product, GDP-Man, as also is found for *Helicobacter pylori* PMI (2). A slight deviation of the 250 μ M GDP-Man lines from the other three lower concentration lines was observed suggesting that the inhibition is attenuated in higher concentrations of the inhibitor (GDP-man). The results suggest that the mannose group in GDP-Man competes with Man-6-p at the PMI active site to regulate the mannose utilization in *P. aeruginosa* PAO1.

1.4.4 An Arg residue participates in the *P. aeruginosa* PMI activity

To identify if PslB is a useful target to combat *P. aeruginosa* infections, it is essential to locate the active site participating in the PMI catalytic activity. It has been shown previously that R304 is an active site residue in a type I PMI of *C. albicans* (21). Although type I and type II PMI share low amino acid sequence homology, their catalytic mechanisms may be similar. To determine whether an Arg is involved in the PMI activity of PslB, this study utilized 2, 3-butanedione to modify Arg in the protein and the PMI activity was determined (22). Figure 1.6.5 shows that the PMI activity decreased with increasing 2, 3-butanedione concentrations and the modification time, revealing that at least one Arg residue in PslB is

involved in PMI catalysis.

1.4.5 Arg408 substitutions abolished the PMI activity of PslB

Based on sequence alignment with other type II PMI, R373, R408, R472 and R479 were chosen and changed to Ala by site-directed mutagenesis. In addition, this study adopted the molecular structure information of *Pyrobaculum aerophilum* bifunctional enzyme phosphoglucose/phosphomannose isomerase (PaPGI/PMI) (23), and selected E410, H411, N433 and E458 for site-directed mutagenesis. The kinetic constants of the wild type and mutant PslB are shown in Table 1.5.5. Substitution of Arg at position 408 to either a Lys or an Ala abolished nearly all of the PMI activity. Other mutant proteins still retained PMI activities and the K_M values were 8- to 20- fold larger compared to those values observed for wild type. The CD spectra (Fig. 1.6.7) of R408A, R408K and wild type PslB are nearly identical, all showing a minimum point at 208 nm and 222 nm, a typical spectrum of high α -helix content protein. The data indicate that there is no major alteration of the secondary structures of the mutant proteins.

Overall, the results indicate that R408, which lies within the well-conserved motif shared by most, if not all, type II PMI is an important residue for PMI catalysis. The residue is likely to participate in the interconversion of sugar moieties by providing the binding of the sugar phosphate group or forming the hydrogen bond of sugar hydroxyl group, stabilizing the

binding between substrates and enzymes.

1.4.6 The R408 mutations did not affect GDP-Man PPase activity of PslB

The fusion of the GDP-Man PPase and PMI domains in the type II PMI implies these two activities may interact with each other. The GDP-Man PPase activity of the PslB deficient in PMI activity was determined and no difference was observed. The K_M values of wild type, R408A and R408K were 0.068 mM, 0.072 mM and 0.078 mM, respectively. The similar K_M values of wild type and mutant PslB provide strong evidence that PMI and GDP-Man PPase are actually two independent domains.

1.4.7 The GMP domain and the PMI domain influence the activities of each other

Based on the domain analysis result of InterProScan, the N-terminal domain (9-297 a.a.) of PslB is GMP domain and the C-terminal domain (325-475 a.a.) of PslB is the PMI domain. Although previous literatures also reported that Type II PMIs own two independent domains (2,6,14,24,25), no article has reported if the PMI and GDP-Man PPase activities would be influenced when Type II PMIs lacked the PMI domain or the GMP domain. To further understand if the separate domains influence the activities of each other, the GMP domain and the PMI domain were cloned into the protein expression vector individually. According to the amino acid sequence alignment result reported by Dr. Leitao J. H. and colleagues (25), the *pslB* DNA fragment of 1-951 (PslB¹⁻³¹⁷) and 1-1086 (PslB¹⁻³⁶²) were cloned into pET30a

to constructed a C-terminal His tag fusion protein. To increase the protein solubility, the *pslB* DNA fragment of 930-1464 ($\text{PslB}^{310-488}$) was cloned into pGEX-5X-1 to constructed an N-terminal GST tag fusion protein. As shown in Fig. 1.6.8, PslB and PslB^{1-362} display the GDP-man PPase activities, but PslB^{317} donot. The K_M values (GDP-man) of PslB and PslB^{1-362} were 0.089 mM and 0.078 mM, respectively. The similar K_M values of PslB and PslB^{1-362} indicated that the GDP-man PPase activity would not be influenced when lacking the C-terminal domain from 363-488. Interestingly, GDP-man PPase activity was lost when lacking the fragment residues from 317-362 predicted to be belonged to the PMI domain (25). Taking those results together, the complete GDP-man PPase activity still required the existence of partial PMI domain. In the case of PMI domain, the time dependent profile (Fig. 1.6.9) displayed that the PMI activity of $\text{PslB}^{310-488}$ were relatively poor than that of PslB . The K_M (Man-6-p) values of PslB and $\text{PslB}^{310-488}$ were 0.92 mM and 2.89 mM, respectively. The K_M value of $\text{PslB}^{310-488}$ decreased 3 folds, indicating that the N-terminal domain is also important for the complete PMI activity. PslB^{1-362} had no PMI activity, revealing that the C-terminal domain was important for PMI activity. May T. B et al. made the similar conclusion using chymotrypsin digestion to produce a 1-kDa C-terminal deletion of AlgA. The chymotrypsin digestion of AlgA retained 81% GMP activity but lost 92% PMI activity (24). In summary, PslB was indeed divided into two independent domains, but they influence

the activities of each other. This result may explain why the two domains fused together.

1.4.8 PslB cannot form protein complex with AlgC

Many of the bifunctional enzymes have been discovered that they catalyze the continuous reactions in the biosynthesis pathway. For example, tryptophan synthase which is commonly found in bacteria, fungi and plants is a bifunctional enzyme that catalyzes the final two steps in the biosynthesis of tryptophan (26). Some bifunctional enzyme, such as PMI-GMPs, catalyzes the noncontinuous reactions. PMI-GMPs participates the first and third steps of the GDP-mannose biosynthesis pathway ($\text{Fru-6-p} \xleftarrow{\text{PslB (PMI)}} \text{Man-6-p} \xleftarrow{\text{AlgC}} \text{PMM} \rightarrow \text{Man-1-p} + \text{GTP} \xleftarrow{\text{PslB (GMP)}} \text{GDP-man} + \text{ppi}$). It is reasonable to speculate that PMI-GMPs are associated with PMM (AlgC) by protein-protein interaction to form the channeling of Fru-6-p to GDM-man (7,27). If PMI-GMP form a protein complex with PMM, it could increase the reaction efficiency by avoiding the loss of any reaction intermediates. In order to clarify this speculation, three PMI-GMPs (*algA*, *pslB* and *wbpW*) and *algC* in *P. aeruginosa* PAO1 were cloned into pET11a-link-NGFP and pMRBAD-link-CGFP respectively for performing the GFP fragment reassembly assay. The bacteria cells harboring the two plasmids were examined by a fluorescence microscope. Only the bacteria harboring pET11a-Z-NGFP and pMRBAD-Z-CGPF displayed the green fluorescence emission (28). None of the bacterial cells containing the PMI-GMP and PMM plasmid pairs emitted

fluorescence signals. Our result does not prove if the PMI-GMPs form protein complex with

PMM or not.



1.5 Tables

Table 1.5.1 Bacterial strains and plasmids used in this study

Strains or Plasmids	Descriptions	Refs. or source
Strains		
<i>E. coli</i>		
BL21 (DE3)	F ⁻ <i>ompT hsdS_B(r_B⁻, m_B⁻) gal dcm</i> (DE3)	Invitrogen
Nova Blue	<i>endA1 hsdR17(r_{K12}⁻ m_{K12}⁺) supE44 thi-1 recA1 gyrA96 relA1 lac F'[proA⁺B⁺lacI^qZΔM15::Tn10]</i> (Tet ^R)	Novagen
XL-1 Blue	<i>recA1 endA1 gyrA96 thi-1 hsdR17 supE44 relA1 lac [F' proAB lacI^qZΔM15 Tn10]</i> (Tet ^r)	Stratagene
Plasmids		
pET28a	Km ^r , His tag protein expression vector	Novagen
pET30a	Km ^r , His tag protein expression vector	Novagen
pGEX-5X-1	Ap ^r , GST tag protein expression vector	GE Healthcare
pET11a-Z-NGFP	Ap ^r , plasmid vector that expresses a fusion of an antiparallel leucine zipper peptide to NGFP	(29)
pET11a-link-NGFP	Ap ^r , plasmid vector designed for fusion of a target protein to the N-terminal fragment of GFP (1-157)	(29)
pMRBAD-link-CGFP	Km ^r , plasmid vector designed for fusion of a target protein to the C-terminal fragment of GFP (158-238)	(29)
pMRBAD-Z-CGFP	Km ^r , plasmid vector that expresses a fusion of an antiparallel leucine zipper peptide to CGFP	(29)
pETPslB	Km ^r , a fragment containing entire <i>pslB</i> (PA2232) coding region cloned into pET30a (NdeI&EcoRI)	this study
pHL17	Km ^r , <i>pslB</i> with the mutation E410A cloned into pET30a	this study
pHL18	Km ^r , <i>pslB</i> with the mutation E411A cloned into pET30a	this study
pHL19	Km ^r , <i>pslB</i> with the mutation E433A cloned into pET30a	this study
pHL20	Km ^r , <i>pslB</i> with the mutation E458A cloned into pET30a	this study
pHL25	Km ^r , <i>pslB</i> with the mutation E373A cloned into pET30a	this study
pHL26	Km ^r , <i>pslB</i> with the mutation E472A cloned into pET30a	this study
pHL27	Km ^r , <i>pslB</i> with the mutation E479A cloned into pET30a	this study

pHL30	Km ^r , <i>pslB</i> with the mutation E408A cloned into pET30a	this study
pHL31	Km ^r , <i>pslB</i> with the mutation E408K cloned into pET30a	this study
pHL24	Km ^r , a fragment containing entire <i>pslB</i> (PA2232) coding region cloned into pET30a (NdeI&HindIII)	this study
pHL29	Km ^r , a fragment containing residues 280-488 of PslB coding region cloned into pET30a	this study
pHL75	Km ^r , a fragment containing residues 1-362 of PslB coding region cloned into pET30a	this study
pHL76	Km ^r , a fragment containing residues 1-317 of PslB coding region cloned into pET30a	this study
pHL77	Km ^r , a fragment containing residues 310-488 of PslB coding region cloned into pET30a	this study
pHL78	Km ^r , a fragment containing residues 1-362 of PslB coding region cloned into pET28a	this study
pHL79	Km ^r , a fragment containing residues 1-317 of PslB coding region cloned into pET28a	this study
pHL80	Km ^r , a fragment containing residues 310-488 of PslB coding region cloned into pET28a	this study
pHL81	Ap ^r , a fragment containing residues 310-488 of PslB coding region cloned into pGEX-5X-1	this study
pHL87	Km ^r , a fragment containing entire <i>algA</i> (PA3551) coding region cloned into pET30a	this study
pHL88	Km ^r , a fragment containing entire <i>wbpW</i> (PA5452) coding region cloned into pET30a	this study
pHL89	Km ^r , a fragment containing entire <i>algC</i> (PA5322) coding region cloned into pET30a	this study
pHL90	Ap ^r , a fragment containing entire <i>algC</i> (PA5322) coding region cloned into pGEX-5X-1	this study
pHL91	Km ^r , a fragment containing entire <i>algC</i> (PA5322) coding region cloned into pMRBAD-link-CGFP	this study
pHL92	Ap ^r , a fragment containing entire <i>algA</i> (PA3551) coding region cloned into pET11a-link-NGPF	this study
pHL93	Ap ^r , a fragment containing entire <i>pslB</i> (PA2232) coding region cloned into pET11a-link-NGPF	this study
pHL94	Ap ^r , a fragment containing entire <i>wbpW</i> (PA5452) coding region cloned into pET11a-link-NGPF	this study

Table 1.5.2 Primers used in this study

Primer name	Primer sequence (5'→3')	Descriptions
Or488-F1	CATATGAACGCCGTCGCCCCGCTG	clone <i>pslB</i> into pET30a
Or488-R1	AAGCTTGGCTTTCTTCTCGTCGCTGG	clone <i>pslB</i> and PslB ²⁸⁰⁻⁴⁸⁸ into pET30a
R373A-F2	CACCGCACGGTCAGCGCGCCCTGG	<i>pslB</i> - pET30a-R373A mutant
R373A-R2	CCAGGGCGCGCTGACCGTGCGGTG	<i>pslB</i> - pET30a-R373A mutant
R408AF1	TGCACCACCATGCCAGCGAGCACTGGAT	<i>pslB</i> - pET30a-R408A mutant
R408AR1	ATCCAGTGCTCGCTGGCATGGTGGTGCA	<i>pslB</i> - pET30a-R408A mutant
R408KF1	ATGCACCACCATAAGAGCGAGCACTGGAT	<i>pslB</i> - pET30a-R408K mutant
R408KR1	ATCCAGTGCTCGCTCTTATGGTGGTGCAT	<i>pslB</i> - pET30a-R408K mutant
IsoE410A-F1	CATCGCAGCGCGCACTGGATCGTGGTC	<i>pslB</i> - pET30a-E410A mutant
IsoE410A-R1	GACCACGATCCAGTGCGCGCTGCGATG	<i>pslB</i> - pET30a-E410A mutant
IsoH411A-F1	CATCGCAGCGAGGCCTGGATCGTGGTC	<i>pslB</i> - pET30a-H411A mutant
IsoH411A-R1	GACCACGATCCAGGCCTCGCTGCGATG	<i>pslB</i> - pET30a-H411A mutant
IsoN433A-F1	CTCCTCAACACCGCGGAATCCACCTTCATCC	<i>pslB</i> - pET30a-N433A mutant
IsoN433A-R1	GGATGAAGGTGGATTCCGCGGTGTTGAGGAG	<i>pslB</i> - pET30a-N433A mutant
IsoE458A-F1	GGTGATGATCGCGGTACAGAGCGGCGAG	<i>pslB</i> - pET30a-E458A mutant
IsoE458A-R1	CTCGCCGCTCTGTACCGCGATCATCACC	<i>pslB</i> - pET30a-E458A mutant
R472A-F1	GGACGACATCGTCGCGTTCAACGACATC	<i>pslB</i> - pET30a-R472A mutant
R472A-R1	GATGTCGTTGAACGCGACGATGTCGTCC	<i>pslB</i> - pET30a-R472A mutant
R479A-F1	CGACATCTACGGTGCCGCCCCCGCCAGC	<i>pslB</i> - pET30a-R479A mutant
R479A-R1	GCTGGCGGGGGCGGCACCGTAGATGTCC	<i>pslB</i> - pET30a-R479A mutant
PMI-f3	CATATGAGCGACATCGGCTCCTGGCA	clone PslB ²⁸⁰⁻⁴⁸⁸ into pET30a
GMP-F	TTACATATGAACGCCGTCGCCCCGCTG	clone PslB ¹⁻³¹⁷ and PslB ¹⁻³⁶² into pET vector

GMP317NR	ATTCTCGAGTCACGAATCGATGTAGCAGTTGC	clone <i>PsIB</i> ¹⁻³¹⁷ into pET-28a
GMP317CR	AATCTCGAGCGAATCGATGTAGCAGTTGCTG	clone <i>PsIB</i> ¹⁻³¹⁷ into pET-30a
GMP362NR	AATCTCGAGTCAGTGGCCGCGACGCTTG	clone <i>PsIB</i> ¹⁻³⁶² into pET-28a
GMP362CR	AATCTCGAGGTGGCCGCGACGCTTGAG	clone <i>PsIB</i> ¹⁻³⁶² into pET-30a
PMI-F	ATTCATATGGTCAGCAACTGCTACATCGATTTCG	clone <i>PsIB</i> ³¹⁰⁻⁴⁸⁸ into pET vector and pGEX-5X-1
PMI-NR	AATGCGGCCGCTCAGGCTTTCTTCTCGTC	clone <i>PsIB</i> ³¹⁰⁻⁴⁸⁸ into pET-28a
PMI-CR	AATGCGGCCGCGGCTTTCTTCTCGTC	clone <i>PsIB</i> ³¹⁰⁻⁴⁸⁸ into pET-30a
PMI GST F	GCGGATCCACGTCAGCAACTGCTACATCG	clone <i>PsIB</i> ³¹⁰⁻⁴⁸⁸ into pGEX-5X-1
3551 F	GCCATATGATCCCAGTAATCCTTTC	clone <i>algA</i> into pET30a
3551 R	AATCTCGAGGCGGCTGCCGGCGACC	clone <i>algA</i> into pET30a
5452 F	AATCATATGCTGATTCCCGTGGTG	clone <i>wbpW</i> into pET30a
5452 R	AATGCGGCCGCGACCACCTGCCGTA	clone <i>wbpW</i> into pET30a
PMM-F	AACATATGAGCACTGCAAAAGCACCGACG	clone <i>algC</i> into pET30a and pGEX-5X-1
pMM-R	AAGCGGCCGCGAAGGGCACGGCAGCGAGG	clone <i>algC</i> into pET30a
pMMgst-F	AAGGATCCCCATGAGCACTGCAAAAGCACCGACG	clone <i>algC</i> into pGEX-5X-1
AN-F	AACTCGAGCATGATCCCAGTAATCCTTTC	clone <i>algA</i> into pET11a-link-NGFP
AN-R	ATGGATCCTCAGCGGCTGCCGGC	clone <i>algA</i> into pET11a-link-NGFP
BN-F	GCATGAACGCCGTCGCCC	clone <i>psIB</i> into pET11a-link-NGFP
BN-R	ATGGATCCTCAGGCTTTCTTCTCGTC	clone <i>psIB</i> into pET11a-link-NGFP
WN-F	GCATGCTGATTCCCGTGGTGCT	clone <i>wbpW</i> into pET11a-link-NGFP
WN-R	ATGGATCCTCAGACCACCTGCC	clone <i>wbpW</i> into pET11a-link-NGFP
MC-F	AATCATGACTATGAGCACTGCAAAAGCACCG	clone <i>algC</i> into pMRBAD-link-CGFP
MC-R	ACGTCCCGAAGGGCACGGGCAG	clone <i>algC</i> into pMRBAD-link-CGFP

Table 1.5.3 Divalent cation effects on PslB

Divalent cation	Relative activity (%) ^b	
	PMI	GDP-Man PPase
Control ^a	9.4 ± 3.6	ND ^c
MgCl ₂	10.1 ± 0.3	100
CaCl ₂	6.1 ± 2.7	38.8 ± 0.1
MnCl ₂	31.7 ± 1.8	38.6 ± 2.0
CoCl ₂	100	86.5 ± 1.3
NiCl ₂	5.5 ± 0.6	9.9 ± 0.2
ZnCl ₂	2.6 ± 0.4	4.7 ± 0.2

^aControl reaction was assayed without adding any divalent cation.

^bThe relative activity was compared to the optimal activity of the divalent cation set as 100% for Co²⁺, in case of PMI and Mg²⁺, in case of GDP-Man PPase.

^cND, Not determined.



Table 1.5.4 Effects of potential inhibitors on the PMI activity

Potential inhibitor ^a	Relative activity (%) ^b
Control	100 ± 2.2
GTP	106.4 ± 2.4
PPi	120.2 ± 3.5
Man-1-P	77.8 ± 2.5
GDP-Man	46.9 ± 3.9
UDP-GlcN	93.3 ± 3.8
UDP-Gal	105.8 ± 6.9
UDP-Glc	87.4 ± 1.4
ADP-Glc	81.9 ± 3.6
TDP-Glc	78.8 ± 1.2

^aThe PMI activity was analyzed in the presence or absence of 0.5 mM potential inhibitors.

^bThe relative activity was calculated by comparing with control, whose activity was set as 100%



Table 1.5.5 PMI kinetic parameters of the wild type or mutant PslB

	K_M (Man-6-p, mM)	K_{cat} (s^{-1}) ^a	K_{cat}/K_M ($mM^{-1}s^{-1}$)
WT	1.18	1.38	1.17
R373A	15.9	0.75	0.05
R408A	ND ^b	ND	ND
R408K	ND	ND	ND
E410A	9.04	2.63	0.29
H411A	16.26	4.41	0.27
N433A	12.92	3.5	0.27
E458A	12.36	3.25	0.26
R472A	23.12	0.25	0.01
R479A	12.28	0.54	0.04

^a K_{cat} was calculated from the equation $V_{max}=K_{cat} \times [E_o]$, where E_o is the molar concentration of PslB. The results are the average of three independent experiments.

^bND, not detected.



1.6 Figures

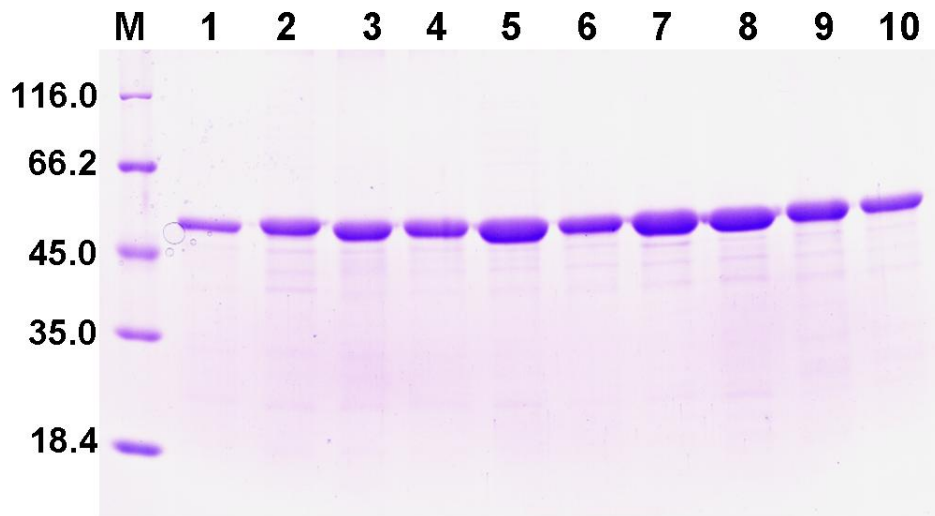
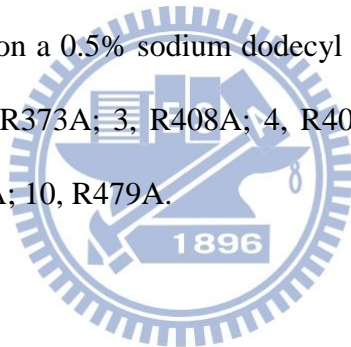


Fig. 1.6.1 Protein purity of wild type and mutant PslB

The samples were resolved on a 0.5% sodium dodecyl sulfate-12.5% polyacrylamide gel. Lanes 1, wild type; 2, R373A; 3, R408A; 4, R408K; 5, E410A; 6, H411A; 7, N433A; 8, E458A; 9, R472A; 10, R479A.



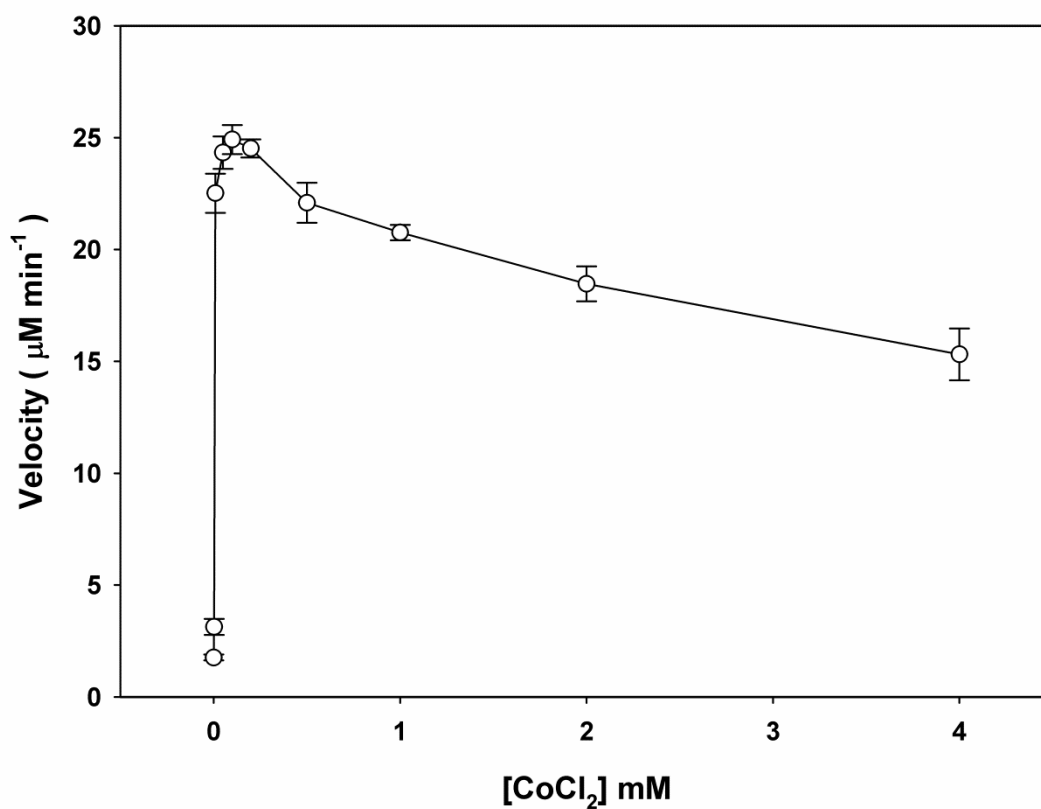


Fig. 1.6.2 Effects of various concentrations of cobalt ion on the PMI activity

The concentrations used in this study were: 0 mM, 0.002 mM, 0.01 mM, 0.05 mM, 0.1 mM, 0.2 mM, 0.5 mM, 1 mM, 2 mM and 4 mM (the X axis). The Y axis is the formation velocity ($\mu\text{M min}^{-1}$) of β -NADPH representing the PMI activity.

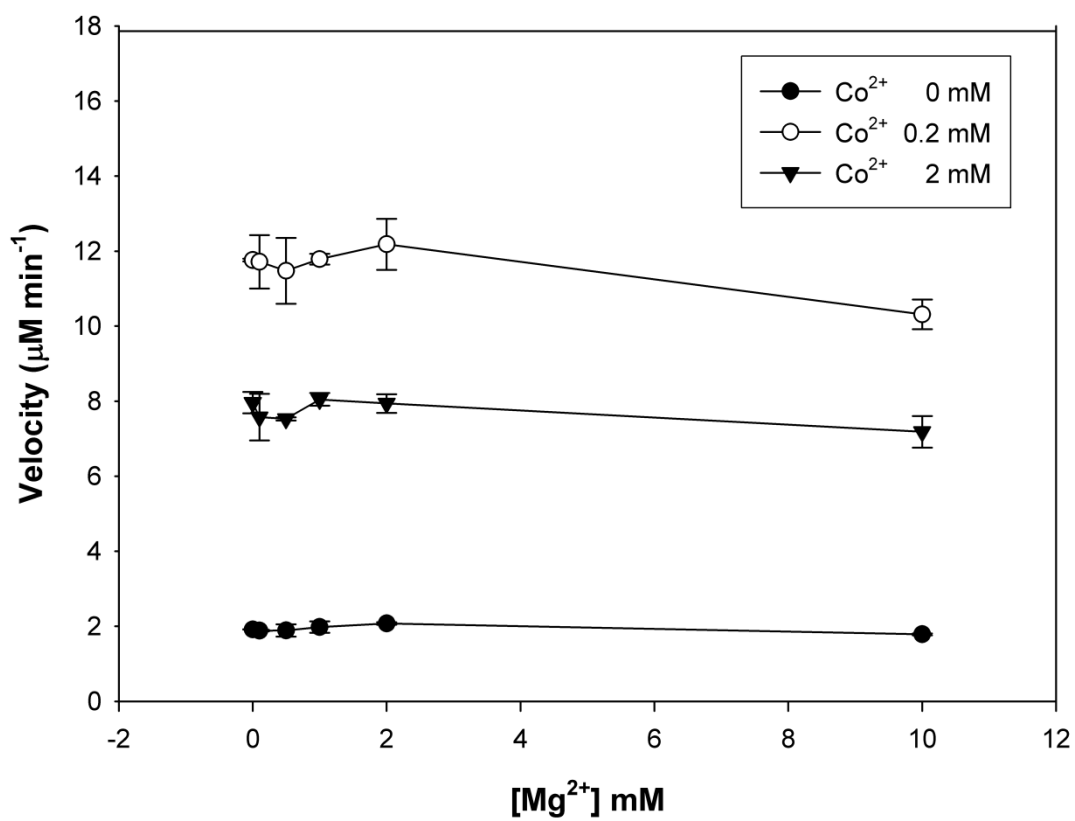


Fig. 1.6.3 Effects of Mg²⁺ on the PMI activity of PslB

The assay was performed in the absence (●), and presence of 0.2 mM (○) or 2.0 mM (▼) Co²⁺.

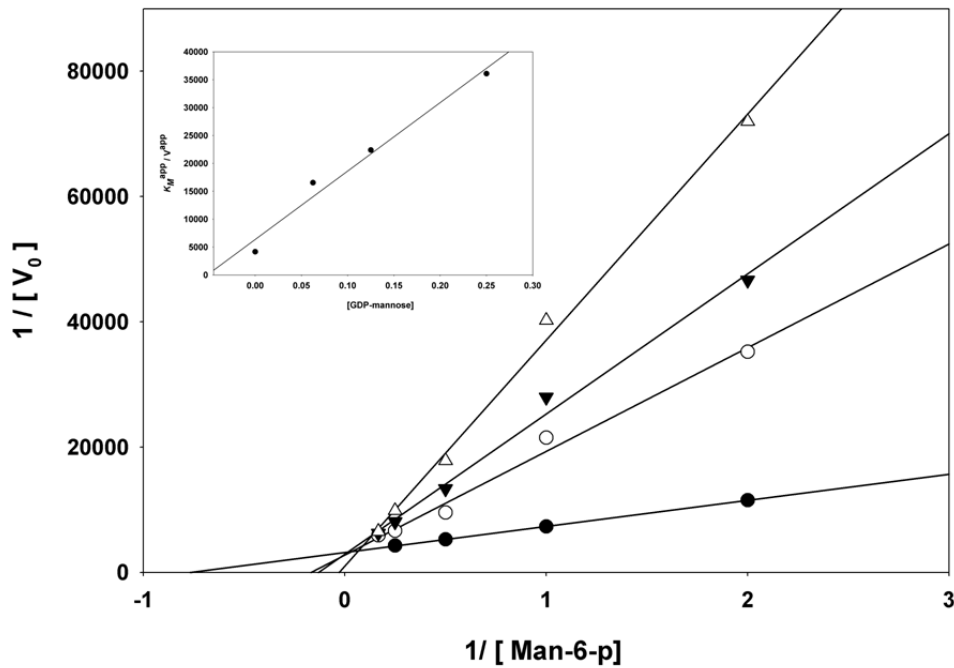


Fig. 1.6.4 Double reciprocal plot at various GDP-Man concentrations

The GDP-Man concentrations shown are \bullet , 0 μM ; \circ , 62.5 μM ; \blacktriangledown , 125 μM ; Δ , 250 μM . The four lines intersect in the vertical axis representing that they have the same V_{max} . The slopes (slope = K_M / V_{max}) of the lines increase in the present of higher concentration of GDP-Man, indicating that their K_M values increase. Overall, this plot shows a competitive inhibition of GDP-Man for PMI activity. The inset illustrates the reciprocal slopes from Fig. 1.6.4 versus GDP-Man concentrations.

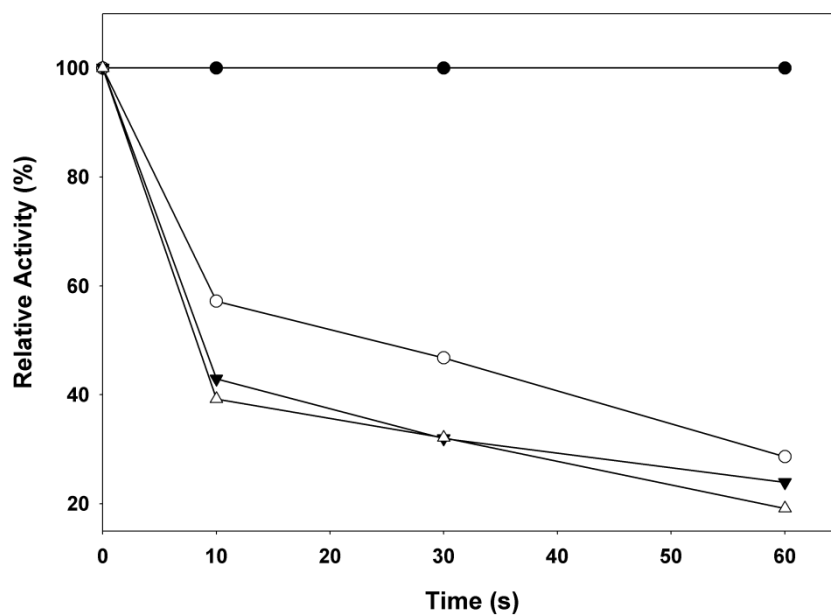
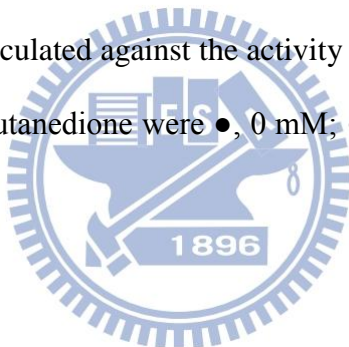


Fig. 1.6.5 Inactivation of PslB by 2, 3-butanedione

Relative activity (%) was calculated against the activity without 2, 3-butanedione. The final concentration of 2, 3-butanedione were ●, 0 mM; ○, 20 mM; ▼, 40 mM; ▽, 80 mM.



```

PslB (297) NGNQVRGESVVLHDVSNICYIDSEPKRLVGAAGVHDLIIIVDTFPDALLVADAARSQDVKFFVAQELKRR
AceF (309) AGNVVVGDVVLEQSHNCYVRSEGMLTAVAGLTDIVLVVTSDAVLAHHRDYAQDVSAVLSQLKMA
HP0043 (284) NVSLNQTPEVFAKESENNLFVFS-HKVSALLGVENLAVIDTKDALLIAHKDKAKDLKALVNEVETN
ManC (298) DGNVLQGRVINKGSRNICYLRSEHRLVVGLGVENLVVVETDDAVLIADRSKAQEIKSVVQLQLEAD
VV0352 (284) NGNAFVGDVKSVDTKNTLVFAKDKLVTTVGVEDLVIVNTKDVAVLVAHKDESQKVKKEIVSOLKAD
XanB (285) CGNAHHDVVIQLDCKNTYAYG-SRLIAMVGLLENVVVETDDAVLVGHRDRIQEVKEVVSQIKSA

```

```

PslB (361) GHDAFRLHRTVSRPWGTYTVLEEGRRFKIKRIVWRBKASLSLQMHHRSEHWIIVVSGMALWENG
AceF (373) RRTEAEIHNRCYRPWGFYEGLIQGERFQVKRIVWYEGKLSLQRHFRHAEHWVVVSGTAVVTRN
HP0043 (347) NQELLQTHTKVYRPWGSYEVLHESGCKYVKILEVWRBNARLSLQKHFRSEHWVVISGMASWELD
ManC (362) GSPEGKARHKIYRPWGAATGVTGEGNRWQVKRISVNEGSSLSLQMHHRHAEHWVVVKGTAIVVERD
VV0352 (348) ERSEVTFHREVYRPWGGKYSVDNGERFQVKRITWRBGAKLSVOMHHRHAEHWIIVVSGTAKVOID
XanB (348) GRSEATWHRKVYRPWGAIDSIDMGQRVQVKRITWRBGATLSLQMHHRHAEHWIIVVSGTAEVTRG

```

```

PslB (425) EREFLLNTNESTFIPAGHSRLSNFGIIDLVMIEVQSGGEYLGEDDIVRFENDIYGRAPASDEKKA
AceF (437) EEKLMLOENESVYIPLGCMHRLSNFGRIPLTLEIYVQSGGEYLGEDDIVRFEDTYGRQ-----
HP0043 (411) HQLFELQANESTYIIPKNTLHRLSNFYGKIPLIIEVQVSGEYVGEDDIVRIDDFNRQNQNA----
ManC (426) GDQLVGENCSTYIIPMGCKHRLSNFGRIPEVLEIYVQSGGEYLGEDDIVRFEDRYGRSDQRIPVQS
VV0352 (412) DTEQFVTENESVYIIPITAVHADENFPGKVDLELEIYVQSGSYLGEDDIVRFEDRYGRVKD-----
XanB (412) EEVLLLTENESTYIIPLGVTHRLSNFEGKLPLELEIYVQSGSYLGEDDIVRFEDTYGR-----

```

Fig. 1.6.6 Amino acid sequence alignment of GDP-Man PPase /PMIs

Only the C-terminal PMI comprising regions of the proteins are shown. The GenBank accession numbers for these proteins are: *P. aeruginosa* PAO1 PslB, NP_250922; *X. campestris* XanB, YP_933589; *Helicobacter pylori* 26695 HP0043, NP_206844; *Gluconacetobacter xylinus* AceF, CAA72316; *Vibrio vulnificus* YJ016 VV0352, NP_933145.

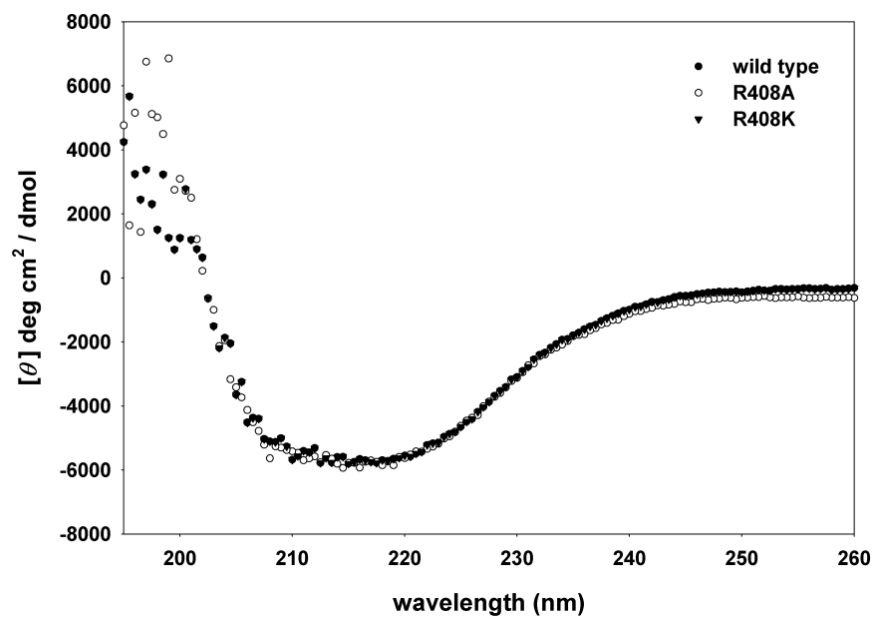
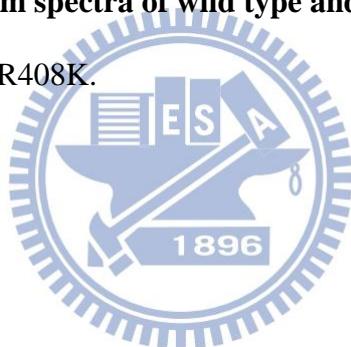


Fig. 1.6.7 Circular dichroism spectra of wild type and mutant PslB

●, wild type; ○, R408A; ▼, R408K.



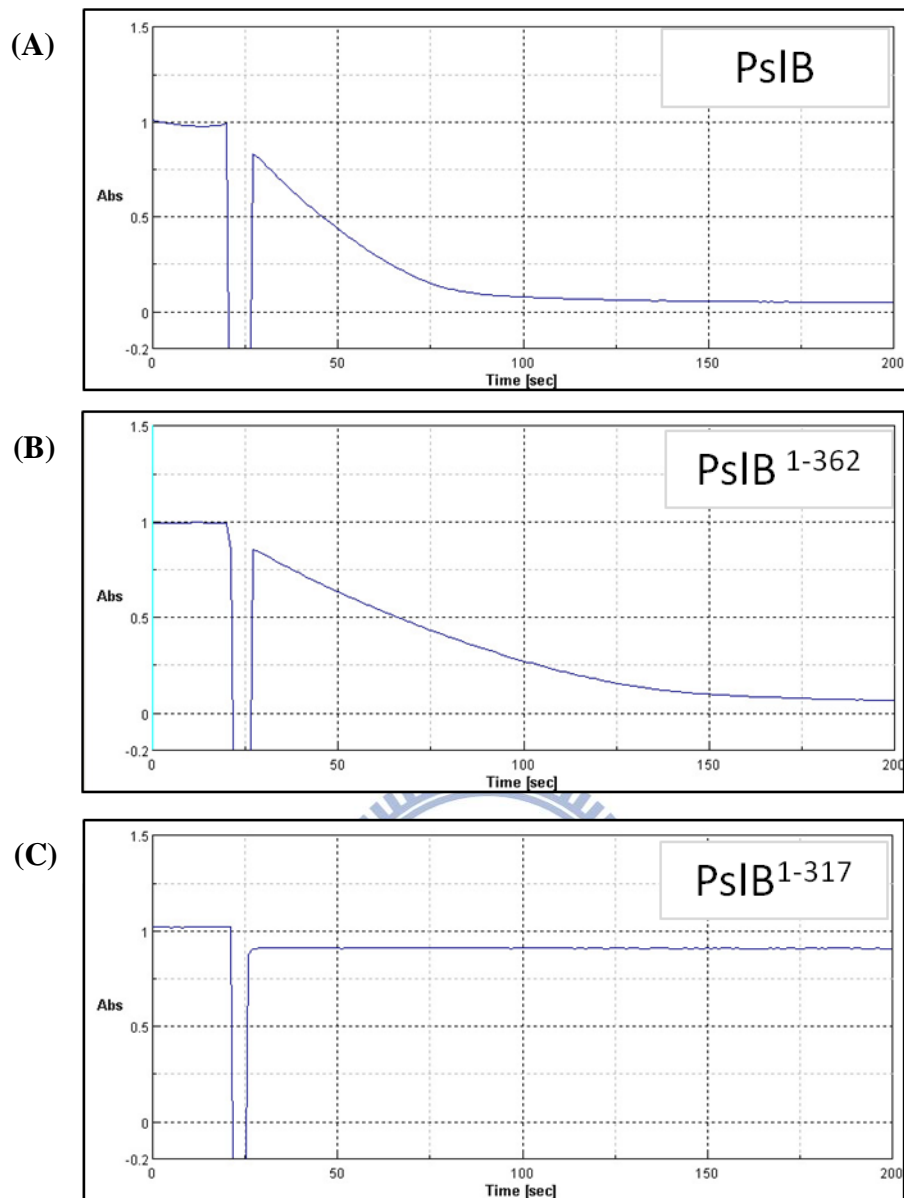


Fig. 1.6.8 Time dependent profiles of the GDP-man PPase activity assay

The profiles exhibited the GDP-Man PPase activity of (A) full length of PsIB (B) the N-terminal GMP region including partial of Man-6-p isomerase domain (C) the N-terminal GMP region of PsIB. The Y axis is the absorption values of β -NADH representing the GDP-man PPase activity.

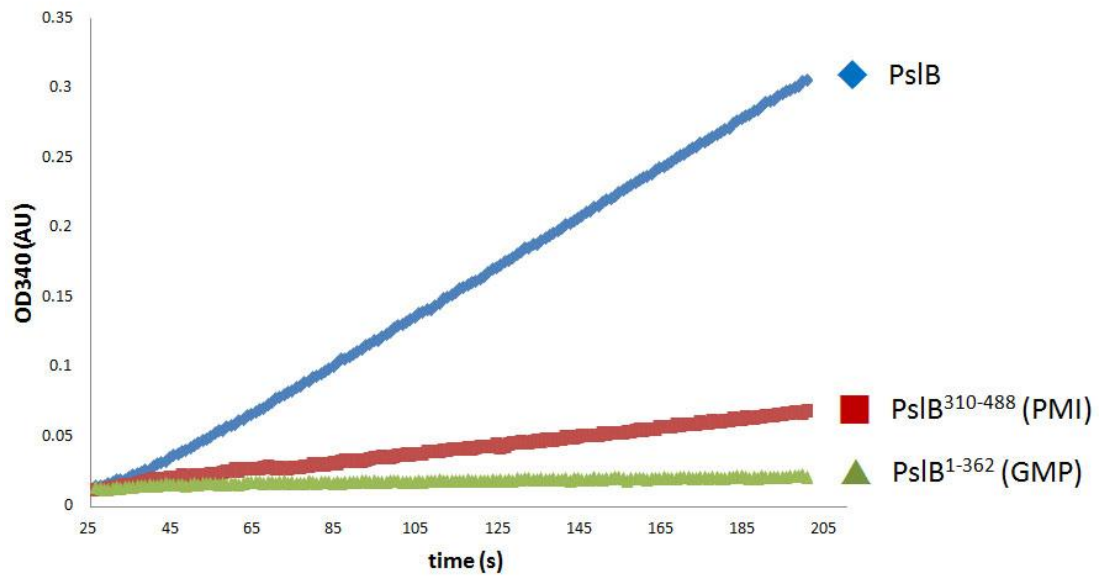
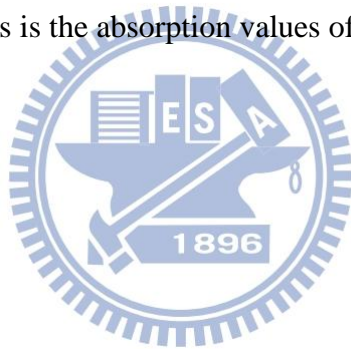


Fig. 1.6.9 Time dependent profile of PMI activity assay

This profile showed the PMI activity of full length PslB was better than that of the PMI domain only. The Y axis is the absorption values of β -NADPH representing the PMI activity.



Chapter2

Characterization of PA3346, a response regulator with dual

Ser protein phosphatase and kinase activities in *P.*

***aeruginosa* PAO1**



2.1 Abstract

Our laboratory has previously observed that the HptB-mediated phosphorelay pathway plays an important role in swarming phenotype and biofilm formation in *P. aeruginosa* PAO1. Upon activation by an environmental stress, sensor kinase (PA1611, PA1976 and PA2824) autophosphorylates itself and then transfers a phosphoryl group to HptB, which then relays the signal to response regulator PA3346. The phosphorylation on PA3346 N-terminal receiver domain results in an increase in its Ser protein phosphatase activity leading to dephosphorylation of the putative anti-sigma factor antagonist PA3347. While the target phosphorylation site on PA3347 has been shown to be located at Ser-56, the corresponding Ser protein kinase and anti-sigma factor remain elusive. Protein domain analysis revealed that the C-terminal region of PA3346 (PA3346^{L408-A571}) contains conserved domains similar to the serine protein kinase/anti-sigma factor SpoIIAB in *Bacillus subtilis*. Thus, we proposed that PA3346-PA3347 forms a partner-switching regulatory module as observed for SpoIIE-SpoIIAB-SpoIIAA in *B. subtilis*. Using standard recombinant DNA techniques and protein purification procedures, we have cloned and purified PA3346^{L408-A571} and PA3347-GST for *in vitro* phosphorylation and GST pull-down assays. The results of *in vitro* phosphorylation assay clearly demonstrated that PA3346^{L408-A571} possesses a kinase activity toward PA3347 and the activity is divalent cation, especially Mg²⁺, Ca²⁺ and Mn²⁺, dependent. The PA3347-S56A mutant protein could not serve as a substrate for the kinase. In the GST pull-down assay, PA3346^{L408-A571} could be co-eluted with PA3347-GST in the presence of ADP. As for the GFP fragment reassembly assay, the bacterial cells harboring the plasmids of PA3346^{L408-A571}-CGFP and PA3347-NGFP display the green fluorescence signals.

These data indicate that PA3346^{L408-A571} is a serine protein kinase/anti-sigma factor playing a key role in the partner-switching regulatory module. In order to identify the specific sigma factor participated in this partner-switching system, *in vivo* bimolecular fluorescence complementation assays were performed and the detail molecular regulation mechanism was reported in this study.

2.2 Introduction

Bacteria mainly use two-component systems (2CS) to regulate gene expressions for rapid adaptation to different environmental challenges (30). A 2CS is usually composed of two modules, a sensor kinase and a response regulator. The sensor kinase can autophosphorylate itself when environmental cue stimulates, and the signal is transmitted through a simple His→Asp pathway or a more complicated His→Asp→His→Asp pathway to activate the cognate response regulator, which mostly functions as a transcription regulator (31). For example, response regulator BvgA in *Bordetella bronchiseptica* is activated by sensor kinase BvgS. Then, the C-terminal DNA-binding domain of BvgA-P binds to *frl* promoter and represses the gene expressions required for flagella biosynthesis, causing a defect in motility (32). Oppositely, MrpAB in *Myxococcus xanthus* positively regulates its own promoter and the expression of *mrpC* (33).

The response regulator PA3346 in the HptB mediated signal transduction pathway in *P. aeruginosa* PAO1 is totally different from transcriptional regulators. The phosphorylation on PA3346 N-terminal receiver domain results in an increase in its Ser protein phosphatase activity and leads to dephosphorylation at Ser-56 of the putative anti-sigma factor antagonist PA3347 (34). More interestingly, the gene organization of PA3346-(unknown Ser protein kinase/anti-sigma factor)-PA3347 is

similar to SpoIIE-SpoIIB-SpoIIAA and RsbU-RsbW-RsbV in *B. subtilis* which are so-called partner switcher system (35). In partner switcher regulatory system, Ser protein kinase /phosphatase modulate the activities of anti-sigma factor antagonist by state conversion between phosphorylated or dephosphorylated form. SpoIIE-SpoIIB-SpoIIAA regulates the sporulation-related gene expression by phosphorylation or dephosphorylation at Ser-58 of the anti-sigma factor antagonist SpoIIAA (36). The phosphorylated state SpoIIAA was an inactive form and the anti-sigma factor SpoIIB was released to form a SpoIIB • σ^F complex for repressing gene transcriptions. In a *Bordetella* species, BtrU-BtrW-BtrV is also a partner switcher system and is required for the production of type III secretion system through the regulation of stress response σ^B (37). However, in the HptB-PA3346-PA3347 system, the Ser protein kinase, anti-sigma factor and specific sigma factor remain unknown. Therefore, the major goal of this study is to search for the Ser protein kinase, which regulates the activity of anti- σ antagonist (36). We recently noted that, by using the InterProScan analysis (<http://www.ebi.ac.uk/Tools/pfa/iprscan/>), the C-terminal region of PA3346 possesses a putative HATPase domain. Hence, our first aim is to determine biochemically whether PA3346 is indeed a Ser protein kinase. It is somewhat unusual if the hypothesis turns out positive, because the Ser protein kinase and phosphatase of partner switcher systems are in two separate protein identities in *B. subtilis* and *Bordetella* species. How the two opposite enzyme activities are regulated in a single protein molecule would be an interesting question to address. Although the enzyme functions of two Ser/Thr protein kinases PpkA and Stk1 in *P. aeruginosa* PAO1 have been proved (38-40), the biochemical and biophysical properties concerning prokaryotic Ser protein kinases are still rarely defined. Therefore, this thesis investigates kinase activity and characterizes the metal ion dependence of the

enzyme by *in vitro* phosphorylation assay. The result of this enzymatic study will help us to understand the regulation mechanism of this system further.

2.3 Materials and Methods

2.3.1 Bacterial strains and growth conditions

E. coli XL-1 Blue was used for plasmid preparation and recombinant DNA manipulation. *E. coli* BL21 (DE3) was used for protein expression. All bacteria used in this study were grown in Luria-Bertain (LB) medium containing ampicillin (100 µg/ml) or kanamycin (25 µg/ml), with 150 rpm shaking at 37°C. Nutrient broth (NB) contains nutrient broth powder (Difco™) and 0.5% glucose (41). M8 minimal (M8) medium contains 64 g/L Na₂HPO₄ · 7 H₂O, 15 g/L KH₂PO₄, 2.5 g/L NaCl, 2 mM MgSO₄, 0.1 mM CaCl₂, 0.5% Casamino acid, 0.4% glucose and 10 mM L-glutamate (42,43). Bacteria strains and plasmids used in this study were listed in Table 2.5.1.

2.3.2 Amino acid sequence alignments

The HATPase region of PA3346, ranging from amino acid position 408 to 571, was used for searching the homologous protein by protein BLAST in the NCBI database, and four proteins predicted as a Ser protein kinase in *Rhodopseudomonas palustris* BisA53 (YP_780133), *Algoriphagus* sp. PR1 (ZP_01718475) Ser-protein kinase RsbW, *Bacillus selenitireducens* MLS10 (ZP_02169479) and *Chloroflexus aggregans* DSM 9485 (YP_002463389) were found. To analyze the conserved region in these Ser protein kinases, four additional proteins, *Geobacillus stearothermophilus* SpoIIAB (AAB81193) (44), *B. subtilis* SpoIIAB (NP_390227) (45) *B. subtilis* RsbW (NP_388353) (46), *Bordetella bronchiseptica* BtrW (NP_888190) (47), were also used in the sequence alignment. The amino acid sequences were analyzed by VectorNTI and the result was shown in Figure 2.6.1.

2.3.3 Cloning, expression and purification of His-tag and GST-tag fusion protein

DNA regions encoding PA3347 and the C-terminal region of PA3346 (1222-1713) were amplified by polymerase chain reaction and cloned into pGEX-5X-1 and pET30a, respectively. Primers used in this study are listed in Table 2.5.2. *E. coli* BL21 (DE3) containing the genes of interest were refreshed in LB medium supplemented with kanamycin or ampicillin with shaking at 37°C until optical density (OD₅₉₅) reached 0.4 to 0.6. Protein expression was induced by adding isopropyl-1-thio-β-D-galactopyranoside (IPTG) to a final concentration of 100 μM, and then the bacteria were propagated at 20°C with 150 rpm shaking for 20 h. The bacterial cells were collected by centrifugation at 5000 rpm for 10 min at 4°C. Cell pellets were washed and resuspended in cold suspension buffer (20 mM Tris-HCl, 140 mM NaCl pH 8.0). The cells were broken by sonication and the cell pellets were removed by centrifugation at 14000 rpm for 20 min at 4°C. His-tagged fusion proteins were purified by Nickel-charged resin (Ni sepharoseTM High Performance, GE Healthcare). The unbinding proteins were washed by wash buffer (20 mM imidazole, 20 mM Tris-HCl, 140 mM NaCl pH 8.0) and the His-tag fusion proteins were eluted by 300 mM imidazole, 20 mM Tris-HCl, and 140 mM NaCl, pH 8.0. The method of induction, protein expression and collection of *E. coli* BL21 (DE3) containing PA3347-GST-tagged fusion plasmid was the same as His-tagged fusion protein described above. The GST-tagged protein were purified via glutathione sepharoseTM 4 fast flow resin (GE Healthcare), washed by PBS buffer and eluted by 50 mM Tris-HCl buffer containing 10 mM reduced form glutathione pH 8.0 (48). Finally, those purified proteins were dialyzed against the dialysis buffer (50 mM Tris-HCl, 200 mM KCl, 10 mM MgCl₂, 1 mM EDTA, 1 mM DTT and 50% glycerol) and stored at -20°C for long-term preservation.

2.3.4 *In vitro* phosphorylation assay

To detect the Ser protein kinase activity, PA3346^{L408-A571} and PA3347 were incubated in buffer containing 100 mM Tris-HCl pH 7.5, 50 mM KCl, 1.5 mM MgCl₂, 1 μCi [γ -³²P] ATP or 2 mM ATP at 37°C for 1 h. The protein ratio of PA3346^{L408-A571} and PA3347 was 1:1; as for *in vitro* phosphorylation assay of another putative anti-sigma antagonist protein PA2797, GST and GST-PA3347 proteins were used as negative control and positive control, respectively. GST-PA2797 (2 μg) was incubated with PA3346^{L407-A571} (1 μg) and 1 mM ATP at 37°C for 10, 30 and 60 min. The reactions were quenched by adding the same volume of SDS-PAGE loading buffer (50 mM Tris-HCl pH 6.8, 100 mM DTT, 2% sodium dodecyl sulfate, 0.1% bromophenol blue, 10% glycerol, and 10% β-mercaptoethanol) and heated at 95°C for 10 min. The phosphorylation pattern was detected by autoradiography or Pro-Q[®] Diamond phosphoprotein gel stain (Molecular Probes, USA). Pro-Q[®] Diamond phosphoprotein gel stain is an in-gel detection method of protein phosphorylation. This fluorescence dye could detect the phosphate group attached on Ser, Thr or Tyr residues (49,50) and the signals could be visualized by using a Typhoon 9200 Imager (GE Healthcare) or a UV Box.

2.3.5 Protein pull-down assays

Glutathione agarose beads were suspended with the equal volume of PBS buffer (pH 7.4). Equal quantity of PA3347-GST (27.4 μg) and PA3346^{L408-A571}-His₆ were incubated with 500 μl of 50% slurry of glutathione agarose beads and 2 mM MgCl₂ in the presence or absence of 2 mM ADP. After end-over-end mixing at 4°C for 2 h, the protein complexes were washed by 1 ml PBS buffer, eluted with 20 mM glutathione

(50 mM Tris-HCl buffer, pH 8.0) and analyzed on a 15% SDS- polyacrylamide gel. As for the protein-protein interaction assay of PA3346-GST and RpoN-His₆, the experimental procedures were the same as described above.

2.3.6 Western blotting analysis

The PA3347-GST and PA3346^{L408-A571}-His₆ proteins on the 15% SDS-polyacrylamide gel were transferred onto a polyvinylidene fluoride (PVDF) membrane (GE Healthcare) at 100 V for 1 h. The blot was blocked in PBS buffer (137 mM NaCl, 2.7 mM KCl, 10 mM Na₂HPO₄, 2 mM KH₂PO₄, pH 7.4) containing 5% skim milk at room temperature for 1 h. Then, the blot was incubated with a monoclonal anti-GST antibody (6G9B9, Novus Biologicals, USA) or a monoclonal anti-His antibody (ab18184, Abcam, UK) at 4°C overnight. After 10-min washes with PBS buffer for three times, a horseradish peroxidase (HRP)-conjugated secondary antibody (Jackson ImmunoResearch, West Grove, PA) was applied to the blot and the incubation was done at room temperature for 1 h. Finally, the signals of the target proteins were revealed by HRP colorimetric assay (Vector[®] NovaRED[™] Substrate kit, Vector Laboratory, USA).

2.3.7 *In vivo* protein-protein interaction assay by GFP fragment reassembly

The vectors used in this study were provided as a gift by Professor Lynne Regan of Yale University (29). Gene PA3347 used as the bait and PA3346 (1222-1713) used as the prey were cloned into pET11a-link-NGFP and pMRBAD-link-CGPF, respectively. The two plasmids were co-transformed into *E. coli* BL21 (DE3) and cultured in LB medium containing 100 μM ampicillin and 35 μM kanamycin at 37°C for 12 to 16 h. To perform the GFP fragment reassembly, ten microliters of the overnight cultures were applied to the LB agar containing the same antibiotics, 100

μM IPTG and 0.05% arabinose. Then, the plates were statically incubated at 20°C for 2 to 3 days. The bacteria cells grown on the plates were re-suspended with PBS buffer and examined under an upright fluorescence microscope (BX-51; Olympus) connected with a CCD camera. The data were analyzed by using the SPOT Advanced Plus Imaging software (Sterling Heights, MI). In the case of searching the putative factors interacting with PA3346⁴⁰⁸⁻⁵⁷¹, all possible genes were cloned into pET11a-link-NGFP and pMRBAD-link-CGPF, respectively. The experimental procedures were the same as described above and the detail information about the possible genes was listed in Table 2.6.3.

2.3.8 Chrome azurol S (CAS) plate assay

The CAS agar plates were prepared on the basis of method described by Schwyn and Neilands (51). Because the preparation for the plates is difficult, we also refer to the step-by-step protocol published by Loudon and Lynee (52). The CAS plate contains 0.1 mM CAS, 0.2 mM HDTMA, 10 μM $\text{FeCl}_3 \cdot 6\text{H}_2\text{O}$, 100 mM PIPES, M9 minimal salt (Sigma-Aldrich[®]), 0.1 mM CaCl_2 , 2 mM MgCl_2 , 0.3% Casamino acid, 0.2% glucose and 1.5% agar. The pH was adjusted to 5.6 with NaOH. *P. aeruginosa* PAO1 wild type and mutant strains were grown overnight in LB medium at 37°C, and then 3 μl of the culture was inoculated onto the CAS agar plate. After 24 h incubation at 37°C, the siderophore production of each bacterial strain was compared according to the orange halo around the colonies.

2.3.9 N-Acyl homoserine lactones (AHL) reporter plate bioassays

The overnight LB culture of *C. violaceum* CV026 was added into the semi-solid LB agar (0.3%, w/v) in the volume ratio of 1:100, mixed well and then poured immediately on the surface of NB, LB or M8 agar plate (1.5%, w/v). After the upper

layer agar solidified, the 200 μ l pipette tips put inversely on the 1.5% agar plate were removed to form wells on the overlaid agar. Each of the wells was filled with 10 μ l overnight LB cultures of *P. aeruginosa* PAO1 wild type or mutant strains, respectively. Then, the plates were kept in the upright position and incubated at 30°C for 24 h. *C. violaceum* CV026 is a mini-Tn5 transposon insertion mutant of *C. violaceum* ATCC 31532, causing a violacein-negative strain (53,54). This purple pigment (violacein) production can be restored by providing the exogenous AHLs. Therefore, the AHLs produced by *P. aeruginosa* strains could be measured qualitatively by examining the purple pigment formed around the wells.

2.3.10 Congo red plate assay

Plates contain Tryptone (10 g/L), Congo red (40 mg/L) and 1% Bacto agar (55,56). Bacteria were inoculated on the surface of the plate by using a sterile toothpick. After 2 days of incubation at 30°C, the colony morphology of each strain was recorded with a Canon camera (PowerShot G10). The assays were performed independently at least three times.

2.4 Result and Discussion

2.4.1 PA3346^{L408-A571} contains the conserved N, G1 and G2 boxes

The protein structure of *B. stearotherophilus* SpoIIAB, a Ser protein kinase and an anti-sigma factor, has been solved. It is revealed that SpoIIAB is structurally distinct to the Hank's type Ser protein kinases (57) while exhibiting high similarities to bacterial two-component histidine kinases and ATPases of the GHKL superfamily (58). SpoIIAB contains three of the four conserved regions in GHKL superfamily, motif I, II and III which corresponded to the N, G1 and G2 boxes in histidine kinase

(58). The C-terminal region of PA3346 contains a histidine-like or Hsp90-like ATPase domain, which belongs to the GHKL superfamily. Sequence alignment performed by VetcorNTI shows that PA3346^{L408-A571} also has N (**E**X₃**N**X₃**H**, x reveals any amino acid), G1 (**D**X**G**X**G**) and G2 (X**G**X**G**X₂) boxes responsible for sigma/anti-sigma factor antagonist binding, Mg²⁺ binding and ADP/ATP binding, respectively (Fig. 2.6.1) (36,37). The result implies that PA3346^{L408-A571} is the Ser protein kinase/anti-sigma factor which we are searching for.

2.4.2 PA3346^{L408-A571} possesses a Ser protein kinase activity toward PA3347

According to the preliminary amino acid sequence analysis, it is possible that PA3346^{L408-A571} can phosphorylate PA3347. Therefore, the C-terminal region of PA3346 was cloned and then purified using Ni²⁺-charged affinity chromatography. The purified PA3346^{L408-A571} protein was incubated with an equal amount of PA3347 and 1 μCi [³²P] ATP at 37°C. Fig. 2.6.2 clearly demonstrates that the intensities of PA3347 phosphorylation signals increase over time, indicating that PA3346^{L408-A571} possesses a protein kinase activity. Besides, the phosphorylation site on PA3347 indeed locates at Ser-56 because a PA3347 variant with a S56A mutation could not be phosphorylated (Fig. 2.6.3) (34). More interestingly, PA3346^{L408-A571} is divalent cation dependence (Fig. 2.6.4). It can utilize at least three kinds of ions and the enzyme activities were in the order of Mg²⁺ >> Ca²⁺ > Mn²⁺. The finding is different from that of PpkA (PA0074), a Ser/Thr protein kinase, which shows Mn²⁺ dependence (38).

2.4.3 PA2797 is not the substrate of PA3346^{L408-A571}

Except PA3347, the hypothetical protein PA2797 is predicted as an anti-sigma factor antagonist based on the result of InterProScan. For further investigation, we also analyzed the amino acid sequence identities and similarities of PA2797 (NP_251487) with PA3347 (NP_252037), *B. subtilis* SpoIIAA (NP_390228) and *B. subtilis* RsbV (NP_388352). Although PA2797 shared only about 10% sequence identity with PA3347, SpoIIAA and RsbV, a conserved **LX₆DSX₂LG** motif (Fig. 2.6.6), where X is any amino acid and S is the target phosphorylation site of Ser protein kinase, was found. Furthermore, PA2797 and PA2798 are the homologs of *B. subtilis* SpoIIAA and SpoIIE. PA2797-PA2798 may form another partner switching system in *P. aeruginosa* PAO1 but lack a specific Ser protein kinase and cognate sigma factor. A recent study also revealed that *P. aeruginosa* PA2797 and PA2798 mutants exhibited an enhanced susceptibility to aminoglycosides (59). Whether PA2797 regulates a yet to be identified sigma factor which confers the bacterial resistance against aminoglycoside through phosphorylation by PA3346⁴⁰⁸⁻⁵⁷¹ remains to be clarified. Therefore, we have cloned and purified PA2797 and included the protein in an *in vitro* phosphorylation assay. As shown in Fig. 2.6.7, both ovalbumin and PA3347 incubated with PA3346⁴⁰⁸⁻⁵⁷¹ and ATP displayed strong fluorescence signals, whereas GST as a negative control did not. GST-PA2797 yielded weak fluorescence signal in the assay, although the signal intensities of GST-PA2797, GST-PA2797 incubated with PA3346⁴⁰⁸⁻⁵⁷¹ in the absence or presence of ATP showed no obvious difference. The result indicates that PA2797 might not be phosphorylated by PA3346⁴⁰⁸⁻⁵⁷¹. Thus, PA3347 is the only substrate of PA3346⁴⁰⁸⁻⁵⁷¹ found. The orphan anti-sigma factor antagonist PA4452 (NP_253142) was not further investigated in this study.

2.4.4 PA3346^{L408-A571} interacts with PA3347 in the presence of ADP *in vitro*

Previous literatures have reported that ADP-containing SpoIIAB and SpoIIAA

formed a stable protein complex (36,60). PA3346^{L408-A571} and PA3347 may behave like an anti-sigma factor and an anti-sigma factor antagonist, respectively. Whether the two proteins can interact with each other was investigated using the GST-pull down assay. The purified PA3347-GST and PA3346^{L408-A571}-His₆ were tested for their binding in the assay and the effect of ADP in protein-protein interaction was also determined. Our finding indicates that in the presence of ADP, PA3346^{L408-A571} could be co-eluted with of PA3347 (Fig. 2.6.8). Comparison of the phosphorylation levels of the freshly purified, calf intestine alkaline phosphatase (CIP) treated, and the fully phosphorylated form of PA3347, it could be concluded that about 10% of the purified PA3347 proteins produced in the heterologous host *E. coli* BL21 (DE3) were phosphorylated, indicating that most of PA3347 proteins are unphosphorylated (Fig. 2.6.5). These results reveal that PA3346^{L408-A571} can bind to the unphosphorylated form of PA3347 in the presence of ADP.

2.4.5 PA3346^{L408-A571} interacts with PA3347 *in vivo*

To further verify whether PA3346^{L408-A571} interacts with PA3347 *in vivo*, a GFP fragment reassembly assay was performed. The DNA fragment containing the coding region of PA3346^{L408-A571} was cloned into pMRBAD-link-CGFP to produce a recombinant protein fused to C-terminal fragment of GFP as the prey. The entire coding region of PA3347 was cloned into pET11a-link-NGFP to produce an NGFP-PA3347 fusion protein as the bait. The protein-protein interaction of the bait and prey can lead to the GFP fragment reassembly (17,29). *E. coli* BL21 (DE3) cells harboring pMRBAD-Z-CGFP and pET11a-Z-NGFP were used as a positive control. As shown in Fig. 2.6.9, the bacterial cells of the positive control and PA3346^{L408-A571}-CGFP and

NGFP-PA3347 pair displayed green fluorescence signals under the fluorescence microscope at an excitation wavelength of 488 nm, whereas no fluorescence emission was detected in negative control cells. The result indicates that PA3346⁴⁰⁸⁻⁵⁷¹ interacts with PA3347 *in vivo*.

2.4.6 PA3346^{L408-A571} cannot interact with RpoN in the presence of ATP *in vitro*

Our data indicated that PA3346^{L408-A571} possessed a Ser protein kinase activity and interacted with the anti-sigma factor antagonist PA3347 *in vitro* and *in vivo*, suggesting that PA3346^{L408-A571} may behave as not only a Ser protein kinase, but also an anti-sigma factor (36,45,47). Like SpoIIE-SpoIIAB-SpoIIAA- σ^F in *B. subtilis*, PA3346-PA3347-unknown sigma factor in *P. aeruginosa* PAO1 might form a partner switcher regulatory system. To clarify if PA3346^{L408-A571} is an anti-sigma factor, it is important to find the unknown sigma factor. In a previous study, it has been proved that the HptB-PA3346-PA3347 cascade regulated the bacterial motility and biofilm formation (34,35,56). In addition, RpoN (σ^{54}) has been reported to be required for the flagella biogenesis and bacterial motility in *P. aeruginosa* (61), *Xanthomonas campestris* (62), *Vibrio fischeri* (63) and *E. coli* MG1655 (64). The *rpoN* mutant of *P. fluorescens* CHA0 displayed reduced swimming and swarming motilities (65). Based on these studies and the results of our phenotype assays, we proposed that RpoN is the possible sigma factor interacting with PA3346^{L408-A571}. Whether RpoN and PA3346^{L408-A571} interact with each other is investigated by using a GST-pull down assay. The purified RpoN-His₆ and GST-PA3346 were tested for their binding in the presence of 1 mM ATP (66). Fig. 2.6.10A shows that RpoN-His₆ and a small amount of GST-PA3346^{L408-A571} were eluted with PBS buffer. When washed by 20 mM

glutathione buffer, only GST-PA3346^{L408-A571} proteins were eluted (Fig. 2.6.10B). The result indicates that RpoN-His₆ could not be co-eluted with GST-PA3346^{L408-A571} in the presence of ATP. Therefore, RpoN might not be the sigma factor we are searching for.

2.4.7 $\Delta hptB$ mutant strain displays a higher production level of exopolysaccharides

In our previous study, analysis of PA3346 and PA3347 gene knock-out mutants revealed that HptB-mediated signaling pathway is associated with biofilm formation (34). Recently, some studies demonstrated that polysaccharides contribute to biofilm formation in nonmucoid strains (67,68). Therefore, we conducted the Congo red plate assay to determine whether the biofilm formation is linked to the production of exopolysaccharides. Congo-red dye has been shown to bind extracellular matrix components, especially the exopolysaccharides. When grown on the Congo red plate, the $\Delta hptB$ mutant (MPA45) colony was completely dark pink, indicating more polysaccharide production. In contrast, PAO1, MJL46 and MJL47 displayed the similar colony morphology. The periphery of PAO1, MJL46 and MJL47 colonies was dark pink and the central was pale white, revealing less polysaccharide production (Fig. 2.6.11). The data is consistent with that of *P. aeruginosa* PAK strain studied by a research group in CNRS, France (56). Thus, based on the result of Congo red plate assay, the biofilm formation regulated by HptB-mediated pathway is in relation to the exopolysaccharide production.

2.4.8 No significant phenotype differences are found in CAS plate assay and AHL reporter assay

There are 24 sigma factors found in *P. aeruginosa* PAO1 (69). In order to know

in advance which sigma factors might participate in the HptB-mediated partner switching regulatory module, we performed the AHL reporter assay and CAS plate assay first. RhlR/RhlI quorum sensing system can regulate the bacterial swarming motility by activating the gene transcription of *rhlAB* and *rhlC* when the concentration of C₄-HSL reaches a threshold (70,71). Moreover, stationary-phase σ factor RpoS negatively regulates the transcription of *rhlI* whose gene product is responsible for the synthesis of C₄-HSL (72). It is interesting to clarify if RpoS regulates the swarming motility through the C₄-HSL-mediated pathway (42,73,74). Using the AHL reporter assay to determine whether *P. aeruginosa* PAO1 wild type and mutant strains produced different amounts of C₄-HSL, we found that regardless the culture medium, (NB, LB or M8 agar), the level of purple pigment produced by the reporter strain *C. violaceum* CV026 shows no significant difference (Fig. 2.6.13). The result indicates that *P. aeruginosa* PAO1 and mutant strains produced comparable amounts of C₄-HSL. This study also interested in PvdS, a σ ECF factor controlling the transcription of pyoverdine biosynthesis genes (75,76). If PvdS participates in the partner switching regulatory system, the Fe³⁺ chelating abilities would be different between *P. aeruginosa* PAO1 wild type, MPA45, MJL46 and MJL47 strains. However, the result of CAS plate assay reveals that the diameters of orange halos around the bacterial colonies are similar (Fig. 2.6.12), indicating that the iron chelating ability of the strains tested has no difference. In summary, RpoS and PvdS may not participate in this HptB-mediated partner switching regulatory system.

2.4.9 Is PA3346^{L408-A571} an anti-sigma factor?

To further investigating the factors interacting with PA3346, a GFP fragment reassembly assay was performed. The genes encoding the sigma factors including RpoH, RpoD, RpoS, RpoN, FiuI, AlgU, SigX, FpvI, PvdS, the uncharacterized σ ECF

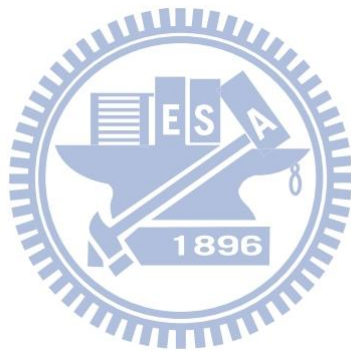
factors PA1351, PA2896, PA3285, the putative σ^{54} -dependent transcriptional regulators FleQ, PA1663, PA2359 (69), putative σ^{54} modulation protein PA4463 and a regulatory protein RsmA (77) are cloned into pMRBAD-link-CGFP or pET11a-link-NGFP, respectively. The plasmids used in this assay are co-transformed into *E. coli* BL21 (DE3) with the PA3346-link-NGFP or PA3346-link-CGFP. The bacterial cells containing the bait and prey vectors are cultured on LB agar plates with appropriate antibiotics and inducers for 3 days at 20°C and then examined under a fluorescence microscope. Although we have tested about 73 combinations of the bait and prey plasmids, the bacterial cells display no fluorescence signal other than the positive control. This result may be due to the conformational incompatibility between the bait and prey GFP fusions or no protein-protein interaction between these factors and PA3346.

Our preliminary result indicates that PA3347 and PA3346^{L408-A571} form a stable protein complex in the presence of ADP. Besides, the phosphorylation of PA3347 by PA3346 leads to the release of PA3347~P from the protein complex (78), agreeing with the mechanism of partner-switching regulatory module that the phosphorylation state of the anti- σ antagonist is an inactive form (47,66,79). The findings reveal that PA3346 might be a SpoIIAB-like anti-sigma factor antagonized with a sigma factor. However, we failed to find the corresponding sigma factor in the GFP fragment reassembly assay. It is possible that PA3346 may function in a manner different from the traditional partner switching system described for *B. subtilis* and other Gram-positive bacteria. For instance, it is reported that the partner switching cascade BtrU-BtrV-BtrW regulates the type III secretion (TTS) in *Bordetella bronchiseptica*, a Gram-negative bacterium causing infectious bronchitis. The authors of this study found that the *btr* partner switching module does not influence the transcription of the

TTS genes but is essential for the regulation of TTS (37). Thus, they proposed that the switching proteins associated with free BtrW (predicted as an anti- σ factor) could be a part of the TTS machinery or another regulatory molecules, but not a sigma factor (47). Furthermore, a similar partner switching system was found in a Gram-negative pathogen *Chlamydia trachomatis* (RsbU-RsbV1-RsbV2-RsbW). No successful experiment results support that *C. trachomatis* RsbW could bind with σ^{66} , σ^{54} or its most likely target σ^{28} . Therefore, the authors consider that the target of *C. trachomatis* switching protein is not a sigma factor but instead is another protein which controls the response functions post-translationally (80). These studies suggest that the switching proteins associated with SpoIIAB-like protein are different from the partner switching system in *B. subtilis*. PA3346 may be associated with a transcriptional factor or a regulatory factor which could be a part of flagella machinery or exopolysaccharide export system. Hence, HptB-PA3346-PA3347 regulatory cascade could regulate the swarming motility and biofilm formation either transcriptionally or post-translationally. There are 5571 open reading frames (ORFs) and at least 550 transcriptional regulators identified in *P. aeruginosa* PAO1 genome (69,81). For the high-throughput screening of the corresponding factors participated in the partner switching regulatory module, it is required to construct a *P. aeruginosa* genome fragment library by using the yeast two-hybrid system (82), bacterial two-hybrid system (83,84) or the bimolecular fluorescence complementation (BiFC) method (29).

Based on the previous work and this study, we suggest that the bacterial swarming motility and biofilm formation are under the regulation of HptB-mediated signaling pathway. The output responses might be controlled through the protein-protein interaction of PA3346^{L408-A571} with either PA3347 or an unknown regulatory factor. Our hypothetical model (Fig. 2.6.14) shows that PA3347, an

anti-sigma factor antagonist, is inactivated by phosphorylation on Ser-56 through the action of Ser protein kinase (PA3346^{L408-A571}). This would lead to the disassociation of PA3346^{L408-A571} from PA3347~P and allow it to bind to the corresponding regulatory factor; When the receiver domain of response regulator PA3346 is phosphorylated, the Ser protein phosphatase activities are increased and result in the dephosphorylation on PA3347 Ser-56. PA3347 is active and could bind to PA3346^{L408-A571} to release the corresponding regulatory factor. Studies are underway to investigate which protein factors participate in this regulatory system. If the model comes out to be true, it might be a novel combination system of two-component system and partner switching regulatory module in Gram-negative bacteria.



2.5 Tables

Table 2.5.1 Bacterial strains and plasmids used in this study

Strains or Plasmids	Descriptions	Refs. or source
Strains		
<i>E. coli</i>		
BL21 (DE3)	F ⁻ <i>ompT hsdS_B(r_B⁻, m_B⁻) gal dcm</i> (DE3)	Invitrogen
XL-1 Blue	<i>recA1 endA1 gyrA96 thi-1 hsdR17 supE44 relA1 lac</i> [F' <i>proAB lacI^qΔM15 Tn10</i> (Tet ^r)].	Stratagene
<i>P. aeruginosa</i>		
PAO1	Nonmucoid wild type strain	Laboratory stock
MPA45	PAO1 Δ <i>hptB</i>	Laboratory stock
MJL46	PAO1 Δ <i>PA3346</i>	Laboratory stock
MJL47	PAO1 Δ <i>PA3347</i>	Laboratory stock
<i>C. violaceum</i> CV026	a mini-Tn5 transposon insertion mutant of <i>C. violaceum</i> ATCC 31532, violacein-negative strain	Laboratory stock
Plasmids		
pET30a	Km ^r , His tag protein expression vector	Novagen
pGEX-5X-1	Ap ^r , GST tag protein expression vector	GE Healthcare
pET11a-Z-NGFP	Ap ^r , plasmid vector that expresses a fusion of an antiparallel leucine zipper peptide to NGFP	(29)
pET11a-link-NGFP	Ap ^r , plasmid vector designed for fusion of a target protein to the N-terminal fragment of GFP (1-157)	(29)
pMRBAD-link-CGFP	Km ^r , plasmid vector designed for fusion of a target protein to the C-terminal fragment of GFP (158-238)	(29)
pMRBAD-Z-CGFP	Km ^r , plasmid vector that expresses a fusion of an antiparallel leucine zipper peptide to CGFP	(29)
pMMB66EH	Ap ^r ; broad-host-range expression vector	Laboratory stock
pHL34	Km ^r , a fragment containing residues 408-571 of PA3346 coding region cloned into pET30a	This study
pHL38	Km ^r , a fragment containing residues 408-571 of PA3346-E46A coding region cloned into pET30a	This study
pHL39	Km ^r , a fragment containing residues 408-571 of PA3346-H54A coding region cloned into pET30a	This study

pHL41	Km ^r , a fragment containing entire PA1097 (<i>fleQ</i>) coding region cloned into pET30a	This study
pHL98	Km ^r , a fragment containing entire PA1663 coding region cloned into pET30a	This study
pE4462	Km ^r , a fragment containing entire PA4462 (<i>rpoN</i>) coding region cloned into pET30a	This study
pHL36	Ap ^r , a fragment containing entire PA3347 coding region cloned into pGEX-5X-1	This study
pE3347-S56A	Ap ^r , a fragment containing entire PA3347-S56A coding region cloned into pGEX-5X-1	Laboratory stock
pHL95	Ap ^r , a fragment containing residues 168-571 of PA3346 coding region cloned into pGEX-5X-1	This study
pHL96	Ap ^r , a fragment containing residues 315-571 of PA3346 coding region cloned into pGEX-5X-1	This study
pHL97	Ap ^r , a fragment containing residues 408-571 of PA3346 coding region cloned into pGEX-5X-1	This study
pHL99	Ap ^r , a fragment containing entire PA2797 coding region cloned into pGEX-5X-1	This study
pHL104	Ap ^r , a fragment containing residues 408-571 of PA3346-E46A coding region cloned into pGEX-5X-1	This study
pHL105	Ap ^r , a fragment containing residues 408-571 of PA3346-H54A coding region cloned into pGEX-5X-1	This study
pHL42	Km ^r , a fragment containing residues 168-571 of PA3346 coding region cloned into pMRBAD-link-CGFP	This study
pHL43	Km ^r , a fragment containing residues 315-571 of PA3346 coding region cloned into pMRBAD-link-CGFP	This study
pHL44	Km ^r , a fragment containing residues 408-571 of PA3346 coding region cloned into pMRBAD-link-CGFP	This study
pHL50	Km ^r , a fragment containing entire PA4462 (<i>rpoN</i>) coding region cloned into pMRBAD-link-CGFP	This study
pHL55	Km ^r , a fragment containing entire PA3622 (<i>rpoS</i>) coding region cloned into pMRBAD-link-CGFP	This study
pHL67	Km ^r , a fragment containing entire PA0576 (<i>rpoD</i>) coding region cloned into pMRBAD-link-CGFP	This study
pHL69	Km ^r , a fragment containing entire PA0376 (<i>rpoH</i>) coding region cloned into pMRBAD-link-CGFP	This study
pHL83	Km ^r , a fragment containing entire PA1097 coding region cloned into pMRBAD-link-CGFP	This study
pHL45	Ap ^r , a fragment containing entire PA4462 (<i>rpoN</i>) coding region cloned into pET11a-link-NGFP	This study
pHL54	Ap ^r , a fragment containing entire PA3622 (<i>rpoS</i>) coding region cloned into pET11a-link-NGFP	This study
pHL59	Ap ^r , a fragment containing entire PA0472 coding region cloned into pET11a-link-NGFP	This study
pHL60	Ap ^r , a fragment containing entire PA0762 coding region cloned into pET11a-link-NGFP	This study
pHL61	Ap ^r , a fragment containing entire PA1776 coding region cloned into pET11a-link-NGFP	This study
pHL62	Ap ^r , a fragment containing entire PA2387 coding region cloned into pET11a-link-NGFP	This study

pHL63	Ap ^r , a fragment containing entire PA2426 coding region cloned into pET11a-link-NGFP	This study
pHL64	Ap ^r , a fragment containing entire PA1351 coding region cloned into pET11a-link-NGFP	This study
pHL65	Ap ^r , a fragment containing entire PA2896 coding region cloned into pET11a-link-NGFP	This study
pHL66	Ap ^r , a fragment containing entire PA3285 coding region cloned into pET11a-link-NGFP	This study
pHL68	Ap ^r , a fragment containing entire PA0376 (<i>rpoH</i>) coding region cloned into pET11a-link-NGFP	This study
pHL71	Ap ^r , a fragment containing residues 29-571 of PA3346 coding region cloned into pET11a-link-NGFP	This study
pHL72	Ap ^r , a fragment containing residues 168-571 of PA3346 coding region cloned into pET11a-link-NGFP	This study
pHL73	Ap ^r , a fragment containing residues 315-571 of PA3346 coding region cloned into pET11a-link-NGFP	This study
pHL74	Ap ^r , a fragment containing residues 408-571 of PA3346 coding region cloned into pET11a-link-NGFP	This study
pHL82	Ap ^r , a fragment containing entire PA0905 coding region cloned into pET11a-link-NGFP	This study
pHL84	Ap ^r , a fragment containing entire PA1663 coding region cloned into pET11a-link-NGFP	This study
pHL85	Ap ^r , a fragment containing entire PA2359 coding region cloned into pET11a-link-NGFP	This study
pHL86	Ap ^r , a fragment containing entire PA4463 coding region cloned into pET11a-link-NGFP	This study
pHL101	Ap ^r , a fragment containing residues 168-571 of PA3346 coding region cloned into pMMB66EH	This study
pHL102	Ap ^r , a fragment containing residues 315-571 of PA3346 coding region cloned into pMMB66EH	This study
pHL103	Ap ^r , a fragment containing residues 408-571 of PA3346 coding region cloned into pMMB66EH	This study

Table 2.5.2 Primers used in this study

Primer name	Primer sequence (5'→3')	Descriptions
His46CF	CATATGCTGGACTGGTTCGGTAAGCTTCG	clone PA3346 ⁴⁰⁸⁻⁵⁷¹ into pET30a
NOTI46CR	GCGGCCGCTGCCTGAGGCGAC	clone PA3346 ⁴⁰⁸⁻⁵⁷¹ into pET30a
C46-E46AF	ACGGTACTCGCCGACTCTATTCTGAAC	PA3346 ⁴⁰⁸⁻⁵⁷¹ - pET30a E46A mutant
C46-E46AR	GTTCGAATAGAGTGCGGCGAGTACCGT	PA3346 ⁴⁰⁸⁻⁵⁷¹ - pET30a E46A mutant
C46-H54AF	AACGCCCTGGAAGCTGGCGTCATCG	PA3346 ⁴⁰⁸⁻⁵⁷¹ - pET30a H54A mutant
C46-H54AR	CGATGACGCCAGCTTCCAGGGCGTT	PA3346 ⁴⁰⁸⁻⁵⁷¹ - pET30a H54A mutant
46-168-GST	CGGGATCCATTCCGGCTGCCTGAACG	clone PA3346 ¹⁶⁸⁻⁵⁷¹ into pGEX-5X-1
46-315-GST	CGGGATCCAAACCTATCCGCTGGATATCG	clone PA3346 ³¹⁵⁻⁵⁷¹ into pGEX-5X-1
GST46CF	GGGATCCCGCTGGACTGGTTCGGTAAG	clone PA3346 ⁴⁰⁸⁻⁵⁷¹ into pGEX-5X-1
GSTCR2	GCGGCCGCTTATGCCTGAGGCGAC	clone PA3346 into pGEX-5X-1
3347GSTR1	GGTCCCTCGAGTCAGCTGATCTTGAAC	clone PA3347 into pGEX-5X-1
3347GSTF2	CTTCGAATTCATGGCCATCACTG	clone PA3347 into pGEX-5X-1
97GSTF	AAGGATCCCCATGAGTACCGGTAATAATCCA	clone PA2797 into pGEX-5X-1
97GSTR	TTGTGACTTAATGGCGCTCCAGGG	clone PA2797 into pGEX-5X-1
rpoNF	CACCCATATGAAACCATCGCTAGTCC	clone <i>rpoN</i> (PA4462) into pET30a
rpoNR	CACCCTCGAGCACCAGTCGCTT	clone <i>rpoN</i> (PA4462) into pET30a
fileQF	CACCCATATGTGGCGCGAAACC	clone <i>fileQ</i> (PA1097) into pET30a
fileQR	CACCAAGCTTATCATCCGACAGGTCGT	clone <i>fileQ</i> (PA1097) into pET30a
aF	ATCATATGTTTCAGCCGCGTACCGCAAC	clone PA1663 into pET30a
aR	ATCTCGAGTCAGGTCCGGGGATCG	clone PA1663 into pET30a
46C168-F	CCATGGCTTCCGGCTGCCTGAACGCCA	clone PA3346 ¹⁶⁸⁻⁵⁷¹ into pMRBAD-link-CGFP

46C315-F	CCATGGCTACCTATCCGCTGGATATCGAAG	clone PA3346 ³¹⁵⁻⁵⁷¹ into pMRBAD-link-CGFP
46C408-F	CCATGGCTCTGGACTGGTCGGTAAGCTTC	clone PA3346 ⁴⁰⁸⁻⁵⁷¹ into pMRBAD-link-CGFP
46CGFP-R	GACGTCCTCCACCTGCCTGAGGCGACCA	clone PA3346 into pMRBAD-link-CGFP
rpoNpBADF	CCATCCATGGCTAAACCATCGCTAGTCCTC	clone <i>rpoN</i> (PA4462) into pMRBAD-link-CGFP
rpoNpBADR	ACGTCCCTGAACCTCCCACCAGTCGCTTGC	clone <i>rpoN</i> (PA4462) into pMRBAD-link-CGFP
spBAD-F	AATCCATGGCTATGGCACTCAAAAAAGAAG	clone <i>rpoS</i> (PA3622) into pMRBAD-link-CGFP
spBAD-R	ACGTCCCCTGGAACAGCGCGTCAC	clone <i>rpoS</i> (PA3622) into pMRBAD-link-CGFP
rpoD-F	AATTCATGACTATGTCCGAAAAGCGCAAC	clone <i>rpoD</i> (PA0576) into pMRBAD-link-CGFP
rpoD-R	ACGTCCCCTCGTCGAGGAAGGAGCG	clone <i>rpoD</i> (PA0576) into pMRBAD-link-CGFP
rpoHBADF	AATCCATGGCTATGACCACTTCTTTGCAACCTGTAC	clone <i>rpoH</i> (PA0376) into pMRBAD-link-CGFP
rpoHBADR	AATGACGTCCCGGCGAGAATCCGCCCTTTCAG	clone <i>rpoH</i> (PA0376) into pMRBAD-link-CGFP
1097-F	AATCCATGGCTATGTGGCGCGAAACCAAAC	clone <i>fleQ</i> (PA1097) into pMRBAD-link-CGFP
1097-R	AATGACGTCCTCCACCATCATCCGACAGGTC	clone <i>fleQ</i> (PA1097) into pMRBAD-link-CGFP
46pET29F	AATGTCGACCATCGTCAGCCGCCAG	clone PA3346 ²⁹⁻⁵⁷¹ into pET11a-link-NGFP
46pET168F	AATGTCGACCTCCGGCTGCCTGAAC	clone PA3346 ¹⁶⁸⁻⁵⁷¹ into pET11a-link-NGFP
46pET315F	AATGTCGACCACCTATCCGCTGGATATCG	clone PA3346 ³¹⁵⁻⁵⁷¹ into pET11a-link-NGFP
46pET408F	AATGTCGACCCTGGACTGGTCGGTAAGC	clone PA3346 ⁴⁰⁸⁻⁵⁷¹ into pET11a-link-NGFP
46pET11aR	AATGGATCCTTATGCCTGAGGCGACCAG	clone PA3346 into pET11a-link-NGFP
11a-rpoNF	ATCTCGAGCGGTGGCTCTAAACCATCGCTAGTC	clone <i>rpoN</i> (PA4462) into pET11a-link-NGFP
11a-rpoNR	ATGGATCCTCACACCAGTCGCTTGCGCT	clone <i>rpoN</i> (PA4462) into pET11a-link-NGFP
s11a-F	AATCTCGAGCATGGCACTCAAAAAAGAAG	clone <i>rpoS</i> (PA3622) into pET11a-link-NGFP
s11a-R	AATAGATCTTCACTGGAACAGCGCGTC	clone <i>rpoS</i> (PA3622) into pET11a-link-NGFP

rpoH11aF	AATCTCGAGCATGACCACTTCTTTGCAACCTG	clone <i>rpoH</i> (PA0376) into pET11a-link-NGFP
rpoH11aR	AATGGATCCTCAGGCGAGAATCCGCCCTT	clone <i>rpoH</i> (PA0376) into pET11a-link-NGFP
0472-F	AATGTCGACCGTGTGACGCGGGTGACGT	clone PA0472 into pET11a-link-NGFP
0472-R	AATGGATCCTCACCGGGGCTCTCCG	clone PA0472 into pET11a-link-NGFP
0762-F	AATCTCGAGCATGCTAACCCAGGAACAG	clone PA0762 into pET11a-link-NGFP
0762-R	AATGGATCCTCAGGCTTCTCGCAACAAAGG	clone PA0762 into pET11a-link-NGFP
1776-F	AATCTCGAGCGTGACGCGCGCCTATG	clone PA1776 into pET11a-link-NGFP
1776-R	AATGGATCCCTATGTTTCGGTTCGCATCTG	clone PA1776 into pET11a-link-NGFP
2387-F	AATCTCGAGCTTGAAAACCATTATCGGG	clone PA2387 into pET11a-link-NGFP
2387-R	AATGGATCCTCAGTCGGCTTCCCATTTCG	clone PA2387 into pET11a-link-NGFP
2426-F	AATCTCGAGCATGTGCGGAACAACGTCTACCC	clone PA2426 into pET11a-link-NGFP
2426-R	AATGGATCCTCAGCGGGCGGGCGCTG	clone PA2426 into pET11a-link-NGFP
1351-F	AATCTCGAGCTTGCGCAGCCGCATCGAG	clone PA1351 into pET11a-link-NGFP
1351-R	AATGGATCCTCAATCGAGTTCGCGCAGGC	clone PA1351 into pET11a-link-NGFP
2896-F	AATCTCGAGCATGCATGCCTCCACCAGC	clone PA2896 into pET11a-link-NGFP
2896-R	AATGGATCCTCATACCGCCACCTCCTCG	clone PA2896 into pET11a-link-NGFP
3285-F	AATCTCGAGCGTGGCGGCGCCTACCGA	clone PA3285 into pET11a-link-NGFP
3285-R	AATGGATCCTCAGCATTGGCCGGTCTCCTC	clone PA3285 into pET11a-link-NGFP
0905-F	AATCTCGAGCGGTGGCTCTATGCTGATTCTGACT	clone PA0905 into pET11a-link-NGFP
0905-R	CGGGATCCTTAATGGTTTGGCTCTTGATC	clone PA0905 into pET11a-link-NGFP
1663-F	AATCTCGAGCGGTGGCTCTATGTTTCAGCCGCGTAC	clone PA1663 into pET11a-link-NGFP
1663-R	AATGGATCCTCAGGTCCGGGGATCGCC	clone PA1663 into pET11a-link-NGFP

2359-F	AATCTCGAGCGGTGGCTCTATGTCCGTCATCACC	clone PA2359 into pET11a-link-NGFP
2359-R	AATGGATCCTCACTTGCCCACCAGCGAGAC	clone PA2359 into pET11a-link-NGFP
4463-F	AATCTCGAGCGGTGGCTCTATGCAAGTCAACATC	clone PA4463 into pET11a-link-NGFP
4463-R	AATGGATCCTCAGCGGGCGCCTACGCC	clone PA4463 into pET11a-link-NGFP
46MF2	CG AGATCTATGTCCCCTATACTAGGTTATTG	clone GST-PA3346 into pMMB66EH
46MR	ATGTCGACTTATGCCTGAGGCGA	clone GST-PA3346 into pMMB66EH
pBAD-F	TAGCGGATCCTACCTGACGC	for DNA sequencing (pMRBAD-link-CGFP)
pBAD-R	TTCGGGCTTTGTTAGCAGCC	for DNA sequencing (pMRBAD-link-CGFP)

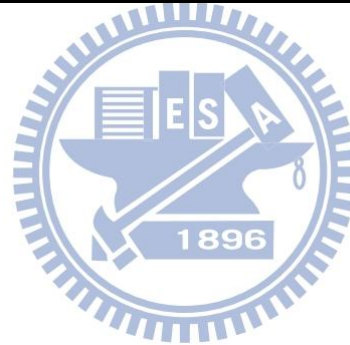


Table 2.5.3 Genes used in the GFP assembly assay

gene index	gene name	description
PA0376	<i>rpoH</i>	RNA polymerase factor sigma-32
PA0472	<i>fiuI</i>	RNA polymerase sigma factor
PA0576	<i>rpoD</i>	RNA polymerase sigma factor RpoD
PA0762	<i>algU</i>	RNA polymerase sigma factor AlgU
PA0905	<i>rsmA</i>	carbon storage regulator
PA1776	<i>sigX</i>	RNA polymerase sigma factor SigX
PA2387	<i>fpvI</i>	RNA polymerase sigma factor
PA2426	<i>pvdS</i>	extracytoplasmic-function sigma-70 factor
PA3622	<i>rpoS</i>	RNA polymerase sigma factor RpoS
PA4462	<i>rpoN</i>	RNA polymerase factor sigma-54
PA1351		sigma-70 factor, ECF subfamily
PA2896		sigma-70 factor, ECF subfamily
PA3285		sigma-70 factor, ECF subfamily
PA1097	<i>fleQ</i>	sigma-54 specific transcriptional regulator; flagellar regulatory protein A
PA1663		sigma-54 dependent transcriptional regulator
PA1945*		sigma-54 specific transcriptional regulator
PA2005*		transcriptional regulator
PA2359		sigma-54 specific transcriptional regulator
PA4463		putative sigma-54 modulation protein

Plasmids containing genes cloned into pET11a-link-NGFP were co-transformed with pHL42 (PA3346¹⁶⁸⁻⁵⁷¹-CGFP), pHL43 (PA3346³¹⁵⁻⁵⁷¹-CGFP) and pHL43 (PA3346⁴⁰⁸⁻⁵⁷¹-CGFP) respectively; plasmids containing genes cloned into pMRBAD-link-CGFP were co-transformed with pHL71 (NGFP-PA3346²⁹⁻⁵⁷¹), pHL72 (NGFP-PA3346¹⁶⁸⁻⁵⁷¹), pHL73 (NGFP-PA3346³¹⁵⁻⁵⁷¹) and pHL74 (NGFP-PA3346⁴⁰⁸⁻⁵⁷¹) respectively. (* Not used in this study)

2.6 Figures

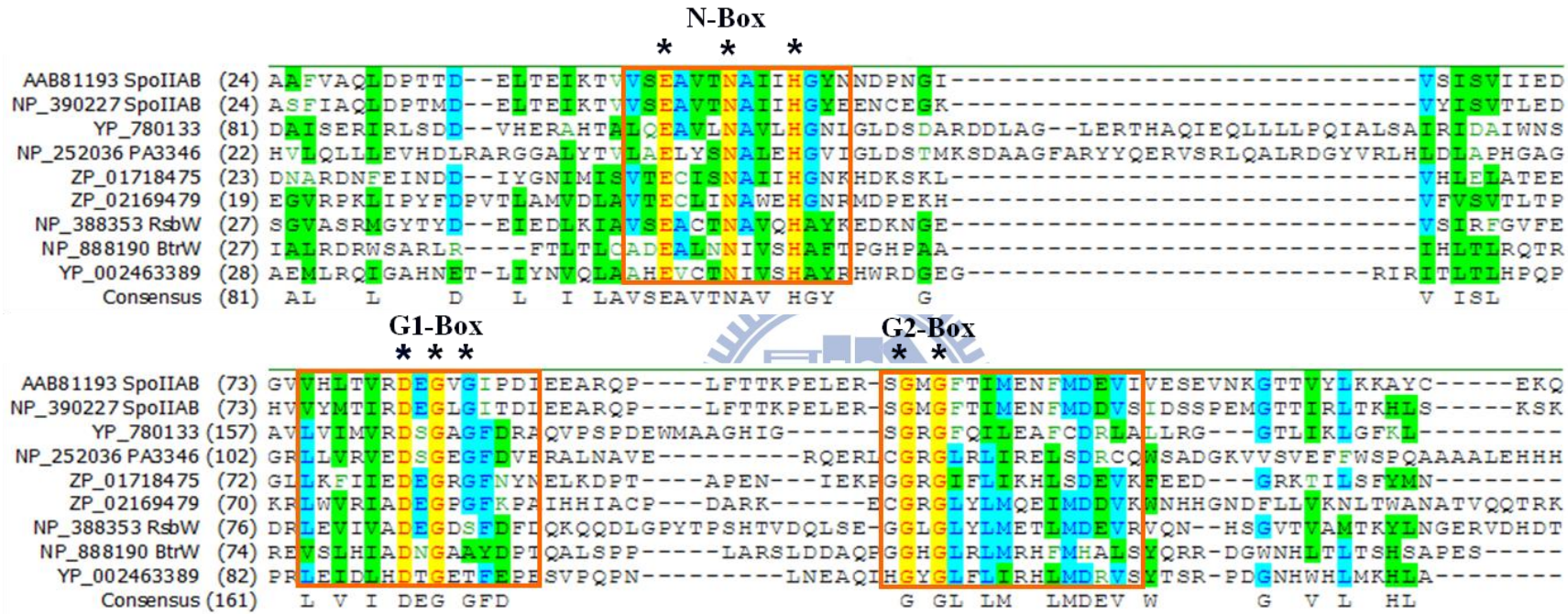


Fig. 2.6.1 Multiple sequence alignment of PA3346^{L408-A571} with other Ser protein kinases.

As the sequence alignment shows, PA3346^{L408-A571} contains conserved N, G1 and G2 boxes. The consensus amino acid residues found in N, G1 and G2 boxes are indicated by star symbol. The bacteria strains and protein accession numbers were as follow: *G. stearothermophilus* SpoIIAB, AAB81193; *B. subtilis* SpoIIAB NP_390227.1; *R. palustris* BisA53, YP_780133; *P. aeruginosa* PAO1 PA3346, NP_252036; *Algoriphagus* sp. PR1 RsbW, ZP_01718475 ; *B. selenitireducens* MLS10, ZP_02169479; *B. subtilis* RsbW, NP_388353.1; *Bd. bronchiseptica* BtrW NP_888190; *C. aggregans* DSM 9485, YP_002463389.

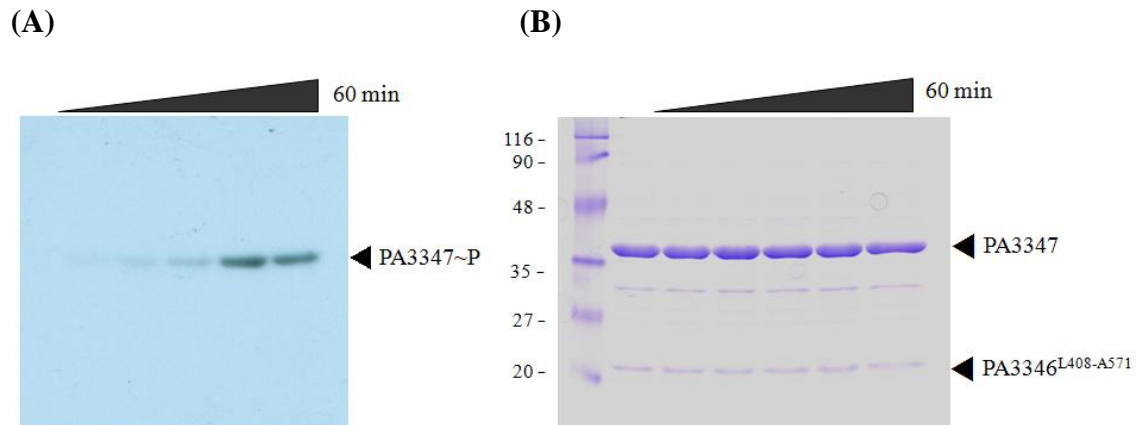
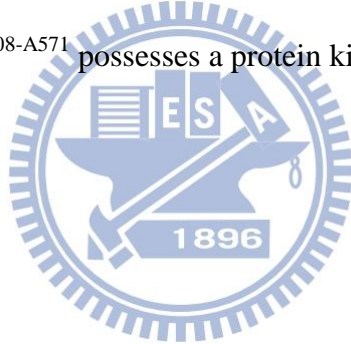


Fig. 2.6.2 Time course analysis of PA3347 *in vitro* phosphorylation.

(A) [γ - 32 P] ATP autoradiogram. (B) SDS-PAGE Coomassie Blue staining. PA3347 (15 μ M) incubated with PA3346^{L408-A571} (15 μ M) and 1 μ Ci [γ - 32 P] ATP at 37°C for different time intervals as follow: 0, 0.5, 1, 5, 15 and 60 min. The result clearly demonstrated that PA3346^{L408-A571} possesses a protein kinase activity toward PA3347.



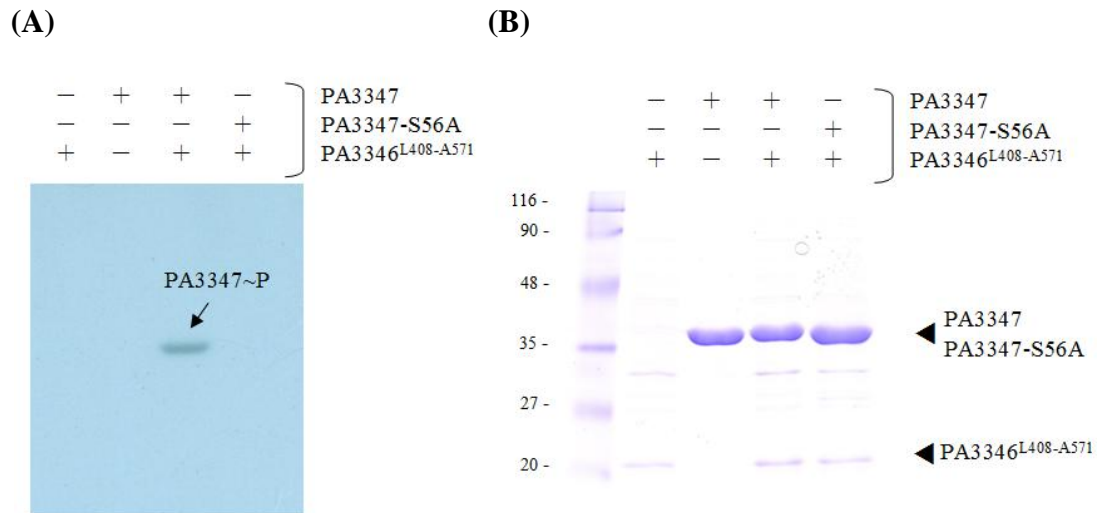
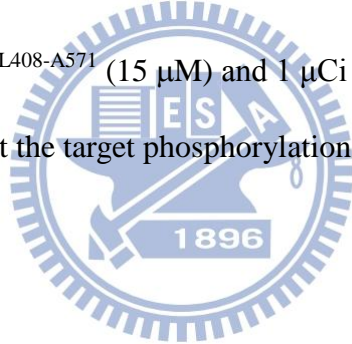


Fig. 2.6.3 *In vitro* phosphorylation assay of purified PA3347 and PA3347S56A mutant protein

(A) [γ -³²P] ATP autoradiogram. (B) SDS-PAGE Coomassie Blue staining. PA3347 (15 μ M) incubated with PA3346^{L408-A571} (15 μ M) and 1 μ Ci [γ -³²P] ATP at 37°C for 10 min. The result indicated that the target phosphorylation site on PA3347 is located at Ser 56.



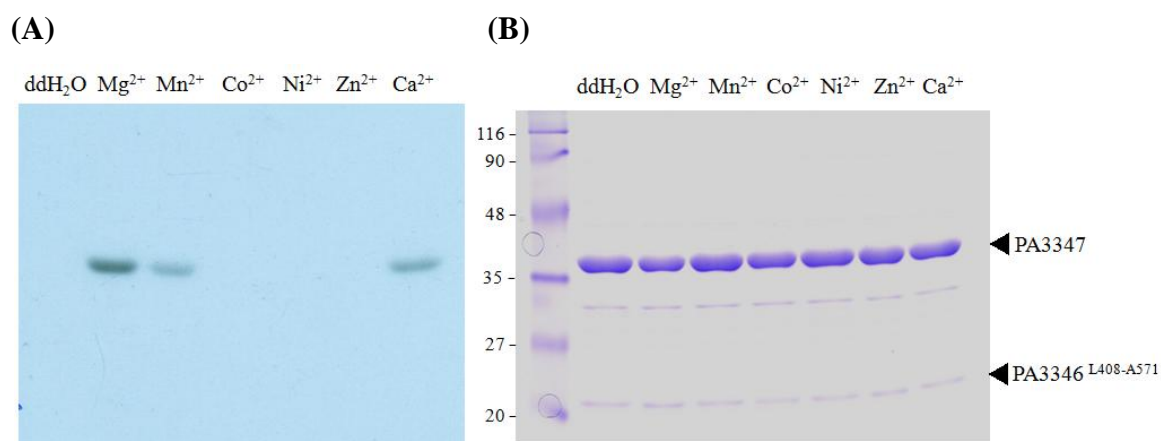


Fig. 2.6.4 Divalent cation dependence on phosphorylation reaction.

(A) [γ -³²P] ATP autoradiogram. (B) SDS-PAGE Coomassie Blue staining. The proteins were reacted with [γ -³²P] ATP and the reaction mixture was resolved on a SDS-polacrylamide gel. PA3347 (15 μ M) incubated with PA3346^{L408-A571} (15 μ M) and 1 μ Ci [γ -³²P] ATP in the presence of 5 mM divalent cation at 37°C for 10 min. The result indicated that the kinase activity is divalent cation, especially Mg²⁺, Ca²⁺ and Mn²⁺, dependent.

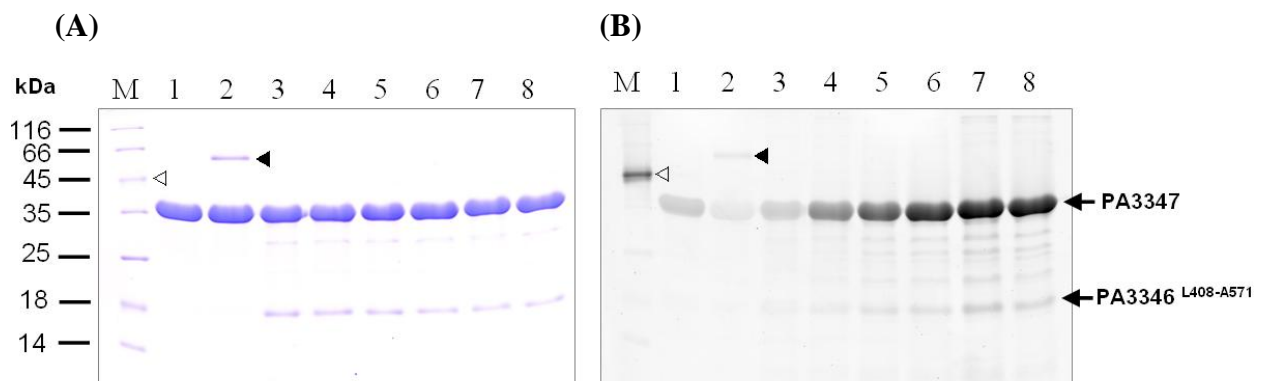


Fig. 2.6.5 Phosphorylation level of PA3347 analysis by Pro-Q Diamond staining

(A) SDS-PAGE Coomassie Blue staining. (B) Pro-Q Diamond staining. M, un-stained protein ladders (Fermentas, USA); 1, PA3347; 2, PA3347 treated with CIP; 3-8, PA3347 incubated with PA3346^{L408-A571} and 2 mM ATP for different time intervals as follow: 0, 5, 10, 20, 40 and 80 min. The signals were revealed by a Typhoon 9200 Imager (GE Healthcare). (Ovabumin is marked by empty arrowheads; calf intestine alkaline phosphatase is marked by filled arrowheads.)

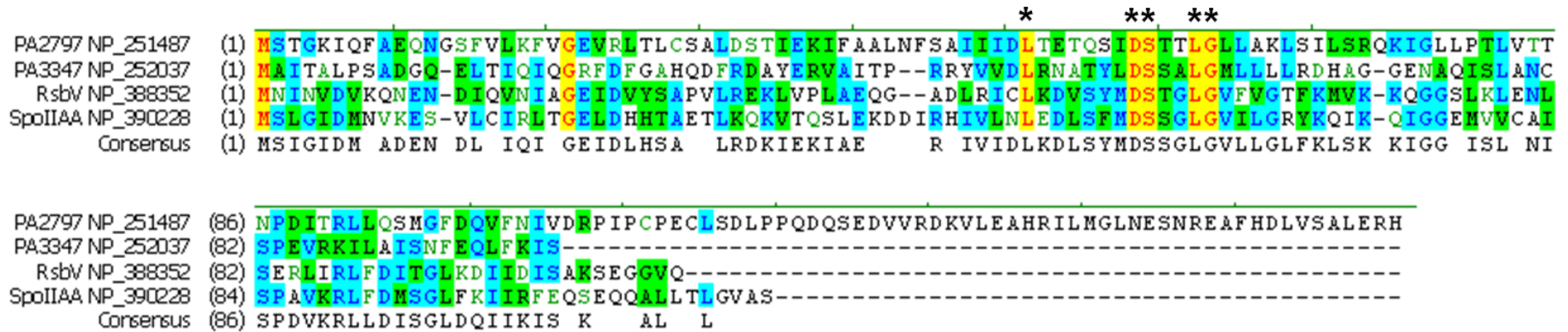


Fig. 2.6.6 Multiple sequence alignment of PA2797 with other anti-sigma factor antagonist.

The bacteria strains and protein accession numbers were as follow: *P. aeruginosa* PAO1 PA2797, NP_251487; *P. aeruginosa* PAO1 PA3347 NP_252037; *B. subtilis* RsbV, NP_388352; *B. subtilis* SpoIIAA, NP_390228. The consensus amino acid residues found in PA2797, PA3347, RsbV and SpoIIA are indicated by star symbol.

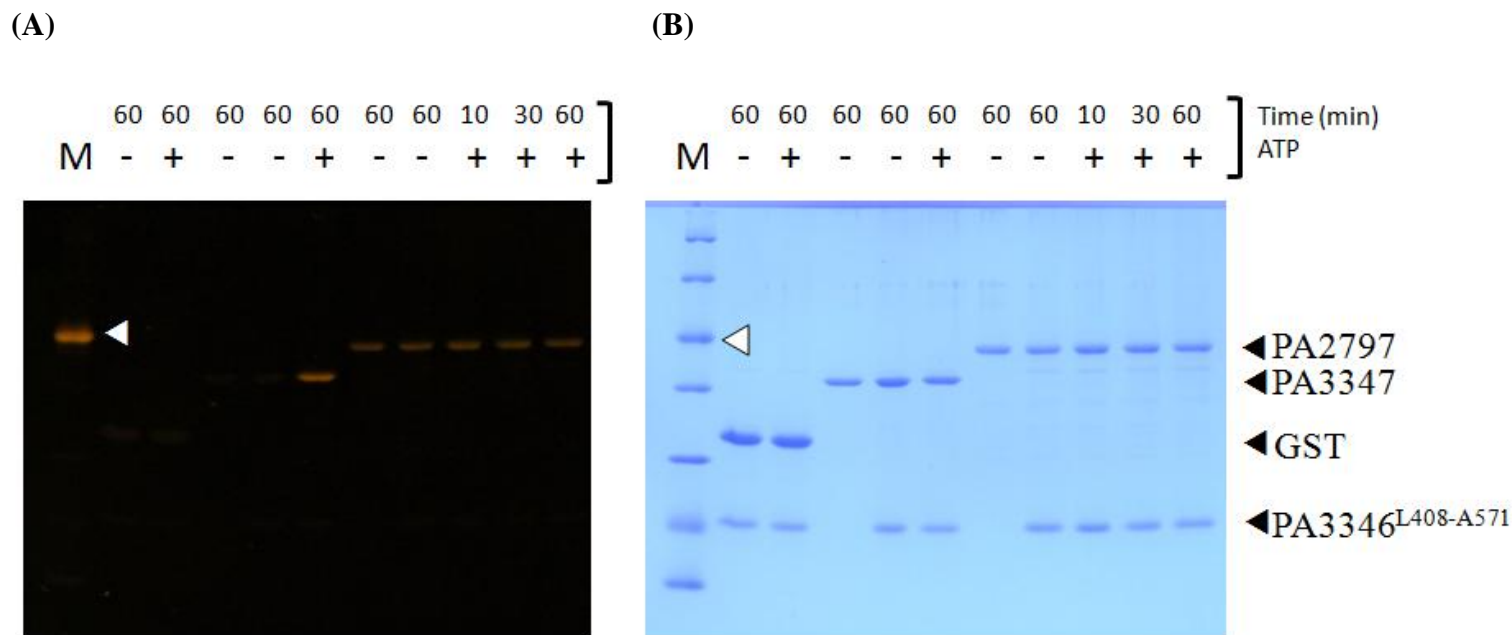


Fig. 2.6.7 *In vitro* phosphorylation of purified GST, GST-PA2797 and GST-PA3347 proteins

(A) Pro-Q Diamond staining. (B) SDS-PAGE Coomassie Blue staining. GST-PA2797 (2 μ g) was incubated with PA3346^{L408-A571} (1 μ g) and 1 mM ATP for different time intervals as follow: 10, 30 and 60 min. The signals were revealed by a UV box. Ovabumin is marked by a white arrowhead. M, unstained protein ladders (Fermentas, USA)

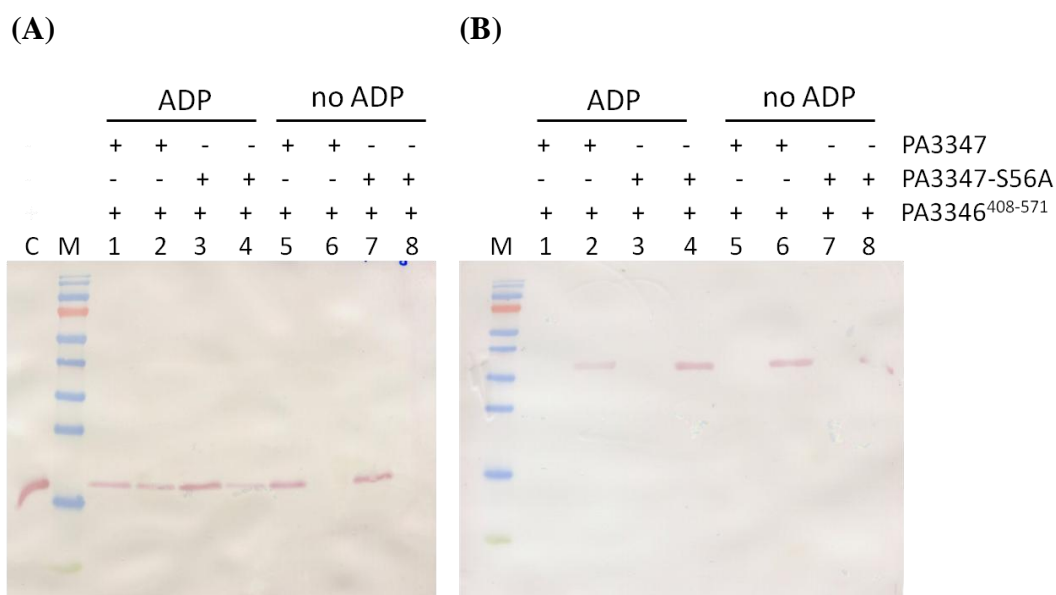


Fig. 2.6.8 Analysis of PA3346^{L408A-A571} and PA3347 protein-protein interaction by using GST pull down assay.

PA3346^{L408-A571} could be co-eluted with PA3347-GST and PA3347-S56A-GST in the presence of 2 mM ADP. Blot was incubated with monoclonal anti-His antibody (A), and with monoclonal anti-GST antibody (B). Lanes 1, 3, 5 and 7: washed with PBS; 2, 4, 6 and 8: eluted with 20 mM glutathione (50 mM Tris-HCl buffer, pH 8.0).

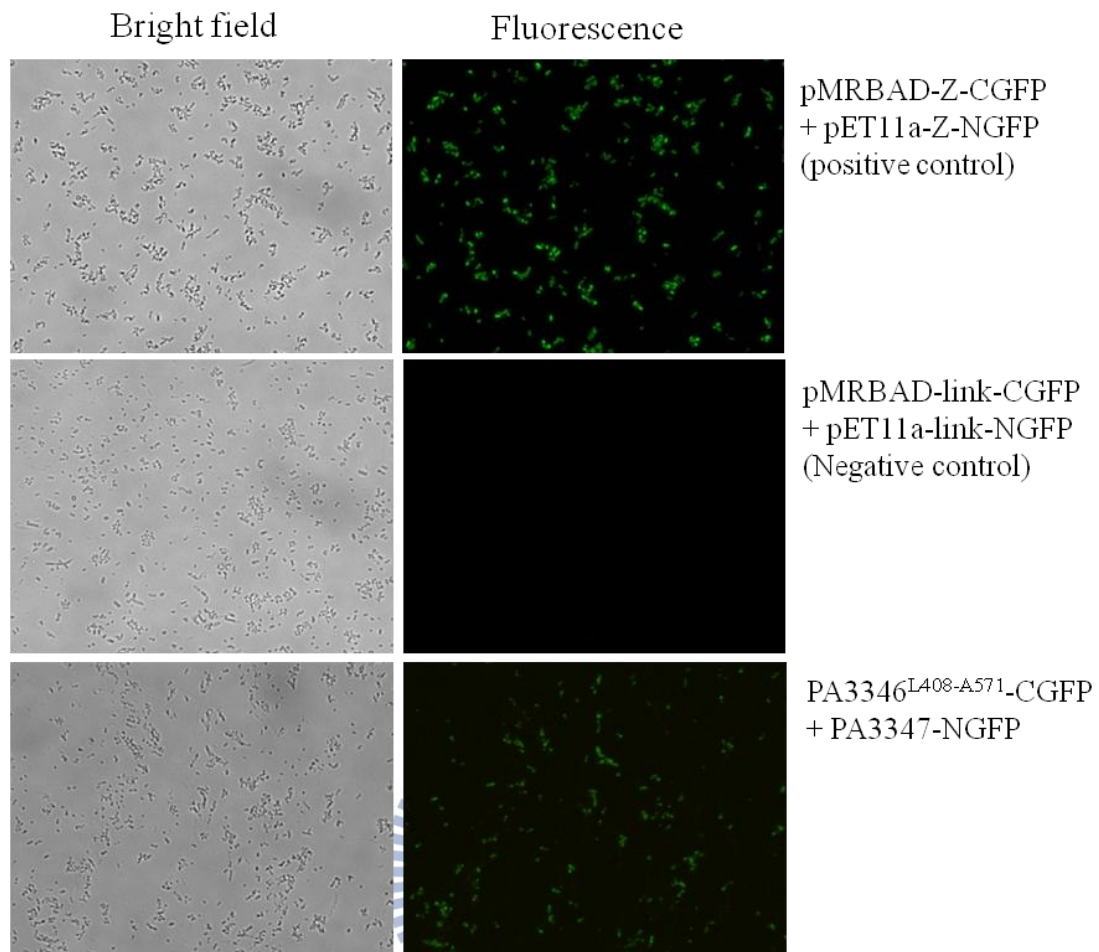


Fig. 2.6.9 Protein interaction of PA3347 and PA3346^{L408-A571} examined using the GFP fragment reassembly assay

E. coli BL21 (DE3) harboring the plasmids indicated at the right side of the graph was grown on LB agar plate containing 100 μ M IPTG and 0.05% arabinose at 20°C for 3 days. The bacterial cells were taken at 200X magnification using an upright fluorescence microscope (BX-51; Olympus). Both the positive control and PA3347/ PA3346^{L408-A571} pairs displayed green fluorescence indicating that PA3347 can interact with PA3346^{L408-A571}.

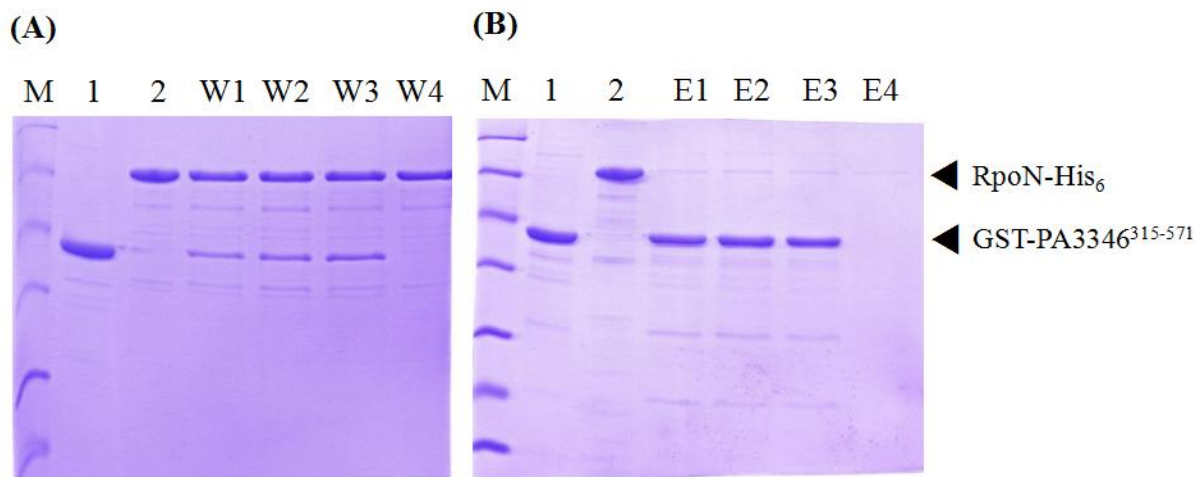
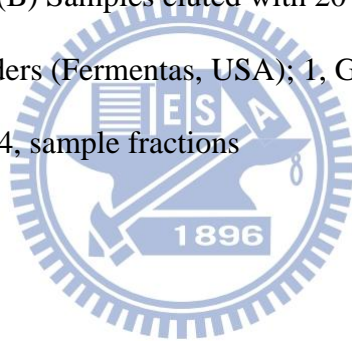


Fig. 2.6.10 Analysis of PA3346 and RpoN protein-protein interaction using GST pull down assay.

(A) Samples washed with PBS. (B) Samples eluted with 20 mM glutathione/50 mM Tris buffer. M, unstained protein ladders (Fermentas, USA); 1, GST-PA3346³¹⁵⁻⁵⁷¹; 2, RpoN-His₆; W1-W4, sample fractions; E1-E4, sample fractions



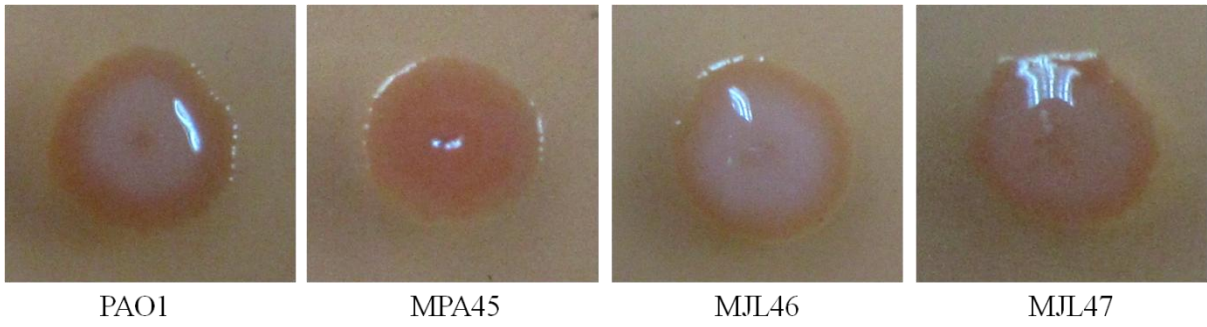
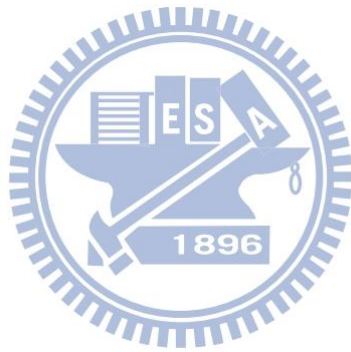


Fig. 2.6.11 Colony morphology of *P. aeruginosa* PAO1 and mutants on Congo red plate

After 2 days of incubation at 30°C, the colony morphology of each of the strains was recorded by a Canon camera (PowerShot G10). The name of the strains was indicated under the photos.



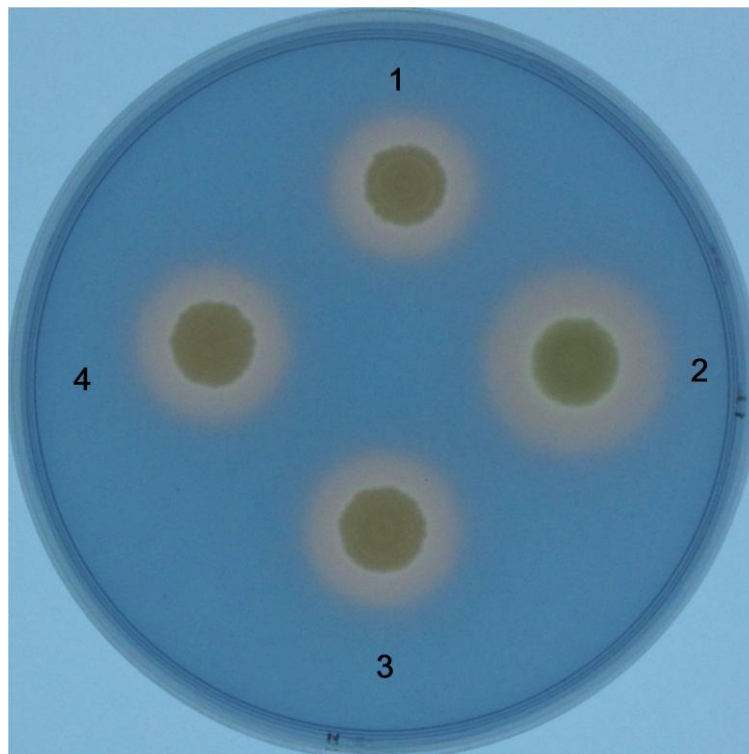


Fig. 2.6.12 The CAS plate assay

The siderophore, a strong iron chelator, removes ferric iron from the CAS/HDTMA complex and resulted in the color changes from blue to orange. The orange halos around the colonies revealed that all strains produced a similar amount of siderophore. The CAS plate assays were performed independently at least three times. 1, PAO1 2, MPA45; 3, MJL46; 4, MJL47.

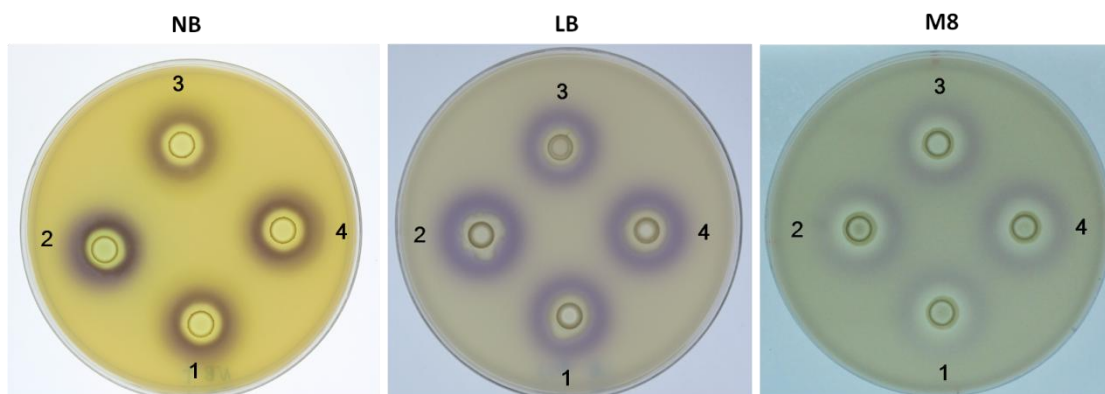
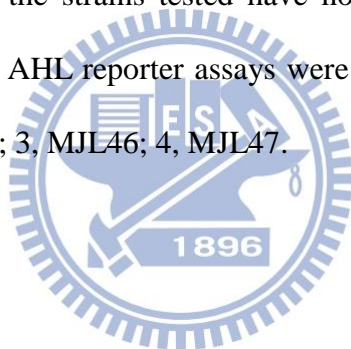


Fig. 2.6.13 The N-Acyl homoserine lactones (AHL) reporter plate bioassays

C. violaceum CV026 was used as a reporter strain to detect the AHL molecules produced by *P. aeruginosa* PAO1 and the mutant strains. By comparing the purple color appeared around the wells, the AHL productions of the strains tested have no significant difference regardless medium used in this assay. The AHL reporter assays were performed independently at least three times. 1, PAO1; 2, MPA45; 3, MJL46; 4, MJL47.



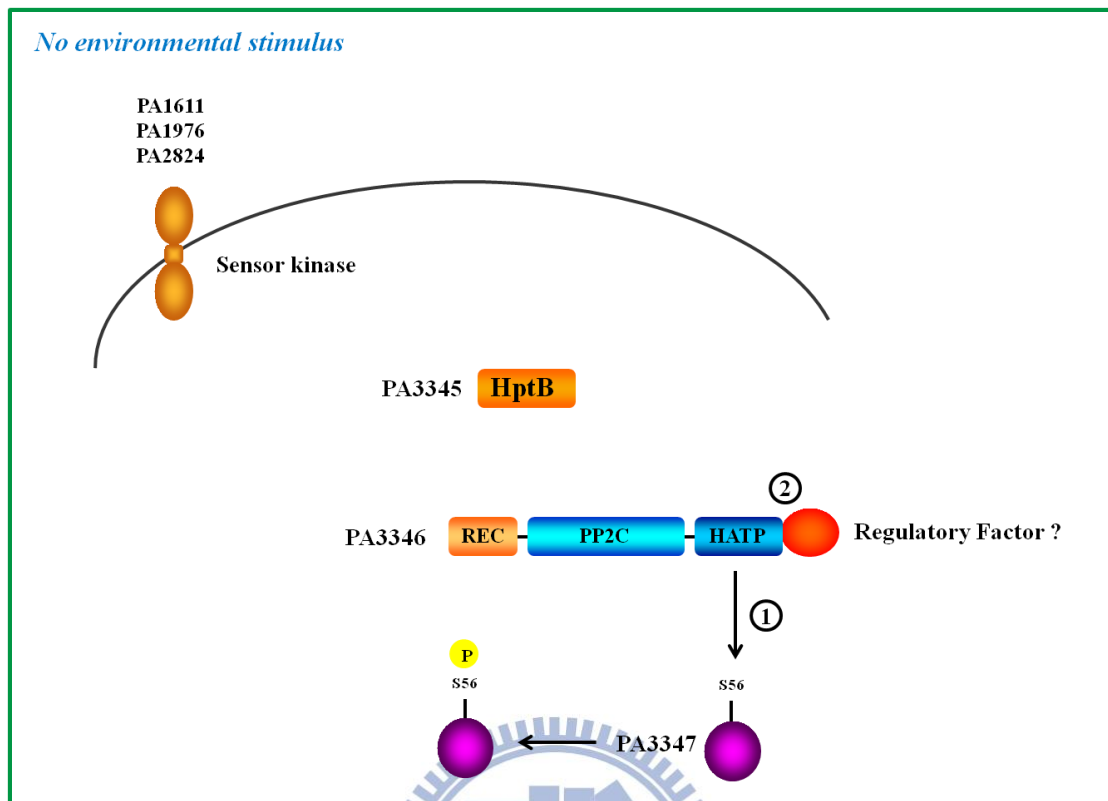


Fig. 2.6.14 A hypothetical model of the combination of the HptB-mediated phosphorelay and partner switching regulatory system.

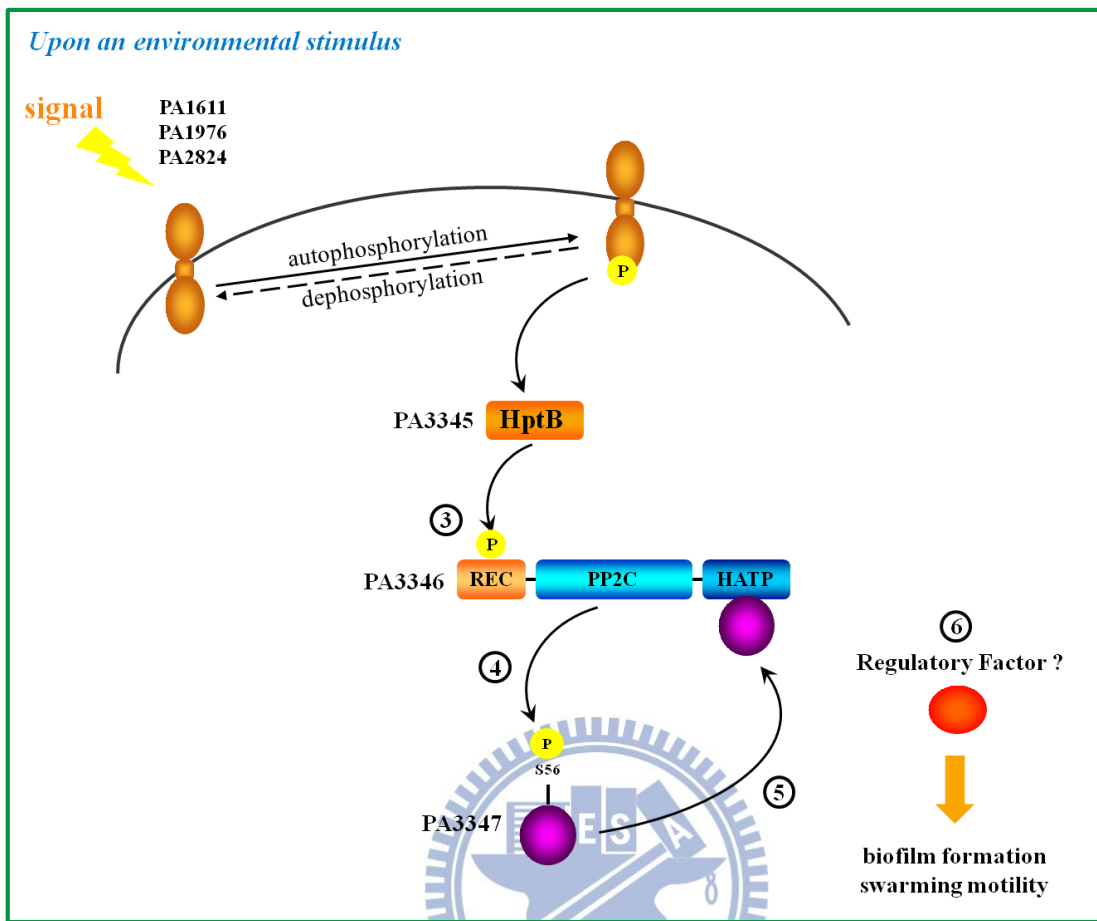
PA3346C is the C-terminal L408-A571 HATP Ser protein kinase domain of PA3346.

(A) No environmental stimulus

① PA3346C phosphorylates the putative anti-sigma factor antagonist PA3347 on Ser56.

PA3347~P is inactive and could not bind PA3346C.

② PA3346C binds a regulatory factor, preventing the occurrence of the downstream response.



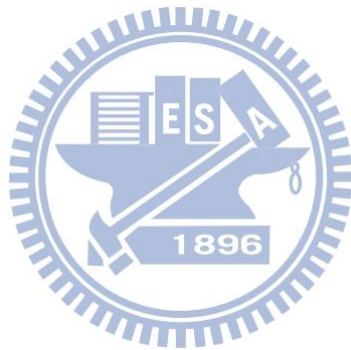
(B) Upon an environmental stimulus

- ③ A sensor kinase (PA1611, PA1976 or PA2824) autophosphorylates itself and transfers the phosphoryl group to HptB, which then relays the signal to response regulator PA3346 (D61 or D68?).
- ④ The phosphorylation on PA3346 N-terminal receiver domain results in an increase in its Ser protein phosphatase activity leading to dephosphorylation of the putative anti-sigma factor antagonist PA3347.
- ⑤ The unphosphorylated form of PA3347 binds PA3346C.
- ⑥ The regulatory factor is released from PA3346C then affects biofilm formation and swarming motility.

Chapter 3

Transcriptome analysis of galactose stress in the *K. pneumoniae*

CG43S3 $\Delta galU$ mutant



3.1 Abstract

K. pneumoniae $\Delta galU$ mutant, which is defective in UDP-Glc PPase, was observed to have a clear growth-inhibition zone on galactose disk diffusion assay. When bacteria were cultivated in M9 minimal medium where 2% glycerol is the sole carbon source, galactose can inhibit the bacterial growth and increase mortality. It is known that the galactose toxicity on $\Delta galU$ mutant was due to the disorder of galactose metabolism and accumulations of toxic galactose metabolites. However, how the toxic intermediates affect the gene expression and cause the cell death remains unclear. Therefore, we study the gene expression profiles of *K. pneumoniae* CG43S3 $\Delta galU$ under the galactose stress by RNA-seq. After analyzing RNA-seq data, we found *galETKM*, *galP*, *lacYZ* and genes responsible for amino acid biosynthesis are upregulated in the presence of galactose. The gene expressions of glycerol metabolism (*pduCDE*), iron-acquisition systems (*sitABCD* and *feoABC*) and 12 regulatory factors (*hns*, *csrA* and 10 transcriptional regulators) are repressed. Notably, H-NS and CsrA are global regulatory proteins controlling a large variety of physiological processes such as carbon metabolism, virulence, bacterial motility and stress response systems. Besides, *E. coli* *csrA* gene was shown to be essential for growth in LB medium and minimal medium. Based on our RNA-seq data and literature review, we speculate that the gene expressions of carbon metabolism and iron-acquisition systems were induced or repressed because of the growth condition. The toxic galactose metabolites might indirectly repress the gene transcriptions of H-NS, CsrA and transcriptional regulators, causing problems on gene transcriptions and translations. Finally, the cell death occurs because of the disorder in bacterial physiology.

3.2 Introduction

D-galactose is a monosaccharide which is transported into cells through a specific transporter (85-87). To enter the glycolytic and the glycans biosynthesis pathway, galactose

needs to be activated and catalyzed by the Leloir pathway enzymes, GalETK (88,89). Galactose is first phosphorylated by galactokinase (GalK) to form Gal-1-P. By the catalysis of Gal-1-P uridylyltransferase GalT, Gal-1-P and UDP-glc are converted into UDP-gal and Glc-1-P. UDP-gal can enter the glycan biosynthesis pathway as a galactosyl donor, or be converted into UDP-glc by UDP-gal epimerase (GalE) (89). In humans, an inherited deficiency in any of the three enzymes leads to the galactose metabolic disorder called galactosemia (90). Galactose intake by galactosemia patients can result in general organ damage. Researchers speculate that the toxic effects might come from the abnormal accumulations of galactose metabolic intermediates, especially Gal-1-P (90-93). Up to the present time, the *in vivo* target(s) for Gal-1-P toxicity remains unclear.

In prokaryotes, galactose is also toxic to the *galETK* deficient strain. *Streptococcus mutans* $\Delta galK$ (94), *Bacillus subtilis* $\Delta galE$ (95), *Salmonella choleraesuis* $\Delta galE$ (96), *Salmonella enterica* serovar Typhimurium $\Delta galE$ (97), *E. coli* $\Delta galT$ (98) are all sensitive to galactose and cannot grow in medium supplemented with galactose. Cell lysis occurred in $\Delta galE$ mutant strains of *B. subtilis* and *S. enterica* when the medium were added exogenous galactose (95,97). As for $\Delta galT$ mutant of *Saccharomyces cerevisiae*, the growth of this GalT-deficient yeast strain stopped 4 h after the addition of 0.2% galactose into YEPgly medium (99). Similar to the case in humans, the toxic effects come from the abnormal accumulations of Gal-1-P or UDP-gal (92,95). In our previous study, we found that galactose is also toxic to *K. pneumoniae* CG43S3 $\Delta galU$ mutant, which is defective in UDP-Glc PPase. The GalU-deficient strain was observed to have a clear growth-inhibition zone on galactose disk diffusion assay. In addition, the colony color of *K. pneumoniae* $\Delta galU$ mutant on MacConkey-0.4% galactose agar displayed pale pink, indicating that the GalU-deficient strain is incapable of fermenting galactose (100,101). The gene *galU* encodes the enzyme

UDP-Glc PPase, which synthesizes UDP-Glc from Glc-1-P and UTP. Though not belonging to the components of the Leloir pathway, GalU plays a role in synthesizing and providing UDP-glc for the enzymatic reaction catalyzed by GalT. Therefore, it is interesting to know why galactose is toxic to bacterial cells with a defective *galU* gene.

In this study, we clarify if the cell death occurs on $\Delta galU$ mutant strain in the presence of galactose by performing the Live/Dead fluorescence stain. To further understand the molecular mechanism of the galactose toxicity, we compared the gene transcriptions of *K. pneumoniae* CG43 $\Delta galU$ mutant in the M9gly medium with or without 0.5% galactose by RNA-seq and revealed the significant differences in gene expression profiles. We hope that the study of galactose effects on *K. pneumoniae* $\Delta galU$ mutant model will help us to understand the pathogenic mechanism of the galactose toxicity at the molecular level.

3.3 Materials and methods

3.3.1 Bacteria strains and growth medium

K. pneumoniae CG43 wild type and $\Delta galU$ mutant strains used in this study are grown in Luria-Bertain medium or M9 medium. M9 minimal (M9) medium contains M9 minimal salt (Sigma-Aldrich[®]), 0.1 mM CaCl₂, 2 mM MgSO₄. The carbon sources used in this study were 2% glycerol, 0.5% glucose or 0.5% galactose. All chemicals were purchased from Sigma-Aldrich[®].

3.3.2 Bacterial growth curve

K. pneumoniae CG43 wild type and $\Delta galU$ mutant strain were grown in LB medium or M9-glycerol medium at 37°C overnight. The overnight bacterial cultures were transferred into LB medium or M9-glycerol medium in the presence or absence of 0.5% galactose for propagation. The optical density of each bacterial culture was measured every hour at the

wavelength of 595 nm by a spectrophotometer (Jasco V-530). The results are the average of three independent experiments.

3.3.3 Disk diffusion assay

Overnight bacterial cultures were spread onto LB agar plates (1.5%, w/v) using cotton swabs. Paper disks impregnated with 3 μ l of 50% galactose were placed on top of the bacterial lawn and the dishes were incubated at 37°C overnight and the diameter of inhibition zone was scored.

3.3.4 LIVE/DEAD[®] BacLight[™] Bacterial Viability assay

K. pneumoniae CG43 $\Delta galU$ mutant strain were grown in M9 medium containing 2% glycerol as carbon source at 37°C overnight. Two milliliters of overnight bacterial culture were transferred into 100 ml fresh M9-glycerol (M9gly) medium for propagation. When the OD₅₉₅ reached to 0.1 to 0.2, galactose was added at the final concentration of 0.5%. After 3 h, the bacteria cells are mixed with the fluorescence dyes (LIVE/DEAD[®] BacLight[™] Bacterial Viability Kits, Molecular Probes) at a volume ratio of 1:1 and incubated at room temperature for 15 min in dark. Three microliters of the bacterial culture-fluorescence dye mixture were applied on slide and examined under a fluorescence microscope. All images were captured with an upright microscope (BX-51; Olympus) connected with a CCD camera. The data were analyzed using the SPOT Advanced Plus Imaging software (Sterling Heights, MI).

3.3.5 RNA purification

The growth condition is the same as described in LIVE/DEAD[®] BacLight[™] Bacterial Viability assay. Fifty milliliters of bacterial culture were transferred to a centrifugal tube and centrifuged at 6000 g for 5 min at 4°C. The supernatant was discarded and the bacterial cells

were re-suspended by adding 5 ml TRIzol[®] reagent (Invitrogen, USA). Then, the bacterial lysate with TRIzol[®] reagent was incubated at room temperature for 5 min to allow complete dissociation of nucleoprotein complexes. One milliliter of chloroform was added into the lysate-TRIzol[®] reagent mixture with vigorously vortex for 15 s. After incubated at room temperature for 3 min, the sample was centrifuged at 12,000 g for 15 min to separate the aqueous phase and organic phase. The aqueous phase (upper layer) was transferred to a fresh RNase-free tube and an equal volume of 70% ethanol was added in the aqueous phase to obtain a final ethanol concentration of 35%. The sample was transferred to a spin cartridge and the RNA was purified by following the standard protocol of PureLink[™] Micor-to-Midi Total RNA Purification Kit (Invitrogen, USA). Finally, total RNA was eluted by 70 µl of RNase-free water (Qiagen).

The next step is to remove the DNA contamination by performing the DNase I digestion. The reaction mixture contains the total RNA, 4.5 mM MgCl₂/DEPC, 10 U DNase I (Promega) and 20 mM Tris-HCl/DEPC pH8.0. After the DNase I digestion mixture was incubated at 30°C for 30 min, an equal volume of phenol/chloroform/isoamylalcohol (25:24:1) was added into it. The mixture was mixed by vigorously vortex for 20 s and centrifuged at the maximal speed for 1 min. After the upper aqueous phase was transferred into a new tube, one tenth volume of 3 M NaCl and 2 volumes of ethanol were added. Then, the sample was stored at -20°C overnight. The next day, the sample was centrifuged at maximal speed for 10 min at 4°C. The supernatant was discarded and the RNA pellet was washed with 500 µl of 70% ethanol at least for 2 times. The sample was centrifuged at 12000 g for 1 min and then the supernatant was carefully discarded. After the RNA pellet was air-dried, forty microliters of RNase-free water were added to dissolve the RNA. The quality and quantity of RNA were examined by NanoDrop Spectrophotometer.

3.3.6 RNA sequencing

KPI and KPII represent the RNA sample of *K. pneumoniae* CG43 $\Delta galU$ and *K. pneumoniae* CG43 $\Delta galU$ challenged with 0.5% of galactose, respectively. The RNA concentrations (OD_{260}/OD_{280}) of KPI and KPII were 1541 ng/ μ l (2.01) and 1028.7 ng/ μ l (1.95). The cDNA library construction and raw data analysis were done by Tri-I Biotech, Inc. (Taipei, Taiwan).

3.4 Result and Discussion

3.4.1 A growth-inhibition zone is observed in *K. pneumoniae* $\Delta galU$ mutant strain in galactose disk diffusion assay

In our previous study, *K. pneumoniae* CG43-17, a Tn5-transposon insertion mutant which is defective in UDP-Glc PPase, showed a clear growth-inhibition zone on galactose disk diffusion assay (100). To further understand if *K. pneumoniae* CG43 $galU$ null mutant is also sensitive to galactose, the disk diffusion assay was performed. The bacterial cultures were applied onto LB agar and the paper disks impregnated with galactose or glucose are placed on the top of the bacterial lawn. As shown in Fig. 3.6.1, after an overnight incubation at 37°C, it is found that both *K. pneumoniae* CG43 wild type and $\Delta galU$ mutant were not sensitive to glucose. However, *K. pneumoniae* CG43 $\Delta galU$ mutant but not the wild type strain showed a clear inhibition zone around the galactose paper disk. The diameter of the inhibition zone is approximately 2.69 ± 0.07 cm. It is known that $galU$ encodes the enzyme UDP-Glc PPase, which synthesizes UDP-Glc from Glc-1-P and UTP. Although GalU is not a component of the Leloir pathway (GalETK), the null mutation of $galU$ makes the bacteria unable to produce UDP-Glc normally that leads to defective galactose metabolism. Finally, the accumulation of toxic intermediates, such as Gal-1-P or UDP-Gal, causes the inhibition of

bacterial growth (95,102,103).

3.4.2 Galactose inhibits growth of *K. pneumoniae* $\Delta galU$ mutant

K. pneumoniae CG43 wild type and $\Delta galU$ mutant strain were grown in LB medium at 37°C overnight. The next day, the bacterial cultures were sub-cultured in fresh LB medium containing various concentrations of galactose. As shown in Fig. 3.6.2, *K. pneumoniae* CG43 wild type strain grew slightly better in the medium containing 0.5% to 5% of galactose, whereas 10% of galactose made the cells grow slower during the log phase. The bacterial growth became normal prior to entering the stationary phase. In addition, the growths of the $\Delta galU$ mutant strain were impaired in the medium containing 2.5%, 5% and 10% of galactose during the log phase, but all of them grew well after 12 h of propagation. Although the $\Delta galU$ strain was sensitive to galactose in disk diffusion assay, the toxicity of galactose to the $\Delta galU$ mutant strain was not obvious in LB broth culture. It might be due to the abundant carbon source in LB medium that the *K. pneumoniae* $\Delta galU$ mutant could bypass galactose metabolism.

To avoid the interference from other carbon sources, the $\Delta galU$ mutant strain was cultured in M9 minimal medium where 2% glycerol was the sole carbon source (104). The $\Delta galU$ mutant strain grew quite slowly in M9gly medium. After about 20 h of propagation, the bacterial cells were sub-cultured into fresh M9gly medium. When the optical density at 595 nm reached to 0.1 to 0.2 AU, the bacterial culture was divided into two equal halves. Galactose was added into one half at the final concentration of 0.5% (w/v). Interestingly, galactose did not immediately affect the growth of the $\Delta galU$ mutant (Fig. 3.6.3A). The phenomenon is similar to the growth response of *Saccharomyces cerevisiae* $\Delta galT$ mutant and *B. subtilis* $\Delta galE$ mutant to galactose. After the addition of galactose for 2 to 4 h, these mutant strains displayed severe growth retardation (95,104). The result may be due to the

accumulation of toxic galactose metabolites after a few hours of propagation to a level sufficient to inhibit cell growth. As shown in Fig. 3.6.3A, 1.5 h after the addition of galactose, it is found that the optical density (OD₅₉₅) of the $\Delta galU$ mutant strain in the M9gly medium supplemented with galactose was approximately half of that without galactose. This result revealed that low concentration of galactose could inhibit the growth of *K. pneumoniae* $\Delta galU$ mutant cultivated in minimal medium where glycerol is the sole carbon source.

3.4.3 Galactose induces death of *K. pneumoniae* $\Delta galU$ mutant

In *B. subtilis* NCIB3610, the *galE* null mutant was sensitive to exogenous galactose. After cultivated in LB medium supplemented with galactose for a few hours, the optical density (OD₆₀₀) of *B. subtilis* *galE* mutant strain was abruptly decreased because high abundance of cell lysis occurred (95). To test whether the cell death of *K. pneumoniae* $\Delta galU$ mutant strain also occurred in the presence of galactose, the bacterial cells treated with galactose for 3 h were collected and subjected to live/dead staining. Fluorescence microscopy imaging showed that all of the cells were alive after 1 h of propagation in M9gly medium (Fig. 3.6.3B, green fluorescence). However, after the addition of galactose for 3 h, increasing numbers of dead bacterial cells (red fluorescence) were observed, suggesting that galactose also induced the cell death of *K. pneumoniae* $\Delta galU$ mutant. Probably because GalU does not play a crucial role in the accumulation of toxic galactose metabolites, the cell death of *K. pneumoniae* $\Delta galU$ mutant was not as dramatic as *B. subtilis* *galE* mutant. Although the cell death rate of *K. pneumoniae* $\Delta galU$ mutant is not higher than 50%, our result is in agreement with previous literatures reporting that galactose is toxic to the bacterial strains deficient in the enzymes of the Leloir pathway (94,95,97,102-104).

3.4.4 Transcriptome analysis of *K. pneumoniae* $\Delta galU$ gene expression profiles under galactose stress

Many literatures have reported that galactose metabolites, especially Gal-1-P, are toxic to bacterial strains deficient in the enzymes of the Leloir pathway (GalETK). Until now, how the toxic intermediates cause the cell death and what the targets of those toxic intermediates are remain elusive (93,104). Therefore, we attempted to find the targets of toxic galactose metabolites and understand the molecular mechanism of the galactose toxicity by performing RNA sequencing. Approximately 10.41 and 10.54 million 150-bp pair end reads from *K. pneumoniae* $\Delta galU$ and *K. pneumoniae* $\Delta galU$ (+Gal), respectively, were generated using Illumina HiSeq 2000 Sequencing System and analyzed by CLC-Genomics Workbench. The transcriptomic data revealed that 44 and 144 genes were up- and down-regulated, respectively more than 2 folds in the *K. pneumoniae* $\Delta galU$ mutant in the presence of galactose. These genes accounted for about 3.84% of the total genes in *K. pneumoniae*. It has been known that adding galactose into growth medium could induce the transcriptions of *gal* regulon (*galETK*) and galactose permease (*galP*) in *Saccharomyces cerevisiae galE* and *galT* mutant strains (104,105). When focus on the upregulated genes of *K. pneumoniae* $\Delta galU$ mutant listed in Table 3.5.1, the expression of the *gal* regulon (*galETKM*) and galactose permease (*galP*) was increased in the presence of galactose consistent with the previous literature. In addition, the *lacYZ* and genes responsible for amino acid biosynthesis were also induced in the *K. pneumoniae* GalU-deficient strain upon galactose stress.

Among the downregulated genes, *pduCDE*, *D364_17595*, and *D364_17590* which are responsible for glycerol metabolism (106) and some sugar transporter genes are repressed. Unexpectedly, two iron-acquisition systems, *sitABCD* and *feoABC*, were also repressed in the presence of galactose (Table 3.5.2). These two gene clusters are regulated by ferric uptake regulator (Fur) and their putative Fur binding boxes were listed in Table 3.5.5 (107). Under iron-replete conditions, dimeric Fur in complex with ferrous ion (Fe^{2+}) binds to the Fur box,

19 bp consensus DNA sequence (GATAAT-GATAAT-CATTATC), preventing *sitABCD* and *feoABC* from transcription (108-111). However, M9gly medium used in this study is deficient in ferrous ion (Fe^{2+}), the repressed transcription of *sitABCD* and *feoABC* under iron-limited condition implied that other regulatory factors might participate. One of the possible regulatory factors is RyhB, a 91 nucleotide non-coding RNA which was induced by iron starvation (112). In *E. coli*, a microarray-based analysis revealed that overproduction of RyhB indirectly repressed the expression of *fhuF*, *feoA* and *feoB* (113). Besides, RyhB was found to repress the expression of *sitA* in *K. pneumoniae* presumably by direct base pairing with *sitA* mRNA (114). To sum up, the transcriptional repressions of *sitABCD*, *feoABC* and genes encoding iron-utilizing proteins might be due to the expression of RyhB in M9gly medium (0.5% galactose).

Interestingly, the genes subjected to galactose-mediated activation and suppression in the *K. pneumoniae* $\Delta galU$ mutant is clustered, suggesting that some transcriptional regulators participate in controlling the gene expression. Therefore, three hundred base pair upstream regions of these gene clusters were analyzed and the putative regulator binding sites were predicted using the bacterial regulon analyzer Virtual Footprint (<http://www.prodoric.de/vfp/>) (115). Most of the promoter regions, including P_{galE} , P_{galP} , P_{pduC} , P_{D364_17615} , P_{sitA} and P_{feoA} were predicted to have a CRP binding box (Table 3.5.3). CRP is a global transcriptional regulator and requires the binding of cyclic AMP (cAMP) for complete activity (116). Up to now, a total of 346 promoters in *E. coli* K12 genome have been proposed to be under the control of cAMP-CRP (117). The cAMP-CRP complex binds to specific sites upstream of promoters, causing transcriptional activation or repression (118). The production of cAMP is reduced in the presence of glucose. When bacteria are grown in glyceol minimal medium or medium supplemented with less-preferred carbon sources, bacteria produce higher levels of

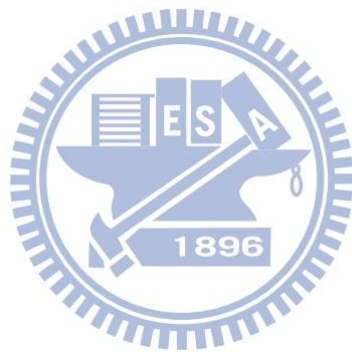
cAMP leading to the formation of cAMP-CRP complex (119-121). Our bacterial culture condition favors more cAMP-CRP complex formation and therefore leads to *galETKM*, *galP*, and *pduCDE* transcription.

In addition to genes involved in carbon metabolism and iron-acquisition, 12 regulatory genes are downregulated in the *K. pneumoniae* $\Delta galU$ mutant under galactose stress. Notably, two global regulators, H-NS and CsrA, were repressed in the presence of galactose. H-NS is homologous to eukaryotic histones and has been extensively studied in *E. coli* and *Salmonella typhimurium* (122,123). H-NS plays important roles in bacterial DNA packaging and silencing genes involved in metabolism, flagellum synthesis, virulence and adaptation to environmental challenges (123-126). However, genes known to be repressed by H-NS were not significantly upregulated in our transcriptome data (124). We also analyzed the upstream promoter regions of P_{lacZ} , $P_{D364-17615}$, P_{pduC} , P_{sitA} , and P_{feoA} . Although extremely conserved H-NS nucleating high-affinity sites were found (Table 3.5.4) (127), no literature has ever reported that these genes are under regulation of H-NS. CsrA, a post-transcriptional regulator, controls a large variety of physiological processes such as central carbon metabolism, virulence, pathogenesis, c-di-GMP synthesis, biofilm formation, quorum sensing as well as bacterial motility and stress response (128-134). CsrA is an RNA-binding protein. The protein binds to a region typically nearby or overlapping with Shine-Dalgarno sequence to block the ribosome binding, resulting in inhibition of translation initiation and rapid mRNA degradation (135-137). In some cases, CsrA served as a positive regulator through binding to the 5' untranslated region to stabilize the mRNA, leading to the enhancement of translation efficiency (138). *E. coli* *csrA* gene was shown to be essential for growth in LB medium and minimal medium supplemented with glycolytic carbon sources (139), revealing the important role of CsrA in bacterial viability. Therefore, based on the RNA-seq results, we proposed that

when *K. pneumoniae* $\Delta galU$ mutant was cultivated in minimal medium supplemented with galactose, the accumulation of toxic galactose metabolites might indirectly target to H-NS, CsrA and several other transcriptional regulators, causing problems on transcription and translation. Eventually, the bacterial growth becomes slow and cell death increases (Fig. 3.6.3B) because of disruption of normal bacterial physiology.

In summary, our transcriptomic results indicate that expression of carbon metabolism and iron-acquisition systems was affected in our culture medium providing galactose stresses. Based on promoter prediction results and literature review, we hypothesized that the transcription of these genes might be under the regulation of cAMP-CRP complex. In addition, *K. pneumoniae* $\Delta galU$ mutant increased the expression of *galETKM* in nutrient-deficient growth condition. However, because GalU deficiency in *K. pneumoniae* interrupts normal galactose metabolism, the higher amounts of GalP and GalETKM in cells may accelerate accumulations of toxic galactose metabolites, which in turn indirectly repress the expression of *hns* and *csrA* whose functions are important in DNA packaging and bacterial viability. Previously, Slepak and colleagues found that ribosomal protein (RP) genes and genes involved in RNA metabolism were repressed in *S. cerevisiae* *galT* mutant challenged with galactose (104). This phenomenon was due to the accumulation of Gal-1-P, the toxic galactose metabolite, in *galT* deficient strain. It was known that these two groups of genes were repressed via signal transduction pathways when *S. cerevisiae* is subjected to external stress stimulus such as hydrogen peroxide, DTT or heat shock. Thus, the authors proposed that “Gal-1-P stress” repressed the transcriptions of RP and RNA metabolism genes through signal transduction pathways responsible for responding to environmental stimulus (104,140). Similarly, the toxic galactose metabolites accumulated in *K. pneumoniae* $\Delta galU$ mutant can be seen as a stress signal and might influence the gene expression via a “known”

signal transduction pathway or regulatory factor. Therefore, understanding which signal transduction pathway or regulatory factor participated in repressing the transcriptions of *hns*, *csrA* and transcriptional regulator genes will bring us to find the *in vivo* target(s) of toxic galactose metabolites. Finally, we hope that the transcriptome study of galactose effects on *K. pneumoniae* $\Delta galU$ mutant helps us to understand how the toxic galactose metabolites cause cell death.



3.5 Tables

Table 3.5.1 Upregulated genes in CG43S3 $\Delta galU$ (+Gal) comparing with CG43S3 $\Delta galU$

Feature ID	Gene Name	Fold Change	Proposed Function
D364_03825	<i>galE</i>	81.26	UDP-glucose 4 -epimerase
D364_03820	<i>galT</i>	54.15	galactose-1-phosphate uridylyltransferase
D364_03815	<i>galK</i>	49.74	galactokinase
<i>galM</i> (D364_03810)	<i>galM</i>	29.80	galactose-1-epimerase
D364_17020	<i>galP</i>	15.74	D-galactose transporter
D364_07970	<i>lacY</i>	23.91	galactoside permease
D364_07975	<i>lacZ</i>	22.76	β -D-galactosidase
D364_20570	<i>dgoR</i>	11.91	galactonate operon transcriptional repressor
D364_20560	<i>dgoA</i>	6.82	2-dehydro-3-deoxy-6-phosphogalactonate aldolase
D364_20555	<i>dgoD</i>	13.22	galactonate dehydratase
D364_20550		5.64	galactonate transporter

(Continued)

Feature ID	Gene Name	Fold Change	Proposed Function
D364_07650		19.87	di- and tricarboxylate transporters, L-tartrate/succinate antiporte
D364_21575	<i>metE</i>	9.73	5-methyltetrahydropteroyltriglutamate-homocysteine methyltransferase
<i>glyA</i> (D364_14465)	<i>glyA</i>	7.64	Ser hydroxymethyltransferase
<i>glnA</i> (D364_20910)	<i>glnA</i>	7.44	glutamine synthetase
D364_17015	<i>metK</i>	7.25	S-adenosylmethionine synthetase
<i>glnH</i> (D364_04210)	<i>glnH</i>	6.02	glutamine ABC transporter periplasmic protein
D364_03465	<i>gltI</i>	5.70	glutamate and aspartate transporter subunit
D364_08005		5.33	5-methyltetrahydropteroyltriglutamate-homocysteine methyltransferase
<i>metQ</i> (D364_01015)	<i>metQ</i>	4.95	DL-methionine transporter substrate-binding subunit
D364_13485	<i>argT</i>	4.85	lysine-, arginine-, ornithine-binding periplasmic protein
D364_13470	<i>hisM</i>	4.76	histidine/lysine/arginine/ornithine ABC transporter permease HisM
D364_03460	<i>gltJ</i>	4.60	glutamate/aspartate ABC transporter permease GltJ

Table 3.5.2 Downregulated genes in CG43S3 $\Delta galU$ (+Gal) comparing with CG43S3 $\Delta galU$

Feature ID	Gene Name	fold change	Proposed Function
D364_17620	<i>dhaT</i>	-38.34	1,3-propanediol oxidoreductase (alcohol dehydrogenase)
D364_17615		-12.23	hypothetical protein
<i>pduC</i> (D364_17610)	<i>pduC</i>	-11.26	propanediol dehydratase large subunit
<i>pduD</i> (D364_17605)	<i>pduD</i>	-16.59	propanediol dehydratase medium subunit
<i>pduE</i> (D364_17600)	<i>pduE</i>	-14.89	propanediol dehydratase small subunit
D364_17595		-14.12	glycerol dehydratase
D364_17590		-12.61	glycerol uptake facilitator GlpF
D364_17580		-7.60	acid-resistance membrane protein
<i>hdeB</i> (D364_16510)	<i>hdeB</i>	-4.96	acid-resistance protein
<i>hdeB</i> (D364_17585)	<i>hdeB</i>	-4.25	acid-resistance protein
D364_23340		-7.02	sn-glycerol-3-phosphate transport system permease
<i>glpA</i> (D364_13220)	<i>glpA</i>	-5.96	sn-glycerol-3-phosphate dehydrogenase subunit A
<i>glpT</i> (D364_13215)	<i>glpT</i>	-4.94	sn-glycerol-3-phosphate transporter
<i>malE</i> (D364_22000)	<i>malE</i>	-8.11	maltose ABC transporter periplasmic protein
D364_22015	<i>malM</i>	-5.86	maltose regulon periplasmic protein
D364_22005		-6.75	ABC-type sugar transport systems, ATPase components
D364_15140		-8.51	PTS system glucitol/sorbitol-specific transporter subunit IIA
<i>srlA</i> (D364_15130)	<i>srlA</i>	-4.08	glucitol/sorbitol-specific PTS family enzyme IIC component

(Continued)

Feature ID	Gene Name	fold change	Proposed Function
D364_15335	<i>sitA</i>	-40.33	iron ABC transporter substrate-binding protein
D364_15340	<i>sitB</i>	-23.93	manganese/iron transport system ATP-binding protein
D364_15345	<i>sitC</i>	-23.24	iron transport system inner membrane permease component
D364_15350	<i>sitD</i>	-12.23	manganese ABC transporter, inner membrane permease protein SitD
<i>feoA</i> (D364_18960)	<i>feoA</i>	-9.36	ferrous iron transport protein A
<i>feoB</i> (D364_18965)	<i>feoB</i>	-7.14	ferrous iron transport protein B
D364_18970	<i>feoC</i>	-10.99	ferrous iron transport protein FeoC
D364_18675	<i>bfd</i>	-30.03	bacterioferritin-associated ferredoxin
D364_05240		-19.35	hypothetical protein;iron permease
D364_05245		-18.90	hypothetical protein; iron uptake system component EfeO
D364_24070	<i>fhuF</i>	-13.22	ferric iron reductase involved in ferric hydroximate transport
D364_10960	<i>tonB</i>	-12.62	transport protein TonB
D364_13700	<i>mntH</i>	-7.93	manganese transport protein MntH
D364_11490		-5.78	ferrichrome-iron receptor
D364_00795		-4.25	iron-hydroxamate transporter substrate-binding subunit
D364_00785		-4.10	ferrichrome outer membrane transporter

(Continued)

Feature ID	Gene Name	fold change	Proposed Function
D364_10085		-8.51	LysR family transcriptional regulator
D364_12135		-7.44	LysR family transcriptional regulator
D364_17675		-6.38	PadR family transcriptional regulator
D364_06175		-5.32	DNA-binding transcriptional activator OsmE
D364_13730	<i>yfeR</i>	-5.05	LysR family transcriptional regulator
D364_01955	<i>bolA</i>	-5.00	transcriptional regulator BolA
D364_11035	<i>hns</i>	-4.78	global DNA-binding transcriptional dual regulator H-NS
D364_04125	<i>ybiH</i>	-4.73	DNA-binding transcriptional regulator
D364_07595		-4.41	DNA-binding transcriptional regulator
D364_18425	<i>envR</i>	-4.08	DNA-binding transcriptional regulator EnvR
D364_23815	<i>cstA</i>	-6.25	carbon starvation protein CstA
D364_15080	<i>csrA</i>	-4.06	carbon storage regulator

Table 3.5.3 Predicted CRP binding site in the upstream region of galactose regulated genes

Gene	CRP binding site		
	5'-TG(T/C)GA:N ₆ :TC(A/G)CA-3'		
<i>P_{galE}</i>	-75	CT <u>T</u> GT:GCTATG: <u>TCACA</u>	-60
<i>P_{galP}</i>	-81	CGTGA:TTATAG: <u>TCACG</u>	-66
<i>P_{D364_17615}</i>	-209	<u>TGTGA</u> :TCGCCC: <u>GCAAT</u>	-194
<i>P_{pduC}</i>	-223	ATT <u>G</u> C:GGGCGA: <u>TCACA</u>	-202
<i>P_{pduC}</i>	-127	AT <u>T</u> TA:TTTTTT: <u>TCACC</u>	-106
<i>P_{sitA}</i>	-68	CTTGT:GCTATA: <u>TAACA</u>	-53
<i>P_{feoA}</i>	-156	CCTGC:AGCGCA: <u>TCATA</u>	-141

Numbers are relative to the position of the translational start codon (Details are found in Appendix II). Nucleobase identical to the consensus CRP binding sequences are underlined.

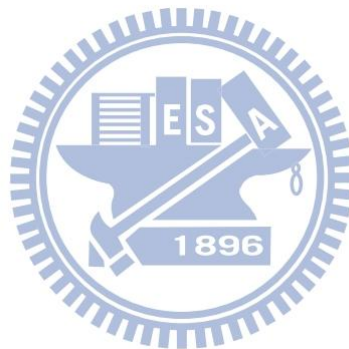


Table 3.5.4 Predicted H-NS binding site in the upstream region of the galactose regulated genes

Gene		H-NS binding site 5'-TCGATAAATT-3'	
<i>P_{lacZ}</i>	-105	<u>TCTGT</u> <u>T</u> <u>AATT</u>	-96
<i>P_{D364_17615}</i>	-283	<u>TCGTT</u> <u>TCAAT</u>	-274
<i>P_{D364_17615}</i>	-185	<u>TCAAT</u> <u>TAATA</u>	-176
<i>P_{pduC}</i>	-10	<u>CCGAT</u> <u>GACA</u>	-1
<i>P_{sitA}</i>	-79	<u>TTTATAA</u> <u>ATA</u>	-70
<i>P_{sitA}</i>	-44	<u>GCTATAA</u> <u>ACG</u>	-35
<i>P_{feoA}</i>	-189	<u>TCAATAA</u> <u>AAAA</u>	-180
<i>P_{feoA}</i>	-20	<u>GCGATAG</u> <u>ACA</u>	-11

Numbers are relative to the position of the translational start codon (Details are found in Appendix II). Nucleobase identical to the consensus H-NS binding sequences are underlined.

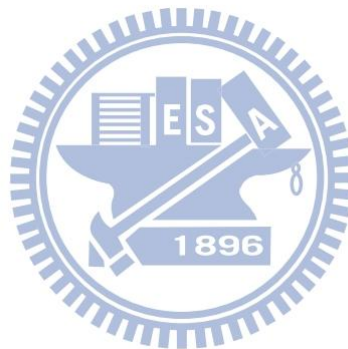
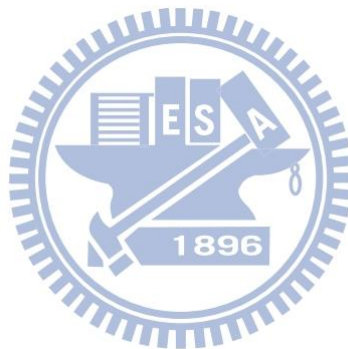


Table 3.5.5 Predicted Fur binding site in the upstream region of the galactose regulated genes

Gene	Fur binding box		
	5'-GATAAT:GATAAT:CATTATC-3'		
<i>P_{sitA}</i>	-99	<u>G</u> <u>C</u> <u>A</u> <u>A</u> <u>A</u> <u>T</u> : <u>A</u> <u>A</u> <u>G</u> <u>A</u> <u>A</u> <u>T</u> : <u>T</u> <u>A</u> <u>T</u> <u>T</u> <u>T</u> <u>T</u> <u>C</u>	-81
<i>P_{feoA}</i>	-134	<u>G</u> <u>A</u> <u>T</u> <u>G</u> <u>A</u> <u>T</u> : <u>A</u> <u>A</u> <u>A</u> <u>A</u> <u>A</u> <u>C</u> : <u>C</u> <u>A</u> <u>T</u> <u>T</u> <u>C</u> <u>T</u> <u>C</u>	-116

Numbers are relative to the position of the translational start codon (Details are found in Appendix II). Nucleobase identical to the consensus Fur binding sequences are underlined.



3.6 Figures

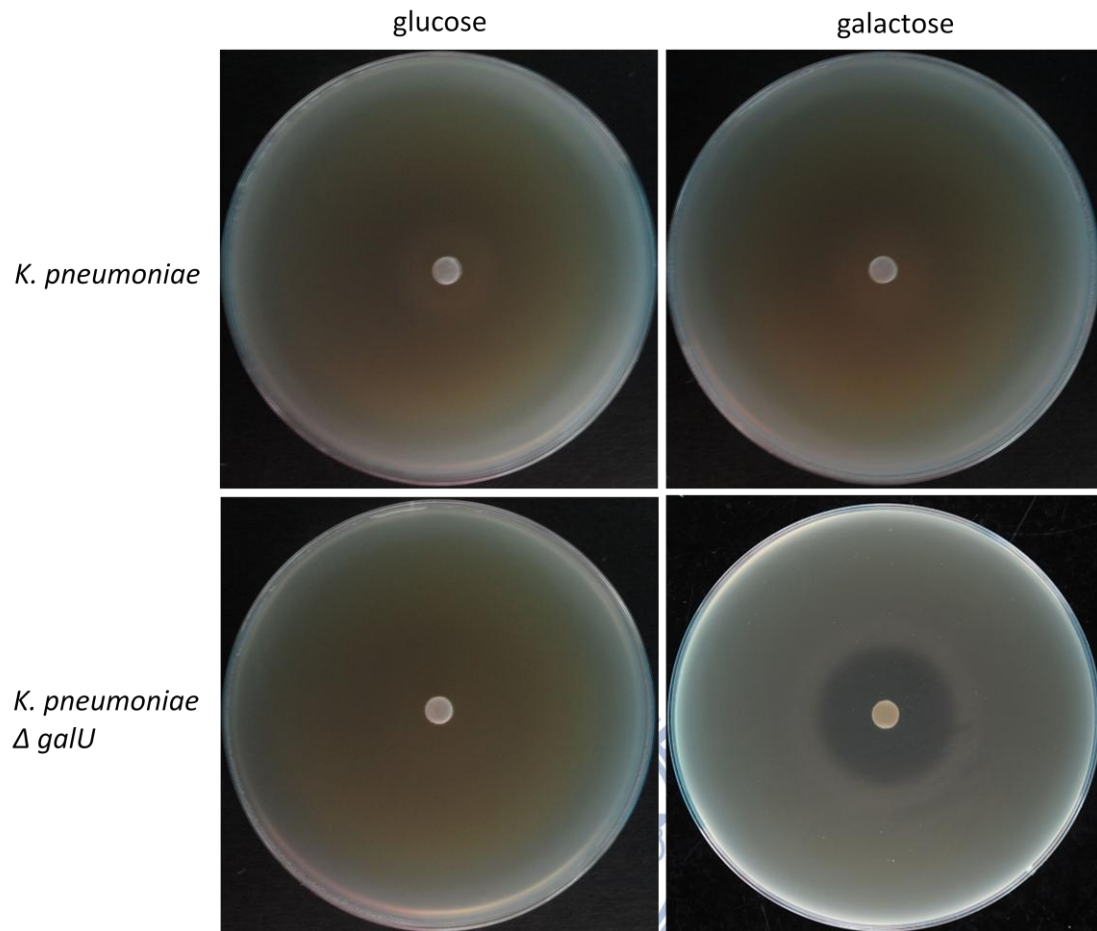


Fig. 3.6.1 Effects of glucose or galactose on *K. pneumoniae* CG43 S3 and $\Delta galU$ mutant using the disk diffusion assay

The bacterial cultures were applied onto LB agar plates and the paper disks impregnated with 3 μ l of 50% galactose or glucose were placed on the top of the bacterial lawn. After an overnight incubation at 37°C, the plates were examined and the pictures were taken by a Canon camera (PowerShot G10).

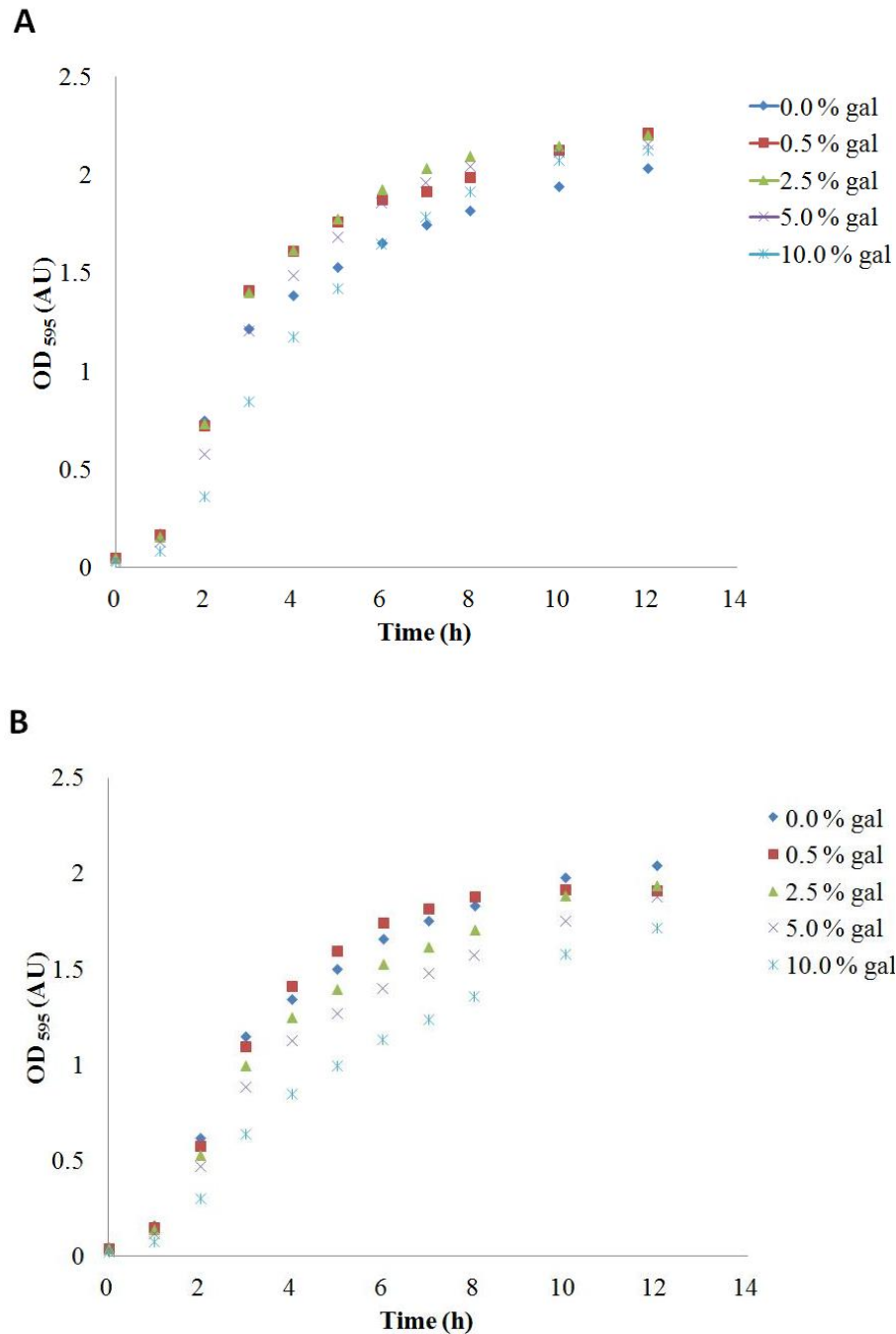


Fig. 3.6.2 Growth curve of *K. pneumoniae* CG43 S3 and the $\Delta galU$ mutant

(A)*K. pneumoniae* CG43 S3 (B)*K. pneumoniae* CG43 $\Delta galU$ mutant. The overnight bacterial cultures were sub-cultured in fresh LB medium containing various concentrations of galactose. The optical density of each bacterial culture was measured every hour at the wavelength of 595 nm by a spectrophotometer (Jasco V-530).

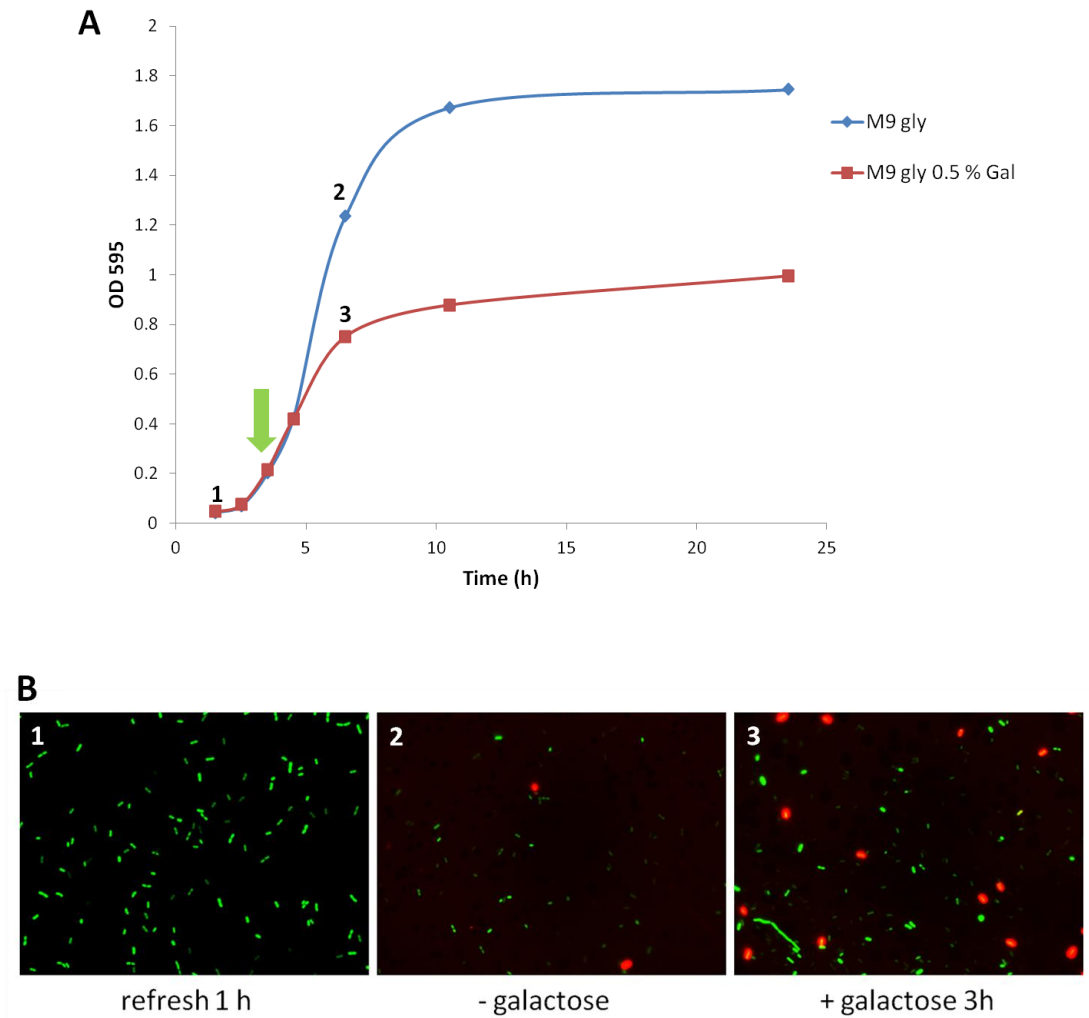


Fig. 3.6.3 The growth curve and Live/Dead cell staining of the *K. pneumoniae* CG43 $\Delta galU$ mutant

(A) Growth curve of *K. pneumoniae* CG43 S3 $\Delta galU$ mutant in M9gly medium containing 0.5% galactose. The green solid arrow indicates the time point at which the galactose is added into bacterial cultures. The numbers represent the time point at which the bacterial cells are collected for Live/Dead cell staining. (B) When the OD₅₉₅ reached to 0.1 - 0.2 AU, galactose was added into the bacterial cultures at the final concentration of 0.5% (w/v). After being treated with galactose for 3 h, the bacterial cells were mixed with the fluorescence dye for 15 min in dark and examined under a fluorescence microscope with a 100x objective lens.

References

1. Cleasby, A., Wonacott, A., Skarzynski, T., Hubbard, R. E., Davies, G. J., Proudfoot, A. E., Bernard, A. R., Payton, M. A., and Wells, T. N. (1996) The x-ray crystal structure of phosphomannose isomerase from *Candida albicans* at 1.7 angstrom resolution. *Nature structural biology* **3**, 470-479
2. Wu, B., Zhang, Y., Zheng, R., Guo, C., and Wang, P. G. (2002) Bifunctional phosphomannose isomerase/GDP-D-mannose pyrophosphorylase is the point of control for GDP-D-mannose biosynthesis in *Helicobacter pylori*. *FEBS letters* **519**, 87-92
3. Rocchetta, H. L., Pacan, J. C., and Lam, J. S. (1998) Synthesis of the A-band polysaccharide sugar D-rhamnose requires Rmd and WbpW: identification of multiple AlgA homologues, WbpW and ORF488, in *Pseudomonas aeruginosa*. *Molecular microbiology* **29**, 1419-1434
4. Proudfoot, A. E., Payton, M. A., and Wells, T. N. (1994) Purification and characterization of fungal and mammalian phosphomannose isomerases. *Journal of protein chemistry* **13**, 619-627
5. Proudfoot, A. E., Turcatti, G., Wells, T. N., Payton, M. A., and Smith, D. J. (1994) Purification, cDNA cloning and heterologous expression of human phosphomannose isomerase. *European journal of biochemistry / FEBS* **219**, 415-423
6. Jensen, S. O., and Reeves, P. B. R. (1998) Domain organisation in phosphomannose isomerases (types I and II). *Biochimica et biophysica acta* **1382**, 5-7
7. Shinabarger, D., Berry, A., May, T. B., Rothmel, R., Fialho, A., and Chakrabarty, A. M. (1991) Purification and characterization of phosphomannose isomerase-guanosine diphospho-D-mannose pyrophosphorylase. A bifunctional enzyme in the alginate biosynthetic pathway of *Pseudomonas aeruginosa*. *The Journal of biological chemistry* **266**, 2080-2088
8. Friedman, L., and Kolter, R. (2004) Two genetic loci produce distinct carbohydrate-rich structural components of the *Pseudomonas aeruginosa* biofilm matrix. *Journal of bacteriology* **186**, 4457-4465
9. Jackson, K. D., Starkey, M., Kremer, S., Parsek, M. R., and Wozniak, D. J. (2004) Identification of psl, a locus encoding a potential exopolysaccharide that is essential for *Pseudomonas aeruginosa* PAO1 biofilm formation. *Journal of bacteriology* **186**, 4466-4475
10. Duggleby, R. G., Peng, H. L., and Chang, H. Y. (1996) An improved assay for UDPglucose pyrophosphorylase and other enzymes that have nucleotide products. *Experientia* **52**, 568-572

11. Sousa, S. A., Moreira, L. M., Wopperer, J., Eberl, L., Sa-Correia, I., and Leitao, J. H. (2007) The Burkholderia cepacia bceA gene encodes a protein with phosphomannose isomerase and GDP-D-mannose pyrophosphorylase activities. *Biochemical and biophysical research communications* **353**, 200-206
12. Makinen, K. K., Makinen, P. L., Wilkes, S. H., Bayliss, M. E., and Prescott, J. M. (1982) Photochemical inactivation of Aeromonas aminopeptidase by 2,3-butanedione. *The Journal of biological chemistry* **257**, 1765-1772
13. Tawfik, D. S. (2002) Modification of Arginine Side Chains with p-Hydroxyphenylglyoxal. in *The Protein Protocols Handbook* (Walker, J. M. ed.), second Ed., Humana Press, Totowa, New Jersey. pp 475-476
14. Koplin, R., Arnold, W., Hotte, B., Simon, R., Wang, G., and Puhler, A. (1992) Genetics of xanthan production in Xanthomonas campestris: the xanA and xanB genes are involved in UDP-glucose and GDP-mannose biosynthesis. *Journal of bacteriology* **174**, 191-199
15. Griffin, A. M., Poelwijk, E. S., Morris, V. J., and Gasson, M. J. (1997) Cloning of the aceF gene encoding the phosphomannose isomerase and GDP-mannose pyrophosphorylase activities involved in acetan biosynthesis in Acetobacter xylinum. *FEMS microbiology letters* **154**, 389-396
16. Pain, R. (2004) Determining the CD Spectrum of a Protein. in *Current Protocols in Protein Science* (John E. Coligan, B. M. D., David W. Speicher, Paul T. Wingfield ed.), John Wiley & Sons, Hoboken, New Jersey. pp Unit 7.6
17. Magliery, T. J., Wilson, C. G., Pan, W., Mishler, D., Ghosh, I., Hamilton, A. D., and Regan, L. (2005) Detecting protein-protein interactions with a green fluorescent protein fragment reassembly trap: scope and mechanism. *Journal of the American Chemical Society* **127**, 146-157
18. Hung, R. J., Chien, H. S., Lin, R. Z., Lin, C. T., Vatsyayan, J., Peng, H. L., and Chang, H. Y. (2007) Comparative analysis of two UDP-glucose dehydrogenases in Pseudomonas aeruginosa PAO1. *The Journal of biological chemistry* **282**, 17738-17748
19. Papoutsopoulou, S. V., and Kyriakidis, D. A. (1997) Phosphomannose isomerase of Xanthomonas campestris: a zinc activated enzyme. *Molecular and cellular biochemistry* **177**, 183-191
20. Hurwitz, C., and Rosano, C. L. (1967) The intracellular concentration of bound and unbound magnesium ions in Escherichia coli. *The Journal of biological chemistry* **242**, 3719-3722
21. Wells, T. N., Scully, P., and Magnenat, E. (1994) Arginine 304 is an active site residue in phosphomannose isomerase from Candida albicans. *Biochemistry* **33**, 5777-5782
22. Rogers, T. B., Borresen, T., and Feeney, R. E. (1978) Chemical modification of

the arginines in transferrins. *Biochemistry* **17**, 1105-1109

23. Swan, M. K., Hansen, T., Schonheit, P., and Davies, C. (2004) Structural basis for phosphomannose isomerase activity in phosphoglucose isomerase from *Pyrobaculum aerophilum*: a subtle difference between distantly related enzymes. *Biochemistry* **43**, 14088-14095
24. May, T. B., Shinabarger, D., Boyd, A., and Chakrabarty, A. M. (1994) Identification of amino acid residues involved in the activity of phosphomannose isomerase-guanosine 5'-diphospho-D-mannose pyrophosphorylase. A bifunctional enzyme in the alginate biosynthetic pathway of *Pseudomonas aeruginosa*. *The Journal of biological chemistry* **269**, 4872-4877
25. Sousa, S. A., Moreira, L. M., and Leitao, J. H. (2008) Functional analysis of the *Burkholderia cenocepacia* J2315 BceAJ protein with phosphomannose isomerase and GDP-D-mannose pyrophosphorylase activities. *Applied microbiology and biotechnology* **80**, 1015-1022
26. Barends, T. R., Dunn, M. F., and Schlichting, I. (2008) Tryptophan synthase, an allosteric molecular factory. *Current opinion in chemical biology* **12**, 593-600
27. Sa-Correia, I., Darzins, A., Wang, S. K., Berry, A., and Chakrabarty, A. M. (1987) Alginate biosynthetic enzymes in mucoid and nonmucoid *Pseudomonas aeruginosa*: overproduction of phosphomannose isomerase, phosphomannomutase, and GDP-mannose pyrophosphorylase by overexpression of the phosphomannose isomerase (*pmi*) gene. *Journal of bacteriology* **169**, 3224-3231
28. Ghosh, I., Hamilton, A. D., and Regan, L. (2000) Antiparallel Leucine Zipper-Directed Protein Reassembly: Application to the Green Fluorescent Protein. *Journal of the American Chemical Society* **122**, 5658-5659
29. Wilson, C. G., Magliery, T. J., and Regan, L. (2004) Detecting protein-protein interactions with GFP-fragment reassembly. *Nature methods* **1**, 255-262
30. Rodrigue, A., Quentin, Y., Lazdunski, A., Mejean, V., and Foglino, M. (2000) Two-component systems in *Pseudomonas aeruginosa*: why so many? *Trends in microbiology* **8**, 498-504
31. Stock, A. M., Robinson, V. L., and Goudreau, P. N. (2000) Two-component signal transduction. *Annual review of biochemistry* **69**, 183-215
32. Akerley, B. J., Cotter, P. A., and Miller, J. F. (1995) Ectopic expression of the flagellar regulon alters development of the *Bordetella*-host interaction. *Cell* **80**, 611-620
33. Lux, R., and Shi, W. (2005) A novel bacterial signalling system with a combination of a Ser/Thr kinase cascade and a His/Asp two-component system. *Molecular microbiology* **58**, 345-348

34. Hsu, J. L., Chen, H. C., Peng, H. L., and Chang, H. Y. (2008) Characterization of the histidine-containing phosphotransfer protein B-mediated multistep phosphorelay system in *Pseudomonas aeruginosa* PAO1. *The Journal of biological chemistry* **283**, 9933-9944
35. Lin, C. T., Huang, Y. J., Chu, P. H., Hsu, J. L., Huang, C. H., and Peng, H. L. (2006) Identification of an HptB-mediated multi-step phosphorelay in *Pseudomonas aeruginosa* PAO1. *Research in microbiology* **157**, 169-175
36. Garsin, D. A., Duncan, L., Paskowitz, D. M., and Losick, R. (1998) The kinase activity of the antisigma factor SpoIIAB is required for activation as well as inhibition of transcription factor sigmaF during sporulation in *Bacillus subtilis*. *Journal of molecular biology* **284**, 569-578
37. Mattoo, S., Yuk, M. H., Huang, L. L., and Miller, J. F. (2004) Regulation of type III secretion in *Bordetella*. *Molecular microbiology* **52**, 1201-1214
38. Mougous, J. D., Gifford, C. A., Ramsdell, T. L., and Mekalanos, J. J. (2007) Threonine phosphorylation post-translationally regulates protein secretion in *Pseudomonas aeruginosa*. *Nature cell biology* **9**, 797-803
39. Mukhopadhyay, S., Kapatral, V., Xu, W., and Chakrabarty, A. M. (1999) Characterization of a Hank's type serine/threonine kinase and serine/threonine phosphoprotein phosphatase in *Pseudomonas aeruginosa*. *Journal of bacteriology* **181**, 6615-6622
40. Motley, S. T., and Lory, S. (1999) Functional characterization of a serine/threonine protein kinase of *Pseudomonas aeruginosa*. *Infection and immunity* **67**, 5386-5394
41. Deziel, E., Comeau, Y., and Villemur, R. (2001) Initiation of biofilm formation by *Pseudomonas aeruginosa* 57RP correlates with emergence of hyperpiliated and highly adherent phenotypic variants deficient in swimming, swarming, and twitching motilities. *Journal of bacteriology* **183**, 1195-1204
42. Kohler, T., Curty, L. K., Barja, F., van Delden, C., and Pechere, J. C. (2000) Swarming of *Pseudomonas aeruginosa* is dependent on cell-to-cell signaling and requires flagella and pili. *Journal of bacteriology* **182**, 5990-5996
43. Tremblay, J., and Deziel, E. (2008) Improving the reproducibility of *Pseudomonas aeruginosa* swarming motility assays. *Journal of basic microbiology* **48**, 509-515
44. Campbell, E. A., Masuda, S., Sun, J. L., Muzzin, O., Olson, C. A., Wang, S., and Darst, S. A. (2002) Crystal structure of the *Bacillus stearothermophilus* anti-sigma factor SpoIIAB with the sporulation sigma factor sigmaF. *Cell* **108**, 795-807
45. Min, K. T., Hilditch, C. M., Diederich, B., Errington, J., and Yudkin, M. D. (1993) Sigma F, the first compartment-specific transcription factor of *B. subtilis*, is regulated by an anti-sigma factor that is also a protein kinase. *Cell*

46. Yang, X., Kang, C. M., Brody, M. S., and Price, C. W. (1996) Opposing pairs of serine protein kinases and phosphatases transmit signals of environmental stress to activate a bacterial transcription factor. *Genes & development* **10**, 2265-2275
47. Kozak, N. A., Mattoo, S., Foreman-Wykert, A. K., Whitelegge, J. P., and Miller, J. F. (2005) Interactions between partner switcher orthologs BtrW and BtrV regulate type III secretion in *Bordetella*. *Journal of bacteriology* **187**, 5665-5676
48. (2000) Purification of Fusion Proteins by Affinity Chromatography on Glutathione Agarose. in *Molecular Cloning, A Laboratory Manual* (Joseph Sambrook, D. W. R. ed.), Cold Spring Harbor Laboratory Press, Cold Spring Harbor, New York. pp 15.36-15.39
49. Schulenberg, B., Aggeler, R., Beechem, J. M., Capaldi, R. A., and Patton, W. F. (2003) Analysis of steady-state protein phosphorylation in mitochondria using a novel fluorescent phosphosensor dye. *The Journal of biological chemistry* **278**, 27251-27255
50. Schulenberg, B., Goodman, T. N., Aggeler, R., Capaldi, R. A., and Patton, W. F. (2004) Characterization of dynamic and steady-state protein phosphorylation using a fluorescent phosphoprotein gel stain and mass spectrometry. *Electrophoresis* **25**, 2526-2532
51. Schwyn, B., and Neilands, J. B. (1987) Universal chemical assay for the detection and determination of siderophores. *Analytical biochemistry* **160**, 47-56
52. Loudon, B. C., Haarmann, D., and Lynne, A. M. (2011) Use of Blue Agar CAS Assay for Siderophore Detection. *Journal of microbiology & biology education : JMBE* **12**, 51-53
53. Latifi, A., Winson, M. K., Foglino, M., Bycroft, B. W., Stewart, G. S., Lazdunski, A., and Williams, P. (1995) Multiple homologues of LuxR and LuxI control expression of virulence determinants and secondary metabolites through quorum sensing in *Pseudomonas aeruginosa* PAO1. *Molecular microbiology* **17**, 333-343
54. McClean, K. H., Winson, M. K., Fish, L., Taylor, A., Chhabra, S. R., Camara, M., Daykin, M., Lamb, J. H., Swift, S., Bycroft, B. W., Stewart, G. S., and Williams, P. (1997) Quorum sensing and *Chromobacterium violaceum*: exploitation of violacein production and inhibition for the detection of N-acylhomoserine lactones. *Microbiology* **143** (Pt 12), 3703-3711
55. Friedman, L., and Kolter, R. (2004) Genes involved in matrix formation in *Pseudomonas aeruginosa* PA14 biofilms. *Molecular microbiology* **51**, 675-690
56. Bordi, C., Lamy, M. C., Ventre, I., Termine, E., Hachani, A., Fillet, S., Roche,

- B., Bleves, S., Mejean, V., Lazdunski, A., and Filloux, A. (2010) Regulatory RNAs and the HptB/RetS signalling pathways fine-tune *Pseudomonas aeruginosa* pathogenesis. *Molecular microbiology* **76**, 1427-1443
57. Zhang, C. C. (1996) Bacterial signalling involving eukaryotic-type protein kinases. *Molecular microbiology* **20**, 9-15
 58. Dutta, R., and Inouye, M. (2000) GHKL, an emergent ATPase/kinase superfamily. *Trends in biochemical sciences* **25**, 24-28
 59. Krahn, T., Gilmour, C., Tilak, J., Fraud, S., Kerr, N., Lau, C. H., and Poole, K. (2012) Determinants of intrinsic aminoglycoside resistance in *Pseudomonas aeruginosa*. *Antimicrobial agents and chemotherapy* **56**, 5591-5602
 60. Lee, C. S., Lucet, I., and Yudkin, M. D. (2000) Fate of the SpoIIAB*-ADP liberated after SpoIIAB phosphorylates SpoIIAA of *Bacillus subtilis*. *Journal of bacteriology* **182**, 6250-6253
 61. Dasgupta, N., Wolfgang, M. C., Goodman, A. L., Arora, S. K., Jyot, J., Lory, S., and Ramphal, R. (2003) A four-tiered transcriptional regulatory circuit controls flagellar biogenesis in *Pseudomonas aeruginosa*. *Molecular microbiology* **50**, 809-824
 62. Yang, T. C., Leu, Y. W., Chang-Chien, H. C., and Hu, R. M. (2009) Flagellar biogenesis of *Xanthomonas campestris* requires the alternative sigma factors RpoN2 and FliA and is temporally regulated by FlhA, FlhB, and FlgM. *Journal of bacteriology* **191**, 2266-2275
 63. Wolfe, A. J., Millikan, D. S., Campbell, J. M., and Visick, K. L. (2004) *Vibrio fischeri* sigma54 controls motility, biofilm formation, luminescence, and colonization. *Applied and environmental microbiology* **70**, 2520-2524
 64. Zhao, K., Liu, M., and Burgess, R. R. (2010) Promoter and regulon analysis of nitrogen assimilation factor, sigma54, reveal alternative strategy for *E. coli* MG1655 flagellar biosynthesis. *Nucleic acids research* **38**, 1273-1283
 65. Pechy-Tarr, M., Bottiglieri, M., Mathys, S., Lejbolle, K. B., Schnider-Keel, U., Maurhofer, M., and Keel, C. (2005) RpoN (sigma54) controls production of antifungal compounds and biocontrol activity in *Pseudomonas fluorescens* CHA0. *Molecular plant-microbe interactions : MPMI* **18**, 260-272
 66. Duncan, L., Alper, S., and Losick, R. (1996) SpoIIAA governs the release of the cell-type specific transcription factor sigma F from its anti-sigma factor SpoIIAB. *Journal of molecular biology* **260**, 147-164
 67. Boyd, A., and Chakrabarty, A. M. (1995) *Pseudomonas aeruginosa* biofilms: role of the alginate exopolysaccharide. *Journal of industrial microbiology* **15**, 162-168
 68. Ryder, C., Byrd, M., and Wozniak, D. J. (2007) Role of polysaccharides in *Pseudomonas aeruginosa* biofilm development. *Current opinion in*

69. Potvin, E., Sanschagrín, F., and Levesque, R. C. (2008) Sigma factors in *Pseudomonas aeruginosa*. *FEMS microbiology reviews* **32**, 38-55
70. Ochsner, U. A., and Reiser, J. (1995) Autoinducer-mediated regulation of rhamnolipid biosurfactant synthesis in *Pseudomonas aeruginosa*. *Proceedings of the National Academy of Sciences of the United States of America* **92**, 6424-6428
71. Rahim, R., Ochsner, U. A., Olvera, C., Graninger, M., Messner, P., Lam, J. S., and Soberon-Chavez, G. (2001) Cloning and functional characterization of the *Pseudomonas aeruginosa* *rhlC* gene that encodes rhamnosyltransferase 2, an enzyme responsible for di-rhamnolipid biosynthesis. *Molecular microbiology* **40**, 708-718
72. Whiteley, M., Parsek, M. R., and Greenberg, E. P. (2000) Regulation of quorum sensing by RpoS in *Pseudomonas aeruginosa*. *Journal of bacteriology* **182**, 4356-4360
73. Bosgelmez-Tinaz, G., and Ulusoy, S. (2008) Characterization of N-butanoyl-L-homoserine lactone (C4-HSL) deficient clinical isolates of *Pseudomonas aeruginosa*. *Microbial pathogenesis* **44**, 13-19
74. Daniels, R., Vanderleyden, J., and Michiels, J. (2004) Quorum sensing and swarming migration in bacteria. *FEMS microbiology reviews* **28**, 261-289
75. Cornelis, P., Matthijs, S., and Van Oeffelen, L. (2009) Iron uptake regulation in *Pseudomonas aeruginosa*. *Biometals : an international journal on the role of metal ions in biology, biochemistry, and medicine* **22**, 15-22
76. Cornelis, P. (2010) Iron uptake and metabolism in pseudomonads. *Applied microbiology and biotechnology* **86**, 1637-1645
77. Burrowes, E., Baysse, C., Adams, C., and O'Gara, F. (2006) Influence of the regulatory protein RsmA on cellular functions in *Pseudomonas aeruginosa* PAO1, as revealed by transcriptome analysis. *Microbiology* **152**, 405-418
78. Bhuwan, M., Lee, H. J., Peng, H. L., and Chang, H. Y. (2012) Histidine-containing phosphotransfer protein-B (HptB) regulates swarming motility through partner-switching system in *Pseudomonas aeruginosa* PAO1 strain. *The Journal of biological chemistry* **287**, 1903-1914
79. Morris, A. R., and Visick, K. L. (2013) The response regulator SypE controls biofilm formation and colonization through phosphorylation of the *syp*-encoded regulator SypA in *Vibrio fischeri*. *Molecular microbiology* **87**, 509-525
80. Hua, L., Hefty, P. S., Lee, Y. J., Lee, Y. M., Stephens, R. S., and Price, C. W. (2006) Core of the partner switching signalling mechanism is conserved in the obligate intracellular pathogen *Chlamydia trachomatis*. *Molecular*

81. Stover, C. K., Pham, X. Q., Erwin, A. L., Mizoguchi, S. D., Warrenner, P., Hickey, M. J., Brinkman, F. S., Hufnagle, W. O., Kowalik, D. J., Lagrou, M., Garber, R. L., Goltry, L., Tolentino, E., Westbrook-Wadman, S., Yuan, Y., Brody, L. L., Coulter, S. N., Folger, K. R., Kas, A., Larbig, K., Lim, R., Smith, K., Spencer, D., Wong, G. K., Wu, Z., Paulsen, I. T., Reizer, J., Saier, M. H., Hancock, R. E., Lory, S., and Olson, M. V. (2000) Complete genome sequence of *Pseudomonas aeruginosa* PAO1, an opportunistic pathogen. *Nature* **406**, 959-964
82. Fields, S., and Song, O. (1989) A novel genetic system to detect protein-protein interactions. *Nature* **340**, 245-246
83. Karimova, G., Pidoux, J., Ullmann, A., and Ladant, D. (1998) A bacterial two-hybrid system based on a reconstituted signal transduction pathway. *Proceedings of the National Academy of Sciences of the United States of America* **95**, 5752-5756
84. Houot, L., Fanni, A., de Bentzmann, S., and Bordi, C. (2012) A bacterial two-hybrid genome fragment library for deciphering regulatory networks of the opportunistic pathogen *Pseudomonas aeruginosa*. *Microbiology* **158**, 1964-1971
85. Henderson, P. J., Giddens, R. A., and Jones-Mortimer, M. C. (1977) Transport of galactose, glucose and their molecular analogues by *Escherichia coli* K12. *The Biochemical journal* **162**, 309-320
86. Szkutnicka, K., Tschopp, J. F., Andrews, L., and Cirillo, V. P. (1989) Sequence and structure of the yeast galactose transporter. *Journal of bacteriology* **171**, 4486-4493
87. Longo, N., and Elsas, L. J. (1998) Human glucose transporters. *Advances in pediatrics* **45**, 293-313
88. Leloir, L. F. (1951) The enzymatic transformation of uridine diphosphate glucose into a galactose derivative. *Archives of biochemistry and biophysics* **33**, 186-190
89. Holden, H. M., Rayment, I., and Thoden, J. B. (2003) Structure and function of enzymes of the Leloir pathway for galactose metabolism. *The Journal of biological chemistry* **278**, 43885-43888
90. Isselbacher, K. J., Anderson, E. P., Kurahashi, K., and Kalckar, H. M. (1956) Congenital galactosemia, a single enzymatic block in galactose metabolism. *Science* **123**, 635-636
91. Donnell, G. N., Bergren, W. R., Perry, G., and Koch, R. (1963) Galactose-1-phosphate in galactosemia. *Pediatrics* **31**, 802-810
92. Gitzelmann, R. (1995) Galactose-1-phosphate in the pathophysiology of

- galactosemia. *European journal of pediatrics* **154**, S45-49
93. Lai, K., Elsas, L. J., and Wierenga, K. J. (2009) Galactose toxicity in animals. *IUBMB life* **61**, 1063-1074
 94. Abranches, J., Chen, Y. Y., and Burne, R. A. (2004) Galactose metabolism by *Streptococcus mutans*. *Applied and environmental microbiology* **70**, 6047-6052
 95. Chai, Y., Beauregard, P. B., Vlamakis, H., Losick, R., and Kolter, R. (2012) Galactose metabolism plays a crucial role in biofilm formation by *Bacillus subtilis*. *mBio* **3**, e00184-00112
 96. Nnalue, N. A., and Stocker, B. A. (1986) Some galE mutants of *Salmonella choleraesuis* retain virulence. *Infection and immunity* **54**, 635-640
 97. Fukasawa, T., and Nikaido, H. (1959) Galactose-sensitive mutants of *Salmonella*. *Nature* **184(Suppl 15)**, 1168-1169
 98. Kurahashi, K., and Wahba, A. J. (1958) Interference with growth of certain *Escherichia coli* mutants by galactose. *Biochimica et biophysica acta* **30**, 298-302
 99. Douglas, H. C., and Hawthorne, D. C. (1964) Enzymatic Expression and Genetic Linkage of Genes Controlling Galactose Utilization in *Saccharomyces*. *Genetics* **49**, 837-844
 100. Chang, H. Y., Lee, J. H., Deng, W. L., Fu, T. F., and Peng, H. L. (1996) Virulence and outer membrane properties of a galU mutant of *Klebsiella pneumoniae* CG43. *Microbial pathogenesis* **20**, 255-261
 101. Lai, Y. C., Peng, H. L., and Chang, H. Y. (2001) Identification of genes induced in vivo during *Klebsiella pneumoniae* CG43 infection. *Infection and immunity* **69**, 7140-7145
 102. Sundararajan, T. A. (1963) Interference with Glycerokinase Induction in Mutants of *E. Coli* Accumulating Gal-1-P. *Proceedings of the National Academy of Sciences of the United States of America* **50**, 463-469
 103. Krispin, O., and Allmansberger, R. (1998) The *Bacillus subtilis* galE gene is essential in the presence of glucose and galactose. *Journal of bacteriology* **180**, 2265-2270
 104. Slepak, T., Tang, M., Addo, F., and Lai, K. (2005) Intracellular galactose-1-phosphate accumulation leads to environmental stress response in yeast model. *Molecular genetics and metabolism* **86**, 360-371
 105. Lohr, D., Venkov, P., and Zlatanova, J. (1995) Transcriptional regulation in the yeast GAL gene family: a complex genetic network. *FASEB journal : official publication of the Federation of American Societies for Experimental Biology* **9**, 777-787

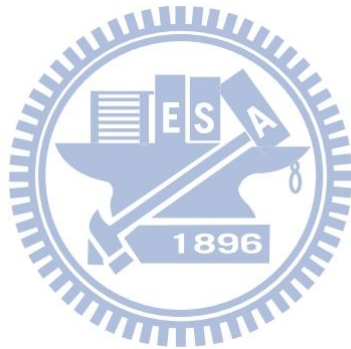
106. Biebl, H., Zeng, A. P., Menzel, K., and Deckwer, W. D. (1998) Fermentation of glycerol to 1,3-propanediol and 2,3-butanediol by *Klebsiella pneumoniae*. *Applied microbiology and biotechnology* **50**, 24-29
107. Lin, C. T., Wu, C. C., Chen, Y. S., Lai, Y. C., Chi, C., Lin, J. C., Chen, Y., and Peng, H. L. (2011) Fur regulation of the capsular polysaccharide biosynthesis and iron-acquisition systems in *Klebsiella pneumoniae* CG43. *Microbiology* **157**, 419-429
108. Janakiraman, A., and Slauch, J. M. (2000) The putative iron transport system SitABCD encoded on SPII is required for full virulence of *Salmonella typhimurium*. *Molecular microbiology* **35**, 1146-1155
109. Ikeda, J. S., Janakiraman, A., Kehres, D. G., Maguire, M. E., and Slauch, J. M. (2005) Transcriptional regulation of sitABCD of *Salmonella enterica* serovar Typhimurium by MntR and Fur. *Journal of bacteriology* **187**, 912-922
110. Weaver, E. A., Wyckoff, E. E., Mey, A. R., Morrison, R., and Payne, S. M. (2013) FeoA and FeoC are essential components of the *Vibrio cholerae* ferrous iron uptake system, and FeoC interacts with FeoB. *Journal of bacteriology* **195**, 4826-4835
111. Griggs, D. W., and Konisky, J. (1989) Mechanism for iron-regulated transcription of the *Escherichia coli* *cir* gene: metal-dependent binding of fur protein to the promoters. *Journal of bacteriology* **171**, 1048-1054
112. Salvail, H., and Masse, E. (2012) Regulating iron storage and metabolism with RNA: an overview of posttranscriptional controls of intracellular iron homeostasis. *Wiley interdisciplinary reviews. RNA* **3**, 26-36
113. Masse, E., Vanderpool, C. K., and Gottesman, S. (2005) Effect of RyhB small RNA on global iron use in *Escherichia coli*. *Journal of bacteriology* **187**, 6962-6971
114. Huang, S. H., Wang, C. K., Peng, H. L., Wu, C. C., Chen, Y. T., Hong, Y. M., and Lin, C. T. (2012) Role of the small RNA RyhB in the Fur regulon in mediating the capsular polysaccharide biosynthesis and iron acquisition systems in *Klebsiella pneumoniae*. *BMC microbiology* **12**, 148
115. Munch, R., Hiller, K., Grote, A., Scheer, M., Klein, J., Schobert, M., and Jahn, D. (2005) Virtual Footprint and PRODORIC: an integrative framework for regulon prediction in prokaryotes. *Bioinformatics* **21**, 4187-4189
116. Fic, E., Bonarek, P., Gorecki, A., Kedracka-Krok, S., Mikolajczak, J., Polit, A., Tworzydło, M., Dziedzicka-Wasylewska, M., and Wasylewski, Z. (2009) cAMP receptor protein from *Escherichia coli* as a model of signal transduction in proteins--a review. *Journal of molecular microbiology and biotechnology* **17**, 1-11
117. Gama-Castro, S., Salgado, H., Peralta-Gil, M., Santos-Zavaleta, A., Muniz-Rascado, L., Solano-Lira, H., Jimenez-Jacinto, V., Weiss, V.,

- Garcia-Sotelo, J. S., Lopez-Fuentes, A., Porron-Sotelo, L., Alquicira-Hernandez, S., Medina-Rivera, A., Martinez-Flores, I., Alquicira-Hernandez, K., Martinez-Adame, R., Bonavides-Martinez, C., Miranda-Rios, J., Huerta, A. M., Mendoza-Vargas, A., Collado-Torres, L., Taboada, B., Vega-Alvarado, L., Olvera, M., Olvera, L., Grande, R., Morett, E., and Collado-Vides, J. (2011) RegulonDB version 7.0: transcriptional regulation of Escherichia coli K-12 integrated within genetic sensory response units (Gensor Units). *Nucleic acids research* **39**, D98-105
118. Kolb, A., Busby, S., Buc, H., Garges, S., and Adhya, S. (1993) Transcriptional regulation by cAMP and its receptor protein. *Annual review of biochemistry* **62**, 749-795
119. Botsford, J. L., and Harman, J. G. (1992) Cyclic AMP in prokaryotes. *Microbiological reviews* **56**, 100-122
120. Gomez-Gomez, J. M., Baquero, F., and Blazquez, J. (1996) Cyclic AMP receptor protein positively controls gyrA transcription and alters DNA topology after nutritional upshift in Escherichia coli. *Journal of bacteriology* **178**, 3331-3334
121. Gorke, B., and Stulke, J. (2008) Carbon catabolite repression in bacteria: many ways to make the most out of nutrients. *Nature reviews. Microbiology* **6**, 613-624
122. Varshavsky, A. J., Nedospasov, S. A., Bakayev, V. V., Bakayeva, T. G., and Georgiev, G. P. (1977) Histone-like proteins in the purified Escherichia coli deoxyribonucleoprotein. *Nucleic acids research* **4**, 2725-2745
123. Schroder, O., and Wagner, R. (2002) The bacterial regulatory protein H-NS--a versatile modulator of nucleic acid structures. *Biological chemistry* **383**, 945-960
124. Hommais, F., Krin, E., Laurent-Winter, C., Soutourina, O., Malpertuy, A., Le Caer, J. P., Danchin, A., and Bertin, P. (2001) Large-scale monitoring of pleiotropic regulation of gene expression by the prokaryotic nucleoid-associated protein, H-NS. *Molecular microbiology* **40**, 20-36
125. Muller, C. M., Dobrindt, U., Nagy, G., Emody, L., Uhlin, B. E., and Hacker, J. (2006) Role of histone-like proteins H-NS and StpA in expression of virulence determinants of uropathogenic Escherichia coli. *Journal of bacteriology* **188**, 5428-5438
126. Bertin, P., Hommais, F., Krin, E., Soutourina, O., Tendeng, C., Derzelle, S., and Danchin, A. (2001) H-NS and H-NS-like proteins in Gram-negative bacteria and their multiple role in the regulation of bacterial metabolism. *Biochimie* **83**, 235-241
127. Lang, B., Blot, N., Bouffartigues, E., Buckle, M., Geertz, M., Gualerzi, C. O., Mavathur, R., Muskhelishvili, G., Pon, C. L., Rimsky, S., Stella, S., Babu, M. M., and Travers, A. (2007) High-affinity DNA binding sites for H-NS provide

- a molecular basis for selective silencing within proteobacterial genomes. *Nucleic acids research* **35**, 6330-6337
128. Timmermans, J., and Van Melderen, L. (2010) Post-transcriptional global regulation by CsrA in bacteria. *Cellular and molecular life sciences : CMLS* **67**, 2897-2908
 129. Romeo, T., Vakulskas, C. A., and Babitzke, P. (2013) Post-transcriptional regulation on a global scale: form and function of Csr/Rsm systems. *Environmental microbiology* **15**, 313-324
 130. Romeo, T., Gong, M., Liu, M. Y., and Brun-Zinkernagel, A. M. (1993) Identification and molecular characterization of csrA, a pleiotropic gene from Escherichia coli that affects glycogen biosynthesis, gluconeogenesis, cell size, and surface properties. *Journal of bacteriology* **175**, 4744-4755
 131. Yang, H., Liu, M. Y., and Romeo, T. (1996) Coordinate genetic regulation of glycogen catabolism and biosynthesis in Escherichia coli via the CsrA gene product. *Journal of bacteriology* **178**, 1012-1017
 132. Wang, X., Dubey, A. K., Suzuki, K., Baker, C. S., Babitzke, P., and Romeo, T. (2005) CsrA post-transcriptionally represses pgaABCD, responsible for synthesis of a biofilm polysaccharide adhesin of Escherichia coli. *Molecular microbiology* **56**, 1648-1663
 133. Yakhnin, H., Pandit, P., Petty, T. J., Baker, C. S., Romeo, T., and Babitzke, P. (2007) CsrA of Bacillus subtilis regulates translation initiation of the gene encoding the flagellin protein (hag) by blocking ribosome binding. *Molecular microbiology* **64**, 1605-1620
 134. Jonas, K., Edwards, A. N., Simm, R., Romeo, T., Romling, U., and Melefors, O. (2008) The RNA binding protein CsrA controls cyclic di-GMP metabolism by directly regulating the expression of GGDEF proteins. *Molecular microbiology* **70**, 236-257
 135. Liu, M. Y., and Romeo, T. (1997) The global regulator CsrA of Escherichia coli is a specific mRNA-binding protein. *Journal of bacteriology* **179**, 4639-4642
 136. Baker, C. S., Eory, L. A., Yakhnin, H., Mercante, J., Romeo, T., and Babitzke, P. (2007) CsrA inhibits translation initiation of Escherichia coli hfq by binding to a single site overlapping the Shine-Dalgarno sequence. *Journal of bacteriology* **189**, 5472-5481
 137. Liu, M. Y., Yang, H., and Romeo, T. (1995) The product of the pleiotropic Escherichia coli gene csrA modulates glycogen biosynthesis via effects on mRNA stability. *Journal of bacteriology* **177**, 2663-2672
 138. Wei, B. L., Brun-Zinkernagel, A. M., Simecka, J. W., Pruss, B. M., Babitzke, P., and Romeo, T. (2001) Positive regulation of motility and flhDC expression by the RNA-binding protein CsrA of Escherichia coli. *Molecular microbiology*

40, 245-256

139. Timmermans, J., and Van Melderer, L. (2009) Conditional essentiality of the *csrA* gene in *Escherichia coli*. *Journal of bacteriology* **191**, 1722-1724
140. Gasch, A. P., Spellman, P. T., Kao, C. M., Carmel-Harel, O., Eisen, M. B., Storz, G., Botstein, D., and Brown, P. O. (2000) Genomic expression programs in the response of yeast cells to environmental changes. *Molecular biology of the cell* **11**, 4241-4257



Appendix I

Table 1 Upregulated genes in CG43S3 $\Delta galU$ (+Gal) comparing with CG43S3 $\Delta galU$ [Fold Change > 4]

Feature ID	Gene Name	Fold Change	Proposed Function
D364_00295		111.59	hypothetical protein
D364_03825	<i>galE</i>	81.26	UDP-glucose 4 -epimerase
D364_03820	<i>galT</i>	54.15	galactose-1-phosphate uridylyltransferase
D364_03815	<i>galK</i>	49.74	galactokinase
	<i>galM</i>	29.80	aldose 1-epimerase
D364_07970	<i>lacY</i>	23.91	galactoside permease
D364_07975	<i>lacZ</i>	22.76	β -D-galactosidase
D364_07650		19.87	Di- and tricarboxylate transporters, L-tartrate/succinate antiporte
D364_02045		16.63	Nitrogen regulatory protein PII
D364_17020	<i>galP</i>	15.74	D-galactose transporter
D364_20555	<i>dgoD</i>	13.22	galactonate dehydratase
D364_20570	<i>dgoR</i>	11.91	galactonate operon transcriptional repressor
D364_21575	<i>metE</i>	9.73	5-methyltetrahydropteroyltriglutamate-homocysteine methyltransferase
D364_12000	<i>ftnA</i>	8.61	ferritin
D364_12155		7.76	LysR family transcriptional regulator
	<i>glyA</i>	7.64	Ser hydroxymethyltransferase
D364_01895		7.52	hypothetical protein
	<i>glnA</i>	7.44	glutamine synthetase
D364_17015	<i>metK</i>	7.25	S-adenosylmethionine synthetase
D364_20110	<i>sbp</i>	7.22	sulfate transporter subunit

D364_20560	<i>dgoA</i>	6.82	2-dehydro-3-deoxy-6-phosphogalactonate aldolase
D364_13460		6.58	N-acetyltransferase GCN5
<i>glnH</i>	<i>glnH</i>	6.02	glutamine ABC transporter periplasmic protein
D364_03465	<i>gltI</i>	5.70	glutamate and aspartate transporter subunit
D364_05135		5.64	hypothetical protein
D364_06380	<i>btuR</i>	5.64	cob(I)yrinic acid a,c-diamide adenosyltransferase
D364_14150		5.64	hypothetical protein
D364_20550		5.64	galactonate transporter
D364_24090	<i>hold</i>	5.64	DNA polymerase III subunit psi
D364_08005		5.33	5-methyltetrahydropteroyltriglutamate-homocysteine methyltransferase
D364_05975		5.33	hypothetical protein
D364_00155		5.17	hypothetical protein
<i>metQ</i>	<i>metQ</i>	4.95	DL-methionine transporter substrate-binding subunit
<i>copA</i>	<i>copA</i>	4.92	copper exporting ATPase
D364_13485	<i>argT</i>	4.85	lysine-, arginine-, ornithine-binding periplasmic protein
D364_13470	<i>hisM</i>	4.76	histidine/lysine/arginine/ornithine ABC transporter permease HisM
D364_04425		4.70	hypothetical protein
D364_08215		4.70	prolyl endopeptidase
D364_02050	<i>amtB</i>	4.66	ammonium transporter
D364_03460	<i>gltJ</i>	4.60	glutamate/aspartate ABC transporter permease GltJ
D364_23750		4.23	hypothetical protein
<i>tpiA</i>	<i>tpiA</i>	4.23	triosephosphate isomerase
D364_06475	<i>yciW</i>	4.18	putative oxidoreductase
D364_20490	<i>yidF</i>	4.08	putative regulator

Table 2 Downregulated genes in CG43S3 $\Delta galU$ (+Gal) comparing with CG43S3 $\Delta galU$ [Fold Change < 4]

Feature ID	Gene Name	fold change	Proposed Function
D364_24080		-187.80	hypothetical protein
D364_10845		-116.33	hypothetical protein
D364_17280		-43.60	biopolymer transport protein ExbD
D364_15335		-40.33	iron ABC transporter substrate-binding protein
D364_17620	<i>dhaT</i>	-38.34	1,3-propanediol oxidoreductase
D364_03070	<i>ychP</i>	-32.96	invasin-like protein
D364_18675	<i>bfd</i>	-30.03	bacterioferritin-associated ferredoxin
D364_14985	<i>nrdH</i>	-27.65	glutaredoxin-like protein
D364_15340	<i>sitB</i>	-23.93	manganese/iron transport system ATP-binding protein
D364_18375		-23.48	TMAO/DMSO reductase
D364_15345	<i>sitC</i>	-23.24	iron transport system inner membrane permease component
D364_05240		-19.35	hypothetical protein; iron permease
D364_05245		-18.90	hypothetical protein; iron uptake system component EfeO
D364_17290	<i>exbB</i>	-16.70	biopolymer transport protein ExbB
	<i>pduD</i>	-16.59	propanediol dehydratase medium subunit
	<i>pduE</i>	-14.89	propanediol dehydratase small subunit
D364_02470		-14.38	hypothetical protein
D364_17595	<i>dhaF</i>	-14.12	glycerol dehydratase
D364_07940		-13.82	membrane protein
D364_17285		-13.47	biopolymer transport protein ExbD
D364_24070	<i>fhuF</i>	-13.22	ferric iron reductase involved in ferric hydroximate transport
D364_07760		-12.76	hypothetical protein

D364_10960	<i>tonB</i>	-12.62	transport protein TonB
D364_17590	<i>glpF</i>	-12.61	glycerol uptake facilitator protein
D364_17615		-12.23	conserved hypothetical protein
D364_15350	<i>sitD</i>	-12.23	manganese ABC transporter, inner membrane permease protein SitD
D364_04235		-11.86	hypothetical protein
lamB	<i>lamB</i>	-11.83	maltoporin
D364_22585		-11.70	hypothetical protein
<i>pduC</i>	<i>pduC</i>	-11.26	propanediol dehydratase large subunit
D364_18970	<i>yhgG</i>	-10.99	ferrous iron transport protein FeoC
D364_22165		-10.63	metal-dependent hydrolases of the beta-lactamase superfamily III
D364_05250		-10.41	hypothetical protein
D364_11245		-9.57	hypothetical protein
<i>feoA</i>	<i>feoA</i>	-9.36	ferrous iron transport protein A
<i>minE</i>	<i>minE</i>	-8.51	cell division topological specificity factor MinE
D364_02520		-8.51	putative oxidoreductase
D364_10085		-8.51	LysR family transcriptional regulator
D364_15140		-8.51	PTS system glucitol/sorbitol-specific transporter subunit IIA
<i>glpE</i>	<i>glpE</i>	-8.51	thiosulfate sulfurtransferase
<i>malE</i>	<i>malE</i>	-8.11	maltose ABC transporter periplasmic protein
D364_15355		-8.03	hypothetical protein
D364_13700	<i>mntH</i>	-7.93	manganese transport protein MntH
D364_10810		-7.69	hypothetical protein
D364_17580		-7.60	acid-resistance membrane protein
D364_10350		-7.44	hypothetical protein
D364_10400	<i>ccmH</i>	-7.44	cytochrome c-type biogenesis protein CcmH

D364_12135		-7.44	LysR family transcriptional regulator
<i>feoB</i>	<i>feoB</i>	-7.14	ferrous iron transport protein B
D364_23380		-7.14	hypothetical protein
D364_23340		-7.02	putative SN-glycerol-3-phosphate transport system permease
D364_05785		-6.91	hypothetical protein
D364_16355		-6.91	P pilus assembly protein, pilin FimA
<i>folA</i>	<i>folA</i>	-6.91	dihydrofolate reductase
D364_22005		-6.75	ABC-type sugar transport systems, ATPase components
D364_17575		-6.73	hypothetical protein
D364_17675		-6.38	PadR family transcriptional regulator
D364_07570		-6.38	DNA-invertase hin
D364_14980		-6.38	hypothetical protein
D364_17170		-6.38	putative fimbrial-like protein
D364_23815	<i>cstA</i>	-6.25	carbon starvation protein CstA
D364_03065	<i>fes</i>	-6.13	enterobactin/ferric enterobactin esterase
D364_22140		-6.03	prepilin peptidase dependent protein C
<i>glpA</i>	<i>glpA</i>	-5.96	sn-glycerol-3-phosphate dehydrogenase subunit A
D364_22015	<i>malM</i>	-5.86	maltose regulon periplasmic protein
D364_11490		-5.78	ferrichrome-iron receptor
D364_21865	<i>aceA</i>	-5.77	isocitrate lyase
D364_09555	<i>yncE</i>	-5.73	putative receptor
D364_07755	<i>ydgD</i>	-5.58	protease ydgD
D364_20650		-5.47	hypothetical protein
D364_03900		-5.32	hypothetical protein
D364_06565		-5.32	peripheral inner membrane phage-shock protein

D364_07495		-5.32	hypothetical protein
D364_19150		-5.32	prevent host death protein, Phd antitoxin
D364_03870		-5.32	hypothetical protein
D364_06175		-5.32	DNA-binding transcriptional activator OsmE
D364_07060		-5.32	hypothetical protein
D364_08000		-5.32	rhodanese-related sulfurtransferase
D364_08070	<i>marC</i>	-5.32	multiple drug resistance protein MarC
D364_10345		-5.32	acetoin reductase
D364_16155		-5.32	hypothetical protein
D364_23515		-5.32	hypothetical protein
D364_14200		-5.14	hypothetical protein
D364_20010		-5.10	hypothetical protein
D364_23840	<i>hpaI</i>	-5.10	2,4-dihydroxyhept-2-ene-1,7-dioic acid aldolase
<i>mobA</i>	<i>mobA</i>	-5.10	molybdopterin-guanine dinucleotide biosynthesis protein MobA
D364_13730	<i>yfeR</i>	-5.05	LysR family transcriptional regulator
D364_04175	<i>ybiL</i>	-5.04	hypothetical protein (DnaK suppressor protein)
D364_01955	<i>bolA</i>	-5.00	transcriptional regulator BolA
<i>hdeB</i>	<i>hdeB</i>	-4.96	acid-resistance protein
<i>glpT</i>	<i>glpT</i>	-4.94	sn-glycerol-3-phosphate transporter
D364_07480		-4.89	hypothetical protein
D364_13625	<i>yfdC</i>	-4.87	formate/nitrite family of transporters
<i>mscL</i>	<i>mscL</i>	-4.87	large-conductance mechanosensitive channel
D364_11025	<i>adhE</i>	-4.87	bifunctional acetaldehyde-CoA/alcohol dehydrogenase
D364_03615		-4.86	hypothetical protein
D364_16285		-4.79	fimbrial-like protein

D364_18400		-4.79	hypothetical protein
D364_11335		-4.79	type VI secretion system protein ImpK
D364_16635		-4.79	putative transposase-like protein
D364_22400		-4.79	hypothetical protein
D364_11035	<i>hns</i>	-4.78	global DNA-binding transcriptional dual regulator H-NS
D364_04125	<i>ybiH</i>	-4.73	DNA-binding transcriptional regulator
	<i>pdxA</i>	-4.68	4-hydroxyThr-4-phosphate dehydrogenase
D364_15075		-4.62	hypothetical protein
D364_08630		-4.61	hypothetical protein
D364_10105		-4.61	hypothetical protein
D364_16440		-4.61	hypothetical protein
D364_07555		-4.54	hypothetical protein
D364_16930		-4.52	putative short-chain dehydrogenase/reductase SDR
D364_20825		-4.48	D-ribose transporter subunit RbsB
D364_17630		-4.47	hypothetical protein
D364_07595		-4.41	DNA-binding transcriptional regulator
D364_22925		-4.38	adenosine-3'(2'),5'-bisphosphate nucleotidase
D364_21215		-4.35	zinc/cadmium-binding protein
D364_00795		-4.25	iron-hydroxamate transporter substrate-binding subunit
D364_06030		-4.25	hypothetical protein
D364_06915		-4.25	hypothetical protein
D364_07385		-4.25	phage replication protein O
D364_08095		-4.25	dihydrodipicolinate synthase
D364_10025		-4.25	hypothetical protein
D364_13235	<i>yfaU</i>	-4.25	2-keto-3-deoxy-L-rhamnonate aldolase

<i>recX</i>	<i>recX</i>	-4.25	recombination regulator RecX
<i>zraP</i>	<i>zraP</i>	-4.25	zinc resistance-associated protein
D364_04170		-4.25	hypothetical protein
D364_07170		-4.25	hypothetical protein
D364_08355		-4.25	hypothetical protein
D364_10140		-4.25	glyoxalase family protein
D364_14240		-4.25	hypothetical protein
D364_17825		-4.25	inner membrane protein YqjF
D364_20635		-4.25	hypothetical protein
D364_22575		-4.25	hypothetical protein
D364_23410		-4.25	hypothetical protein
<i>hdeB</i>	<i>hdeB</i>	-4.25	acid-resistance protein
<i>entF</i>	<i>entF</i>	-4.23	enterobactin synthase subunit F
D364_07870		-4.12	hypothetical protein
D364_00785		-4.10	ferrichrome outer membrane transporter
D364_18425	<i>envR</i>	-4.08	DNA-binding transcriptional regulator EnvR
<i>srlA</i>	<i>srlA</i>	-4.08	glucitol/sorbitol-specific PTS family enzyme IIC component
D364_02705		-4.08	putative periplasmic protein
D364_15080	<i>csrA</i>	-4.06	carbon storage regulator
D364_08100		-4.04	alcohol dehydrogenase
D364_20205	<i>nudF</i>	-4.04	ADP-ribose pyrophosphatase
<i>narI</i>	<i>narI</i>	-4.04	nitrate reductase 1 gamma subunit

Appendix II

P_{galE}

TGCGGAAGATGCCCCGACTGTATTACCCATCGCCTGGCGTTTCGTTCCCAGTGGAGACGG
TTACTTATCAGCTCGCCCCGTGGCCTGACGCCCCCTGTCGGGGATCGAAAGATCCCT
GGTATTTTTTCAGAAAAATAGCGCCAAAATAATATAATGACATGTTTTTAAAGAAAAATAT
ATTCAATGATATCATTTCGCCCTTGAGTGTAACGATTCCACTAACTTGTGCTATGTCACA
CTTTTCACTTCTTTGATATGCTATCTTCTCACAAACGATAAGCCGAATGGAGCGAATC
ATGAAAGTCTGGTTACAGGTGGTAGCGGTTACATTGGAAGTCATACCTGCGTTCAACTG

CRP binding box

P_{galP}

CGCGCGGCCGCCACAAAATGAAAGCGATTACATAGTAAAGACTGTCACCTTCTGCCAAA
GACGCTATCTCTGTACCCATTTTTTACAATGTTACATATTGTTTCGGTCAACTCTGATT
ACCGTTTTTCAAATGTCGTCTATCCTTGTATATTGCTGATTTAAAAAGCATTTAATG
AATTACGTTTCTTTACCTTTGTGGAACGATTACACAGCGTGAATTATAGTCACGTTTTT
TTACCGACGAGTGTCTACCCTAACCATCGACAGAATCAATAACTCAACTGGAGGGCGTT
ATGCCTGACAACAAAAACAAGGGCGTTCGAACAAGACTATGACGTTCTTCGTCTGTTTC

CRP binding box

P_{lacZ}

CGGGCTGACACCACCTCAGGACGGTTCAGCACCCGGGAGACCGTCTGCTGGGACACGCC
GCGGCGGGGCGACATCCTCCAGGGTTGCGGTACGACGCGGCATCTTTTCTCTCAGTAA
TAACAATGTCGTGCGCTAACATTTATGTTTAAACGCGCGACAAAAACAGCGCTTCGTCC
H-NS
CCGTTTTCGTGATCGTCTGTTAATTTTCGATTCCCCCGAGATTGCTGGACAAAACAAATTA
CCCGATAACGTTAATCATCCTGTTTAGCGAACGACAATTTCTGACTTACCGGGGTTAAT
ATGCAAATTAGCGATACCGGCCGAGCCACACTCCTGACTTTCACGCCGCTCCTCGCCCGT

P_{pduC}

CCGCCATGATTTAGTCAATAGGGTTAAATAGCGACGGCAAAGCGTAATTAAGGGCGTTT
CRP binding box
TTTATTAATTGATTTATATCATTTGCGGGCGATTCACAATTTTTATTTTTGCCGGCGGAGTA
AAGTTTCATAGTGAAACTGTCGGTAGATTTTCGTGTGCCAAATTGAAACGAAATTAATTT
CRP binding box
ATTTTTTTCACCACTGGCTCATTAAAGTTCGCTATTGCCGGTAATGGCCGGGCGGCAA
H-NS
CGACGCTGGCCCGGCGTATTTCGCTACCGTCTGCGGATTTACCTTTTTCGATGAACA
ATGAAAAGATCAAACGATTTGCAGTACTGGCCAGCGCCCGTCAATCAGGACGGGCTG

P_{D364_17615}

H-NS
AAAAAATAAATTTAATTTTCGTTTCAATTTGGCACACGAAATCTACCGACAGTTTCACTAT
CRP binding box H-NS
GAAACTTTACTCCGCGGCAAAAATAAAAAATGTTGATATAAATCAAT
TAATAAAAAACGCCCTTAATTACGCTTTGCCGTCGCTATTTTAAACCCTATTGACTAAATC
ATGGCGGGCGACAAAATAACGCTGACAAAATAAAGCAAGCCAACCGAATGGTAATAGT
TTTTACTATCGCCCCCTACTGACTATTCGCGCCAGCGTTATCCTGGTGCGGGAGAGAATG
ATGAACAAGAGCCAACAAGTTTCAGACAATCACCTGGCCGCCGCCAGAAAATGGCGGG

P_{sitA}

TGCTGGATAACTGTATTCAGCGTATTCGCAGCCTGATTGACGACCGGCCAACCTTCACCG
CCGAGGGCCGCTCGCTGGCTGGCCGCCTGATCCCCGCGCCAGTCGGTCGCCGATATCTCTT
GATCTTCGCCCGGTTGGCGCCGGGCCAGACTTACCTCCCCTTTTCGCGCTTTCGTTTCCC

Fur binding box H-SN

GGCTCATTATTACCCACGCATGCAAATAAGAATTATTTTCATTTATAAATAGCTTGTGCT
CRP binding box H-SN

ATATAACATAGCAATGGCTATAAACGCTGGGAAATTAACCACACCATTGCGAGGGATCCT
ATGCTACACCTGACATCGCTGAAATCATTGCTGCTGGCCAGCGCGCTGGCTCTGCTGGCC

P_{feoA}

GGCAGCGAAATTAATATTTTCATTTTCGTTAACTTCAGAAACCTTAATTAACATTAGATC
H-NS

GCCGAAATAATATTTTCGCGCATTTTTGATTACAGGCTGACTTTGCGGCATATCAATAAAAA

CRP binding box Fur binding box

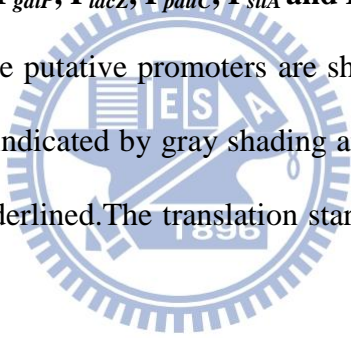
GGTGATTTTCACTTTAAAAATAGCCTGCAGCGCATCATAATGTATTGATGATAAAAAACCA
TTCTCATTATCATCGATTACAGAACGTTTTTTTTCTTTTTTCGTTGGCTACGGTCCCCGGC

H-NS

GCAACTGCCTCCAGGCGTCCGGAAAATTCTTCTTCGGTTAGCGATAGACAAGTAGGCCCT
ATGCAATTCACACCTGATAGTGCGTGGAATAATTACCGTTTTTCTCGCGATATTAGCCCA

Sequence analysis of P_{galE}, P_{galP}, P_{lacZ}, P_{pduC}, P_{sitA} and P_{feoA}

The sequences containing the putative promoters are shown. The predicted CRP, Fur and H-NS binding sites are indicated by gray shading and nucleobase identical to the consensus sequences are underlined. The translation start codon (ATG) is indicated in bold face and font border.



Curriculum Vitae

Esther, Hui-Ju Lee

E-mail: esther.bt93g@nctu.edu.tw

Education

Date	Degree	Institute
2000-2004	B.S.	Department of Applied Chemistry, National Chiao Tung University
2004-2007	M.S.	College of Biological Science and Technology, National Chiao Tung University
2007-Present	Ph.D.	College of Biological Science and Technology, National Chiao Tung University

Publication

A. Journal Papers:

1. **Lee HJ**, Chang HY, Venkatesan N, Peng HL (2008) Identification of amino acid residues important for the phosphomannose isomerase activity of PslB in *Pseudomonas aeruginosa* PAO1. *FEBS Letters* 582 (23-24): 3479-3483
2. **Lee HJ**, Ho MR, Bhuwan M, Hsu CY, Huang MS, Peng HL, Chang HY (2010) Enhancing ATP-based bacteria and biofilm detection by enzymatic pyrophosphate regeneration. *Analytical Biochemistry* 399 (2): 168-173
3. **Lee HJ**, Ho MR, Tseng CS, Hsu CY, Huang MS, Peng HL, ChangHY (2011) Exponential ATP amplification through simultaneous regeneration from AMP and pyrophosphate for luminescence detection of bacteria. *Analytical Biochemistry* 418 (1): 19-23
4. Bhuwan M, **Lee HJ**, Peng HL, Chang HY (2012) Histidine-containing phosphotransfer protein-B (HptB) regulates swarming motility through partner-switching system in *Pseudomonas aeruginosa* PAO1 strain. *Journal of Biological Chemistry* 287 (3): 1903-1914
5. Young YF, **Lee HJ**, Shen YS, Tseng SH, Lee CY, Tai NH, Chang HY (2012) Toxicity mechanism of carbon nanotubes on *Escherichia coli*. *Materials Chemistry and Physics* 134 (1): 279-286

B. Conference:

1. **Lee HJ** and Peng HL (2006) Important Residues in Phosphomannose Isomerase of *Pseudomonas aeruginosa* PAO1. The 11th Conference on Bacteriology, 23 Aug-25 Aug, Taiwan.
2. **Lee HJ** and Peng HL (2007) Important Residues in Phosphomannose Isomerase of *Pseudomonas aeruginosa* PAO1. 107th ASM general meeting, 18-25 May, Toronto, Canada.
3. **Lee HJ**, Ho MR, Hsu CY, Yang SY, Kuo YC, Huang MS and Chang HY (2008) Detection of bacteria in water by using an ADP-glucose pyrophosphorylase coupling ATP regeneration system, Taiwan Society of Microbiology Conference, 29 November, Taipei, Taiwan.
4. **Lee HJ**, Bhuwan M, Liu DY, Chang HY and Peng HL (2009) A novel signaling system with a combination of HptB-mediated multistep phosphorelay and partner-switching regulatory modules in *Pseudomonas aeruginosa* PAO1. The Poster Competition of College of Biological Science and Technology, National Chiao Tung University, 21 May, Hsinchu, Taiwan.
5. Bhuwan M, **Lee HJ**, Peng HL and Chang HY (2009) Corroborate the significance of PA3347, an antisigma antagonist, in flagellum induced virulence and partner-switching regulatory module for HptB mediated two component system in *Pseudomonas aeruginosa*. The 14th Conference on Bacteriology, 26-28 August, Taiwan.
6. Bhuwan M, **Lee HJ**, Peng HL and Chang HY (2011) HptB-PA3346-PA3347 is a swarming regulating partner switching module in *Pseudomonas aeruginosa* PAO1. 13th International Conference on Pseudomonas, 04-07 September, Sydney, Australia